DELTA FORM AND PROCESS: A FLUME STUDY

by

A. K. Azizul Hoq Bhuyia

B.Sc. (Hons.) University of Dacca, Bangladesh, 1964

M.Sc., University of Dacca, Bangladesh, 1965

A THESIS SUBMITTED IN PARTIAL FULFILLMENT OF

THE REQUIREMENTS FOR THE DEGREE OF

MASTER OF SCIENCE

in the Department

of

Geography

SIMON FRASER UNIVERSITY

July 1980

APPROVAL

Name: A.K. Azizul Hoq Bhuiya

Degree: Master of Science

Title of Thesis: Delta Form and Process: A Flume Study

Examining Committee:

Chairman: Roger Hayter

Edward J. Hickin
Senior Supervisor

Michael C. Roberts

Colin C. Crampton

Knut R. Fladmark
External Examiner
Associate Professor
Department of Archaeology
Simon Fraser University

Date of Approval: July 23rd 1980

PARTIAL COPYRIGHT LICENSE

I hereby grant to Simon Fraser University the right to lend my thesis, project or extended essay (the title of which is shown below) to users of the Simon Fraser University Library, and to make partial or single copies only for such users or in response to a request from the library of any other university, or other educational institution, on its own behalf or for one of its users. I further agree that permission for multiple copying of this work for scholarly purposes may be granted by me or the Dean of Graduate Studies. It is understood that copying or publication of this work for financial gain shall not be allowed without my written permission.

Title of Thesis/Project/Extended Essay

Delta Form and Process: A Flume Study

Author: _____
(signature)

A.K. Azizul Hoq Bhuiya
(name)

August 5, 1980
(date)

ABSTRACT

Sedimentation dynamics at a river mouth represent a complex set of interacting processes. The interaction of the river effluent and the ambient water is the most fundamental of these processes. However, the vast majority of delta studies have merely described the morphology in general terms and have ignored the relevant fluid dynamics theory. Furthermore, there is poor understanding of the interaction of processes and forms, and of which parameters are most important in the interpretation of geomorphic, geologic, and hydrologic characteristics of deltas. Past studies sought an analogy between the theory of free jets and the dynamics of water and transported sediments at river mouths. The free-jet model proposed that the pattern of fluid and sediment dispersal, and consequent deposition, are directly related to the fluid dynamics of jet diffusion.

In order to test the appropriateness of the jet analogy as a model of the formation and development of deltas, a small-scale flume experiment was performed. The study explored the relationship between axial jet diffusion and deltaic deposition, and described interactions and interdependencies among flows, sediment transport conditions and the morphological delta pattern. The important results of the flume experiment are:

1. The sedimentation process associated with delta formation

does not conform to axial jet diffusion, although a dynamic similarity has been found to hold in the hydraulic expansion of the jets at different discharge regimes and in sediment free flow conditions.

2. Delta morphometry is functionally related to the changing scale of flow and sediment transport rate. For a given sediment discharge rate an increase in flow velocity causes a relative rate of increase in the longitudinal length of the delta with concomitant decrease in both vertical and lateral growth rate. Conversely, at a given discharge of water, an increase in sediment supply rate tends to retard the relative rate of longitudinal advance, a mechanism effectively related to compensatory increases in both lateral and upward growth of the deltaic mass.
3. The surficial delta features, such as submerged natural levees, shoals and bars, and pattern of distributaries, are directly related to the nature and degree of flow divergence occurring over the the delta platform.
4. The foreset deposit constituted the gross structural organization of the laboratory deltas. The cross bedded structure of the foreset deposit is directly related to high bed load transport and the phenomenon of flow separation.

These findings stress the interdependency and interaction of processes and forms; an intricate association conditioned by the changing flow scale and sediment transport conditions.

ACKNOWLEDGEMENTS

I would like to express my gratitude to the many people who were forced to suffer from my continued need for assistance, discussion, and encouragement at different stages of this study.

I am most grateful to Ted Hickin for serving as my senior supervisor. His encouragement and support in undertaking the flume experiment, and subsequent advice and guidance to refine and sharpen my thinking and writing were invaluable. My gratitude is also extended to Michael Roberts and Colin Crampton, whose offices were always open to me for discussion and assistance. I am also thankful to them for their close reading, comments, and editorial assistance.

I would like to thank Ian Hutchinson for providing much needed help during the construction of the flume. Assistance from friends and fellow graduate students, especially from Jim Prior, Larry King, Michael MacPhee, Amanat Khan, and Abdullah Al-Mamun, Wayne Luscombe, Pood Lai, and Ken Rood is gratefully acknowledged and appreciated.

I would also like to thank Len Evenden for his close reading and critical comments.

I would like to thank Knut Fladmark, Department of Archaeology, Simon Fraser University, for serving as my external examiner.

I am very grateful to Bernard Curtin who single-handedly

helped me to type the thesis.

I am indebted to Mr. John Helliwell, Director, Foreign Student Affairs, the Canadian Bureau of International Education for financial assistance at the time of my greatest need. Tom Peucker's help is also deeply appreciated.

Finally, I would like to express my deep sense of gratitude to my wife, Setara, for her assistance in varying capacities, patience, and when my entusiasm waned, her encouragement and wits; and to my daughter, Angela, who never failed to receive me with innocent smiles.

A. TABLE OF CONTENTS

LIST OF TABLES

LIST OF FIGURES

LIST OF PHOTO-PLATES

I. Introduction

1.1 The General Problem

The patterns of fluid and sediment dispersal and consequent deposition at a river mouth represent a complex set of interacting processes. The interaction of the river effluent and ambient water is the most fundamental of these processes. River effluent discharges into a basin, resulting in diffusion of the outflow momentum and in a consequent loss of transporting power, which leads to delta formation and development. Barrell (1912) defined a delta as 'a deposit, partly subaerial, built by a river into or against a permanent body of water'. The shape, size and composition of deltas are affected by many factors. The principal controls are hydraulic parameters, sediment properties, rate of sediment transport, off-shore energy conditions, density difference between the inflow and basin water, basin morphology, subsidence, and climate. Processes and forms are interrelated, but their interaction is not precisely known.

Attempts to define and understand the development of delta morphology have increased in recent decades. However, the vast majority of delta studies by geographers and geologists have

merely described the morphology in general terms and have ignored the relevant fluid dynamics theory. As a result, no analytical method has yet been developed to relate the fluid processes active at a river mouth to the morphology of the resultant delta. In 1953 Charles C. Bates sought an analogy between the Tollmien (1926) theory of free jets and the dynamics of water and transported sediment at river mouths. The model of delta formation before Bates' paper (1953) was that proposed by Gilbert in 1885. In the interim, much attention was given to the detailed descriptions of deltaic features and little to the processes responsible for these deposits. Although the jet analogy continues to appear in recent literature (Crickmay 1955; Jopling 1960, 1962, 1963, 1964, 1965; Axelsson 1967; Bonham-Carter and Sutherland 1967; Coleman and Wright 1967, 1971), few experimental attempts have been made to investigate the appropriateness of this model. Furthermore, there is a poor understanding of which parameters are the most important in the interpretation of geomorphic, geologic, and hydrologic characteristics of deltas.

1.2 Aim of the Study

The twofold general aim of the present study is to isolate and describe some of the hydraulic factors which control delta morphology, and to examine the viability of the jet analogy as a

model of the formation and development of deltas.

Delta morphology, during the constructional phase, appears largely to be dependent on the flow conditions and nature of transported materials. But our knowledge of deltaic sedimentation is insufficient to explain the precise role of these variables. One problem is the choice of which variables are independent and which are dependent when the processes and forms are interrelated and interacting. In fact the choice depends on both temporal and spatial characteristics of the sedimentation system. The present study focuses on the discharge and the rate of sediment transport as independent variables and seeks to answer questions about the mode of formation and development of deltas (dependent variable) in a variety of discharge and sediment transport conditions. This choice is made because the present study regards a 'steady state' channel, which maintains the continuity of discharge and sediment transport, as independent of any external process or form occurring in the basin at the time scale of the investigation.

In order to examine delta processes and forms within a reasonable time, a small-scale laboratory experiment under homopycnal inflow conditions[1] has been chosen as the basic data source. It is assumed that the ambient water is stationary in the sense that the offshore energy (tides, waves, currents),

---

[1] Homopycnal flow conditions (Bates, 1953) mean river water and ambient water are equally dense and inflow enters into a water body as an axial jet.

water level and other physical conditions of the basin are constant or absent. Given these assumptions, the main objectives of the study are to investigate the influences of variation in discharge and sediment transport on the velocity-field and on the diffusion of the jet, on the mode of sediment dispersal and deposition, and on the formation of delta morphology.

The ultimate aim of this study is to contribute to the understanding of sedimentation at river mouths. It represents a first step in solving problems related to sedimentation dynamics at a river mouth.

1.3 The Perspective of a Laboratory Experiment

In searching for order and unifying tendencies in natural processes, a useful strategy in geomorphological enquiry has been to perform small-scale experiments in a laboratory situation. King (1966) noted that "the small-scale model experiment is of the greatest utility when there is a need to control many variables and study in isolation, a situation which is not possible in nature". Hickin (1970) found experiments to be useful for examining "combinations of conditions" through easy manipulation of the variables while recognising that the "flume experiment is considerably simpler than its natural counterpart." He emphasized that "an understanding of the simple case makes the analysis of the real situation somewhat less

formidable".

The complexity involved in the interaction of variables such as flow discharge and sediment transport in the formation of deltas can be illustrated by simple yet fundamental flume experiments. A flume experiment often suffices to describe the general behaviour of a geomorphic system in somewhat controlled conditions. This may help to formulate principles concerning processes of transfer of energy and be of importance in understanding the physical forces and forms in nature. A flume experiment is, however, of little rigorous use if explicit correspondence in nature is found to be unresolved.

1.4 Organization of the Study

The various topics in the study correspond approximately with their chronological treatment. Chapter 2 provides a review of the pertinent literature. In addition to outlining the ideas and views of the jet analogy, the review includes an examination of experimental works concerned with process and form of deltaic deposits. Chapter 3 presents the specific assumptions and hypotheses of the present investigation. The hypotheses are based on my analysis of past studies reported in the literature. The validity of the hypotheses are discussed in the concluding chapter.

Chapter 4 outlines the methods and procedures adopted in

the experiment. It also provides a discussion of the design and engineering of the model, instrumentation and control-devices used in the experiments.

Experimental data and analyses are presented in chapter 5. It provides an interpretation of the data based largely on the correlation among the variables.

Chapter 6 is devoted to the interpretation and discussion of the results, to the synthesis of the experimental findings, and to identifying the limitation of the experiments. Conclusions drawn from this exercise provide the basis for recommendations for future research.

II. The Jet Analogy and Other Views of Delta Formation

2.1 Introduction

Although there is a considerable literature on deltas, little is known about the processes controlling delta morphology. Gilbert (1885) proposed that the loss of flow competence resulting in deposition at the river mouth was the main mechanism of delta formation. His model of flow deceleration resulting in the tripartite structure of a delta is now recognized as the classic theory of delta formation.

In 1953, Charles. C. Bates published the Rational Theory of Delta Formation which considered progressive deconcentration of effluent momentum to be a result of jet diffusion into a standing body of water. He reviewed the works of Gilbert (1885), Forel (1904), Lipsey (1919), Dent (1924), Tollmien (1926), Russell (1936), Auerbach (1939), Fisk (1944), Albertson et al. (1950), Simons (1951), Shepard (1951), Cobb (1952), Crowell (1952), Ewig (1952), Glen (1952), Heegen (1952), Holle (1952) and others. The processes active at the mouth of the Mississippi were considered by Bates to confirm the contention that a delta is "a deposit built by jet flow into or within a permanent body of water".

The fluid dynamics of jet expansion were first investigated theoretically by Tollmien (1926). He applied Prandtl's (1925) momentum-transport theory to solve the mixing problems of a jet issuing into the same medium at rest. Tollmien's theory has been further developed and tested experimentally by workers in such varied fields as aerodynamics, chemical, heating, and hydraulic engineering. However, for the purpose of the present study, the work of Albertson et al. (1950) is particularly relevant.

2.2 Diffussion of a Submerged Jet (M. L. Albertson et al. 1950)

Albertson et al. (1950) published detailed characteristics of jet diffusion into a stationary 'infinite' volume of the same fluid. According to their observations, when water moves out, shear along the jet boundary generates turbulent eddies with lateral mixing which progresses both inward and outward with distance from the outlet. Newton's second law of motion requires that such mixing produces two balanced reactions: 1) fluid within the jet is gradually decelerated, and 2) fluid from the surrounding region is gradually accelerated or entrained. As a result, the constant velocity-core of the jet decreases steadily in lateral extent and continuity considerations demand that this velocity reduction lead to an increase in the total flow area. The limit of this 'zone of flow establishment' is reached when the mixing region has penetrated the axis of the jet (Figure 1).

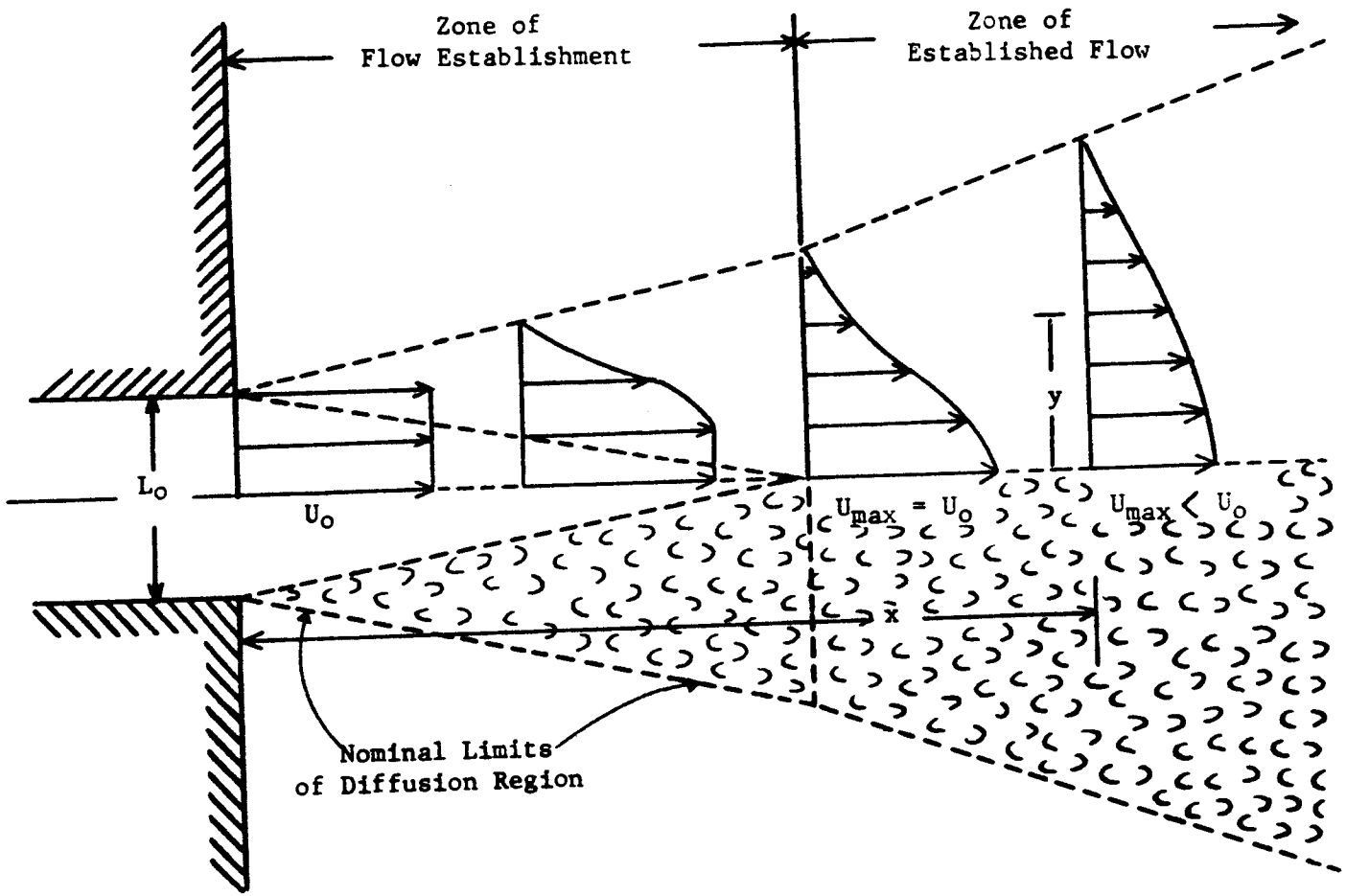

Figure 1. Schematic Representation of Jet Diffusion
(After Albertson et al., 1950)

Once the axis velocity begins to decrease, the diffusion process continues without essential change. Further entrainment of the surrounding fluid by the expanding eddy region is balanced by a continuous reduction in the velocity of the entire central region. This is the 'zone of established flow' (Figure 1).

A similar effect occurs in the energy conditions of the jet. A reduction in the velocity of the jet flow necessarily represents a decrease in kinetic energy, causing an irrecoverable loss of power. More explicitly, reaction between a jet and the surrounding fluid into which it is discharged produces a 'pronounced degree of instability' in the mixing zone. As a result, 'the kinetic energy of the oncoming flow is steadily converted into kinetic energy of turbulence', and later acts as an agent of dissipation of the kinetic energy. The analysis by Albertson et al. (1950) illustrates the principles which are, in many respects, common to most theories of jet diffusion.

2.3 The Rational Theory of Delta Formation (C. C. Bates, 1953)

In 1953 Charles C. Bates futher developed the theoretical and empirical results of Albertson et al. (1950) He reasoned that the pattern of deposition which results in the formation of deltas is closely related to the pattern of jet diffusion. His

reasoning is based on two assumptions: that a major river discharging into a lake, gulf, or ocean produces a 'free' jet flow in the water body, and that "the amount and type of sediment transport per unit mass of water are functions" of the flow-velocity of the river.

Bates (1953) considered two types of jet flow: axial (three-dimensional) jet and plane (two-dimensional) jet, depending on the relative density difference between river water and basin water. These two types of jet flow are conceptualized under three conditions of entrance flow. If river water and basin water are equally dense, the spreading of the inflowing water occurs in a three-dimensional form which constitutes an axial jet flow. On the other hand, if the density of the inflowing water is more (or less) than that of the water body into which it enters, the river water spreads in a two-dimensional way forming a plane jet flow.

Bates (1953) demonstrated that the ratio of U/Uo is a function of Dz and of X in the axial jet but a function of Dy and of X in the plane jet (Figure 2), where

U = the centreline velocity at any point

Uo = the centreline velocity at the point of issuance

Dz = the diameter of the circular orifice

Dy = the width of the slot

X = the distance downstream from the orifice

He pointed out that the 'zone of flow establishment' extends a

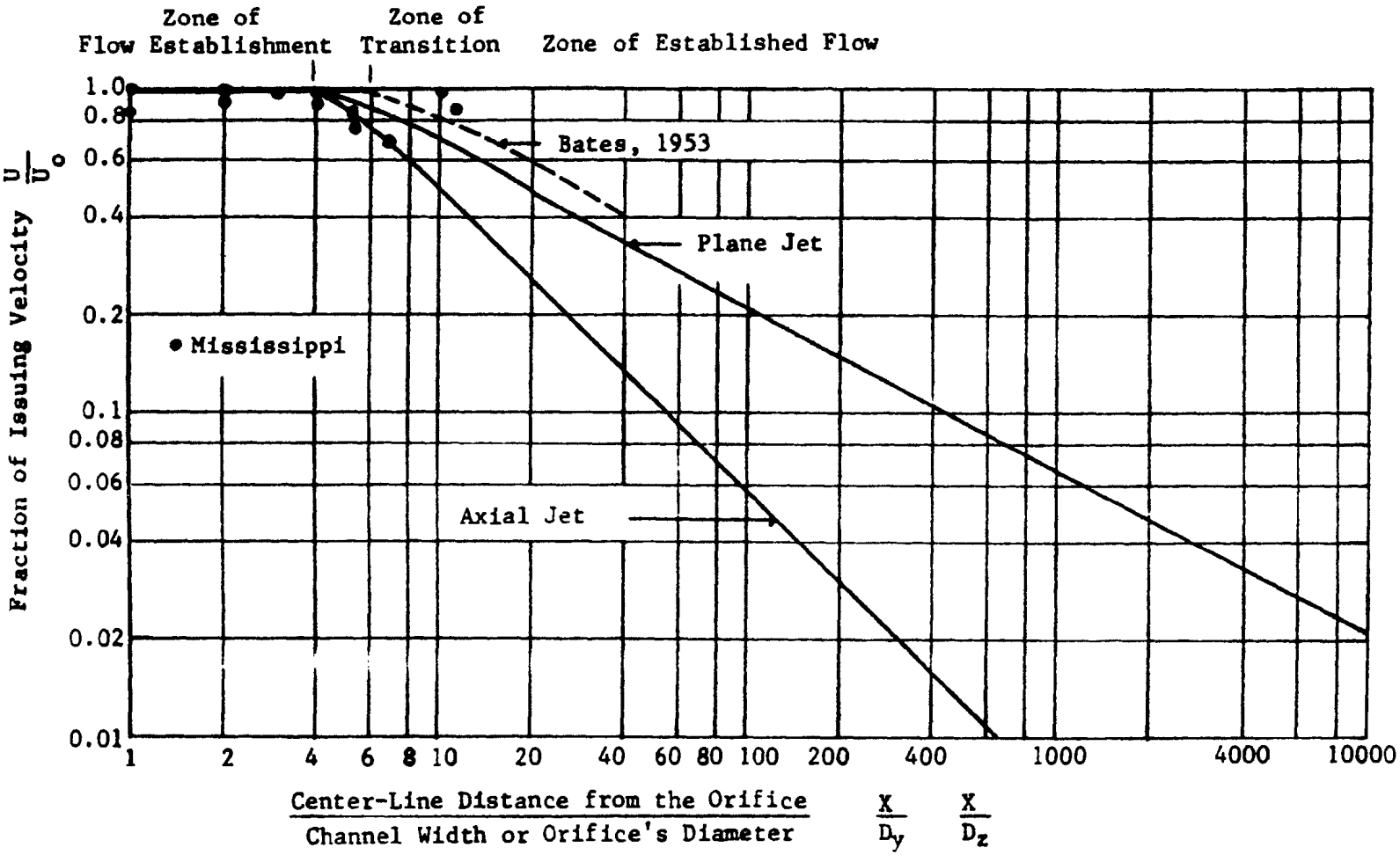

Figure 2. Center-Line Velocity in Plane and Axial Jets according to Theory, Experiment, and Field-Observations (After Bates, 1953)

distance of 4Dz (axial) and 4Dy (plane) from that of the orifice. His modifications to the presentation of Albertson et al. (1950) include the apparently arbitrary definition of 'zone of transition', and equally arbitrary limitations of the terminal areas of diffusion along the jet axis which extends to a distance of 200Dz from the orifice in the case of axial jets and 2000Dy in the case of plane jets (Figure 2). These are arbitrary in the sense that no criteria were assigned to their delimitations. Moreover, progressive deceleration of flow along the jet axis necessarily represents reduction in velocities ranging from the initial to the infinitesimal which, at least theoretically, tends to extend indefinitely.

Bates (1953) postulated that three types of inflow, each defined by the relative density difference of the river water to that of the basin, would result in a particular type of deltaic deposit:

1. Hyperpycnal inflow: This type of inflow occurs when a more dense fluid discharges into a less dense fluid-body of the same medium. The density differences are due to the content of suspended sediments, dissolved solid load, or temperature difference. The common connotations attached to this type of flow are underflows, bottomflows, or density currents.[1]

---

[1]Turbidity or density currents are usually defined (Howard, 1953; Middleton, 1965, 1966; Church and Gilbert, 1975) as underflows that owe their density difference from the surrounding water to their content of sediment in suspension rather than to temperature or dissolved load differences.

Because of the density difference, the flow expansion and diffusion is restricted only to lateral and longitudinal directions. As a result, the flow pattern is two-dimensional (plane jet).

Such inflow is possible when sediment-charged and cold river water plunges beneath the clearer lake water and flows down to the lake bottom. This type of underflow persists for a distance along the basin bottom as a clearly defined flow and is subjected to gravitational acceleration (Harleman: 1961, 1963).

Bates (1953) notes that a 'submarine delta', a deposit which forms at the mouth of a submarine canyon, results from hyperpycnal inflow conditions (Figure 3a).

2. Homopycnal inflow: This type of inflow results if the density of the inflowing river water is about the same as that of the basin water. Such a condition is thought to prevail when a river enters into a well-mixed fresh-water lake with the same water temperature. Because of equal density, the expansion and mixing of inflow river water into the basin is three-dimensional and is termed an axial jet. This type of inflow is closely related to 'interflow' which is intermediate between the underflow and surface-flow (Church and Gilbert, 1975).

The delta which forms under the homopycnal inflow conditions is the classical type with top-, fore- and

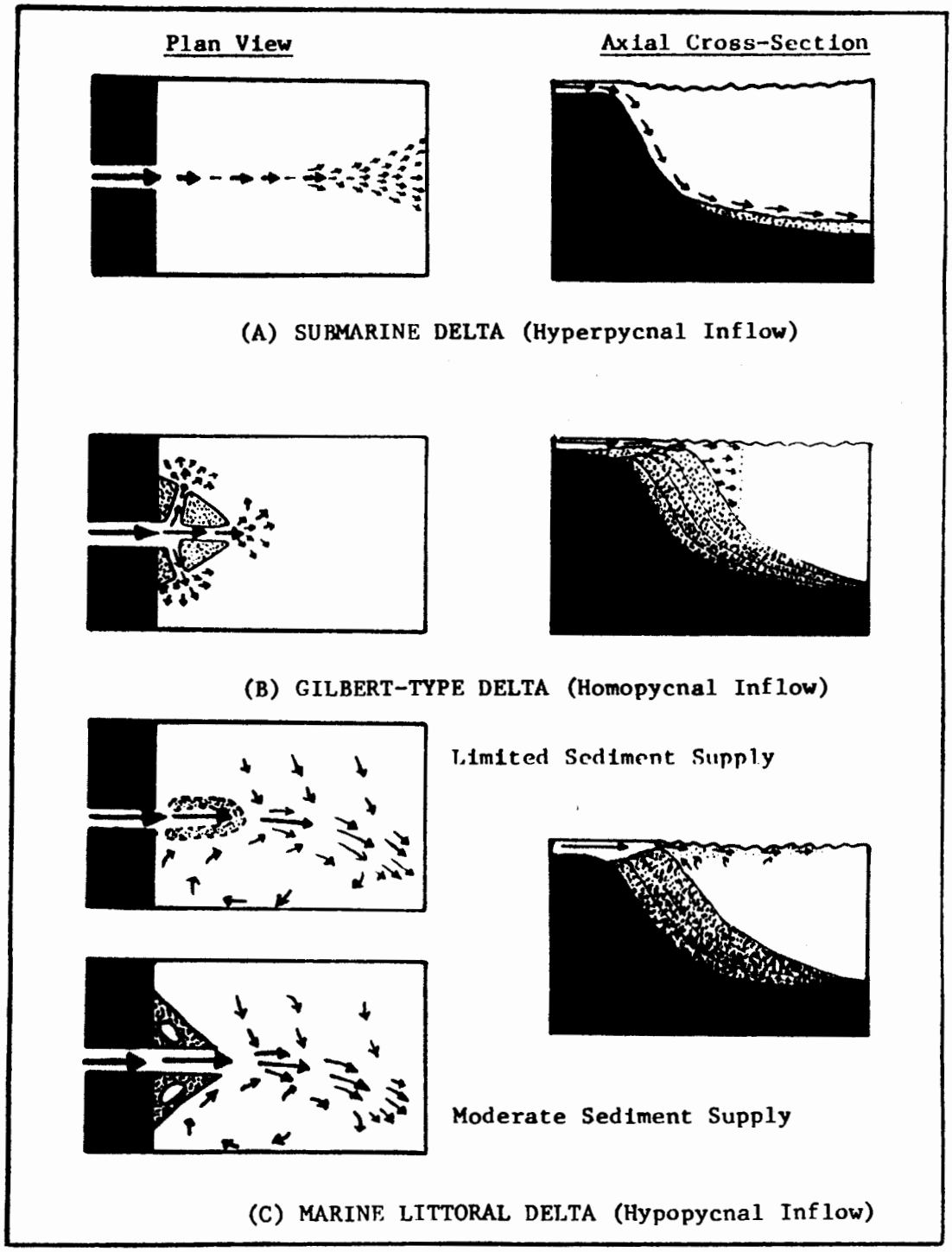

Figure 3. Schematic diagram of basic types of inflow into basins and subsequent deltaic deposits (After Bates, 1953)

bottom-set beds as described by Gilbert (1885). The axial expansion of the jet causes rapid deceleration of the outflowing fluid. This results in the development of flat topset beds flanking the channel which change to foreset beds resting at an angle of repose. Bottomset beds are formed by the deposition of the fine-grained materials in the deeper part of the basin (Figure 3B).

3. Hypopycnal inflow: Bates (1953) considered that almost all major rivers discharging into the sea or saline water would comply to hypopycnal inflow conditions. The condition implies that the saline water of the sea is more dense than the inflowing river water. This density difference inhibits vertical mixing between more dense basin water and less dense river water. As a result, the less dense river water tends to float to the top of the basin water and expands only in lateral and longitudinal directions forming a two-dimensional jet. This type of inflow is equivalent to surface flow which forms when the density of the inflowing river water is less that that of the body into which it flows, causing the river water to spread on the surface (Church and Gilbert, 1975).

According to Bates (1953) two types of deltaic deposit, depending on the magnitude of the discharge, would result in the hypopycnal situation. If the magnitude of the channel discharge is small, a lunate bar gradually builds up at a

distance of 4 to 8 times outlet width from the mouth. And if the discharge is moderate to large, a cuspate, arcuate, or bird-foot delta will form (Figure 3c).

The form of the diffusion pattern and the associated deltaic deposit were thought by Bates (1953) to depend on the relative density between the river and basin water rather than on the outlet form. This is in direct contrast to the ideas of Albertson et al. (1950).

Bates (1953) suggested that the formation of submerged natural levees would occur along the flanks of a jet in the zone of flow establishment. He further argued that, in the zone of transition, rapid deposition of bed-load would develop a transverse bar across the channel. Linkage of this transverse with the flanking levees will create a lunate bar, which eventually blocks the mouth of the outlet. If stream flow is to continue into the basin, the transverse bar or the submerged levee must be cut. As a result, the main channel must split into a system of distributaries: a typical pattern associated with the delta formation. The frequency of channel splitting will be higher in the case of an axial jet.

2.4 Limitations of the Free Jet Model of Delta Formation

Many of the basic assumptions and boundary conditions for submerged free jets are not applicable in the context of natural

deltas. Modifications and additions to Bates' (1953) proposed theory of delta formation are necessary before it is of use in interpreting sedimentation dynamics at river mouths. The following discussion of the limitations of the specified parameters is considered to be of great importance in modelling delta formation.

2.4.1 Density difference

Bates (1953) was much concerned with the relative density differences between effluent and ambient water and their influences on the axial and plane jets. This is reflected in his recognition of different types of deltas. Crickmay (1955) claimed that the jet would have a plane form of two-dimensional pattern whether or not there is a density difference. He mentioned that natural inflows are vastly more complicated than implied by the free jet model and that consideration of boundary conditions, sediment property and quantity, and mode of sediment transportation are more important and their effects are more pronounced than previously believed.

On the question of density difference, Bell found that a density contrast of 0.01% might be sufficient to cause flow separation. To Jopling (1960), a more realistic and effective contrast is in the range of 0.02% to 0.05% because of mixing and dilution. Axelsson (1967) noted, a contrast of 0.03% is

sufficient to form density currents in Lake Laitaure. All their findings suggest that vertical as well as lateral diffusion will be inhibited by density contrasts between the effluent and the ambient water. On the other hand, Bates (1953) found that the Mississippi river discharging into the saline water of the Gulf of Mexico inhibits vertical mixing because of density differences.

Density differences appear to provide somewhat stable and distinct boundaries which prevent lateral as well as vertical mixing. Although Bates (1953) is correct in emphasizing the importance of density differences in defining the nature of diffusion off river mouths, his idea that density difference inhibits only vertical diffusion has been seriously questioned. Axelsson (1967) pointed out that the relevance of jet analogy in hyperpycnal and hypopycnal inflow is invalid. He found that the density currents (caused by density difference) spread out in a way which is quite different from that of free jets. He mentioned, however, that the homopycnal inflow conditions, as proposed by Bates, will provide valuable information on the general flow conditions in the immediate vicinity of the distributary mouth, which can be related to the general trend of deposition and sorting of suspended sediment.

Wright (1970) indicated that the turbulent plane jet model is not applicable to the surface water debouching from the South Pass (Mississippi River) under normal conditions. His findings

are more compatible with Takano's (1954, 1955) generalized model of a homogenous surface layer of fresh water which spreads laterally with variable lateral exchange above the denser sea water. Under such conditions, continuity is maintained by a corresponding decrease in the vertical thickness of the fresh layer. Bonder (1969) explained the outflow trends at the Sulina mouth of the Danube River in terms of a model similar to that of Takano (Wright, 1970).

2.4.2 Submerged free jet

This condition implies that the pattern of jet diffusion is not affected by boundaries on any side of the expanding jet. Bates (1953, 1955) regarded the conditions of free jet to be valid in natural deltaic situations.

A river outlet is always bounded by the air-water interface. The presence of the air-water interface which provides a relatively frictionless boundary may be ignored. But the possible interference from low sloping basin sides and bottom cannot be dismissed. Elrod (1954) reported that a jet cannot be considered completely free of its surroundings if the cross-section area of the jet is greater than one-fifth of the total cross-sectional flow area of the region through which it passes. Jopling (1960) found that if the frontal slope over which the flow expands is less than 10°, the flow will not

separate from the boundary at all.

The effect of interference by the basin sides and bottom is vital to the concept of free jet flow, particularly for hyperpycnal and for many cases of homopycnal inflow conditions. Because such interference generates wall turbulence, it not only affects the mean velocity distribution, but greatly alters the pattern of sediment dispersal and subsequent deposition. For these reasons alone, jets off river mouths can scarcely be considered 'free'.

2.4.3 Infinite basin fluid.

The assumed infinite basin fluid is questionable because no natural basin is infinite in volume. A finite basin volume implies, however, that a return flow must be generated to replace the entrained basin water caused by the expanding jet. Singamsetti (1966) noted that, if the velocity of the return flow is small, its effect will be negligible. Jopling (1960) reported that the return flow plays a significant role in the development of tangential cross-bedding (regressive ripples) under certain conditions.

2.4.4 Stationary basin fluid

Natural fluid bodies are seldom in a state of rest. In most deltaic environments, the longshore currents, the wave actions,

and tidal influences are inevitably present. They are likely to affect significantly the pattern of jet diffusion, thus altering the depositional pattern of the entrained sediment.

Scruton (1953, 1956), on the basis of field data from the mouth of the Mississippi, reported that the effect of waves and currents was much more pronounced than Bates' (1953) analogical views on delta formation indicated. In fact, he suggested that the jet analogy be abandoned except in a small area just outside the river mouth. Wright (1970) found the surface effluent patterns of the South Pass being widely diffused and boundaries more poorly defined because of a considerable degree of influence exerted by winds and waves irrespective of their overall directions of movement. He also noted that the wind- and wave-induced surface turbulence increases lateral diffusion in a noticeable way.

2.4.5 Form and stability of the outlet

It is well known in hydrodynamics that the pattern of jet diffusion, either in plane or axial form, depends on the geometry of the efflux. Albertson et al. (1950) treated both the infinite slot (two-dimensional mixing) and the circular orifice (three-dimensional mixing). To this, Elrod (1954) added the rectangular outlet where the expanding jet is of the axial type. The outlet form seems to have obvious implications in the delta

situation because the closest approach to a natural river outlet is rectangular in shape as discussed by Elrod. This point was critically raised by Crickmay (1955). In spite of this criticism Bates (1953, 1955) defined the pattern of jet diffusion strictly by mixing properties of the fluids having relative density differences and argued that the density contrast and boundary effects would restrict the hyperpycnal and hypopycnal inflows to plane jet form.

Deltas are composed almost entirely of movable sediment and are associated with some degree of feedback between process and response. The adjustment of process and form in the presence of continuous deposition of sediment causes the channel outlet to migrate basinward. From this consideration alone, the assumption of a stable orifice in a natural situation is questionable.

Bates' (1953) infers that maximum sediment deposition along the margins of the zone of flow establishment and within the transition zone causes a lunate bar around the outlet. The lunate bar thus formed reduces the flow area for outflow which is, in turn, adjusted by an overall increase in the channel width through the splitting of the master stream into two or more distributaries. He further suggested that the velocity tends to decrease over the distributary mouth bar.

Bates' description of the velocity decrease over the distributary mouth bar is not in agreement with the findings of Scruton (1956) who found that velocity increases over the

distributary mouth bar. Jopling (1963) reported that these bars did not form in his laboratory studies. He noted, however, that jet flow was initiated in the 'rapidly varying flow regime' at the top of the foreset beds.

Scruton (1956) futher discussed that the formation of a distributary mouth bar results from the bed load deposition which is conditioned by vertical flow separation. Such deposition occurs at the point where flow separation first begins. Jopling suggests, that the deposition of bed load will take place even before this point because of reduction in the channel flow velocity associated with the M1 backwater curve effect.

It is important to note that lateral separation may occur before vertical separation is possible in the homopycnal situation. In addition, continuous deposition of sediment will cause shifting of the channel outlet. Bonham-Carter and Sutherland (1967) have considered this in their computer simulation model of deltaic sedimentation, but the possibility of vertical separation was neglected in their study; they assumed that hypopycnal conditions would form a two-dimensional jet. Like Bates, they also ignored the consideration of bed load.

The above discussion on the question of outlet-form and stability illustrates that there are greater complexities concerning the true pattern of flow than are normally assumed. A

model ignoring such considerations will probably generate errors of large magnitude in describing the outflow pattern and the subsequent deposition.

2.4.6 Steady, uniform water and sediment flow.

In geomorphology, the analogy between landform evolution and an open system in a steady state[2] is often drawn for the sake of statistical-mechanical formulation. Many geomorphologists, as noted by Chorley (1962), have described certain landforms as an open system in steady state. The steady state is, however, considered to depend on conditions imposed by the boundaries of the system, and is maintained only as long as external conditions remain unchanged. Abrahams (1968) conceived the steady state as "rarely one of precise poise, and continual fluctuations about the most probable condition can be expected in accordance with the magnitude and frequency of the fieldforce and overshooting of feedback mechanisms". Gilbert (1880) mentioned that every segment of a stream affects those below it by discharge and debris. An important difference between natural conditions and the stable canal theories was drawn by Dozier (1973). In most rivers there is a great deal of variation both

---

[2]Dozier (1973) broadly defined an open system as "one which can exchange matter and energy with its surroundings, and a steady state exists when the system remains constant in composition, even though continuous irreversible processes involving the import and export of matter and energy take place."

in discharge and sediment load operating over a range of time scales. In fact, a state of randomness of variability manifested with the feedback mechanisms of process and form is more likely to be present in the deltaic situation than the assumed state of uniformity. For this reason, Bates' (1953) assumption of steady and uniform velocity in the natural stream is not valid.

The common vertical velocity profile of an open channel is logarithmic in form. Thus, a constant velocity core in the zone of flow establishment, as hypothesized by Bates (1953), cannot be regarded as valid. Bonham-Carter and Sutherland have recognized this in their model of delta formation. Their solution has been to assume that plane jets with outlet velocities determined by the height above channel bed can be piled on top of each other to give a reasonable picture of the resultant vertically asymmetric mean velocity pattern. The effect of the logarithmic velocity on turbulent diffusion is important in the homopycnal situation.

In the studies of open channel flow and fluvial morphology there has been a search for the dominant discharge which controls the channel geometry. Wolman and Leopold (1957) and Nixon (1959) considered the bankful discharge as the dominant discharge. Kuiper (1960) suggested that the bankful stage is the dominant control in the formation of deltas. A similar approach may be used in defining discharge for the jet diffusion model.

Both the character of sediment transport and the flow pattern is important in delta formation. The bulk of materials in most rivers is transported in suspension or as bed-load and their character and quantity also vary significantly with time and space. The effect of these variations on the pattern of flow diffusion is considerable. Bates (1953) assumed that the amount and type of sediment transported per unit mass of water are direct functions of the velocity of the stream flow. But his analogy ignored bed load transport. Even then, his assumed conditions of suspended load are not very meaningful in the natural situation. This is evident from the findings of Benson and Thomas (1966). They plotted suspended sediment discharge against stream discharge for nine rivers in the U.S.A. The result suggests that, although a modal value usually exists, almost the same amount of suspended load is transported over a large range of discharges. In addition, Axelsson (1967) pointed out that it is not necessarily the homopycnal inflow which results in the formation of foreset beds in deltas, but rather they are formed when bed-load transportation occurs right up to the mouth. Jopling (1963) took a similar view.

Singamsetti (1966) in his study of sediment diffusion within the jets found that, because of inertial and gravitational effects, the eddy diffusivity for sediment will usually differ from the eddy diffusivity of water. The ratio of these two diffusivity rates was found to be dependent on flow

and particle Reynolds Numbers. It was concluded that the particle inertia would cause the sediment to lag behind the fluid. However, he suggested that, because of circular motion in eddies, small particles (within the Stokes's range) will tend to be thrown out in front of the fluid particles and thus will tend to move down the axis more quickly than the fluid. Consideration of sediment diffusion in jets, and thus the depositional patterns, need to be related to particle and fluid diffusivities.

2.5 Other Contributions to the Theory of Delta Formation

In addition to the preceding discussion, the following contributions by different authors are considered relevant in the present context of delta formation.

2.5.1 G. F. Bonham-Carter and A. J. Sutherland

Bonham-Carter and Sutherland (1967) developed a computer-simulation model for deltaic deposition utilizing the jet analogy, which essentially dealt with the variables important in the constructive phase of delta building. They calculated the trajectories of sediment particles which were subjected to the forward movement of jet flow and settling due to gravity. Their findings suggest that the shape and foreset slope of the delta depend on the discharge and sediment grain

size. They also concluded that branching of delta distributaries is strongly influenced by the relative rate of sedimentation at the front of the delta, in contrast to that at the margins of the flow regions.

2.5.2 L. S. Borichansky and V. N. Mikhailov

Borichansky and Mikhailov (1966) conducted experiments from which they derived equations describing the lateral velocity field. They recognized four factors which affect current spreading: 1) The greater the depth in a basin, the narrower the lateral extent of the flow; 2) as the depth of the basin increases, the transition reach of the flow becomes narrower; 3) a submerged bar causes a sharp widening of the flow; and 4) the greater the bottom-roughness of the basin, the more swiftly the bar widens.

2.5.3 A. V. Jopling.

Jopling (1960, 1962, 1963, 1963, 1965) carried out several experiments on vertical flow separation. He calculated deposition on the delta front from a consideration of grains suspended in the inflowing stream, and the grain size distribution and fall velocities assuming quasi-laminar flow. Jopling's experimental results demonstrate that the diffusion boundary, representing the limit of penetration of the eddies of free-turbulence shear, is tilted at an angle of approximately

5.5° to the horiztontal (Figure 4). The velocity in the zone of no diffusion, however, decreases away from the delta lip, accompanied by a compensatory rise in the water level. Jopling (1960, 1963) used depth-ratio[3] and dip angles in front of the distributaries in the study of flow separation. He found that when the depth-ratio is low and dip angle high, the abrupt vertical boundary expansion causes the flow to separate from the bottom, and the flow pattern over the foreset slope bears a similarity to that of a three-dimensional jet. And if the depth-ratio is high and the dip angle low, the flow separation is only lateral, forming a two-dimensional jet.

2.5.4 R. J. Russell.

Russell (1967) viewed the jet flow as a two-dimensional form. He stated that the river outflow continues forward as a result of the initial momentum and flares laterally into a lake or sea, because of discontinuity of confinement imposed by the fixed banks of the river. The flaring of the outflow increases the area between threads of most intense turbulence and exchange. The exchange process sends most of the entrained materials toward the margins of quiet water, which then build submarine natural levees on the outer sides of each thread. He further pointed out that the flaring of outflow is also

---

[3]Depth-ratio (Jopling; 1960, 1963): the ratio of distributary mouth depth to that of the basin in front of the distributary.

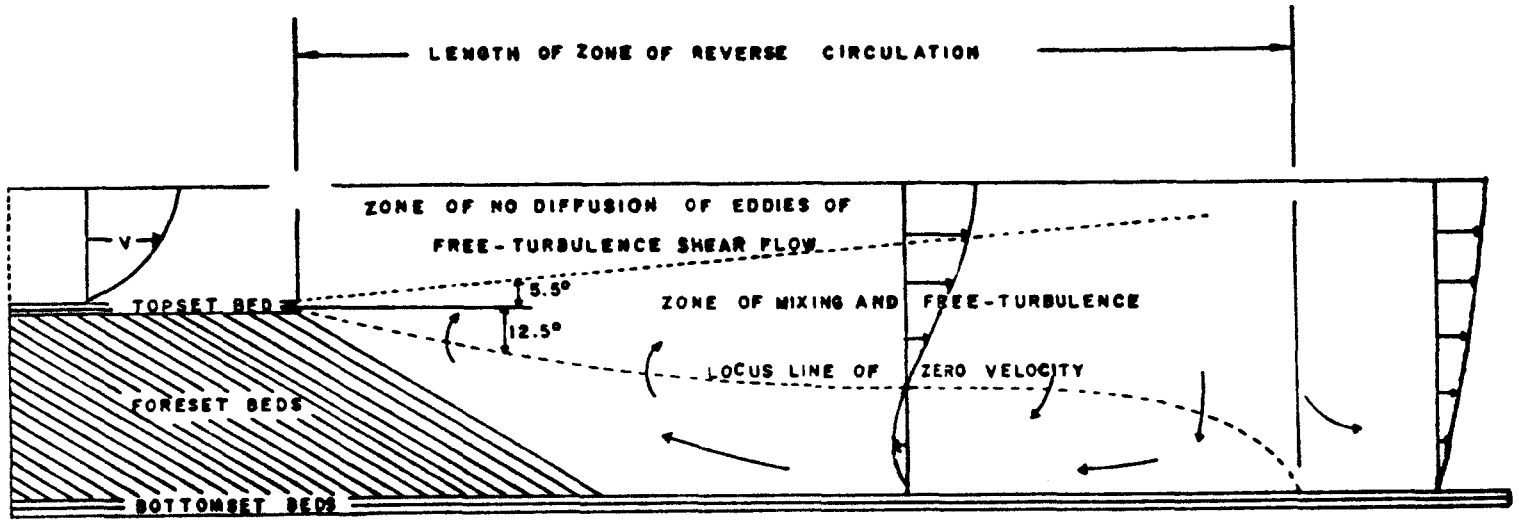

Figure 4. Schematic representation of the zonal terminology for flow expansion over a tabular unit of cross-bedding deposited as a small laboratory delta (After Jopling, 1964)

associated with the widening of the mid-channel water area where reductions in flow velocity are evident. As a result, deposition occurs at the mid-channel, creating a shoal. The channel divides around the shoal into two distributaries, each of which develops its marginal threads of maximum turbulence. The process of subdivision of each new channel, as noted by Russell (1967), continues in geometric progression along with the delta growth if unopposed by wave actions or longshore currents (Figure 5).

2.6 Conclusion

Although many critical views of Bates' (1953) model are presented in the preceding discussion, these do not detract from the fundamental contribution that he has made to the study of deltas. Real delta-building processes are very complicated, involving many factors rather than a single dominant one. It is important to understand the effective roles of the interdependent and interacting variables such as hydraulic factors, sediment load on the bed and in suspension, sediment diffusivity, basin morphology, off-shore energy conditions, etc. A useful first step towards this end is to study some of them in isolation under controlled conditions.

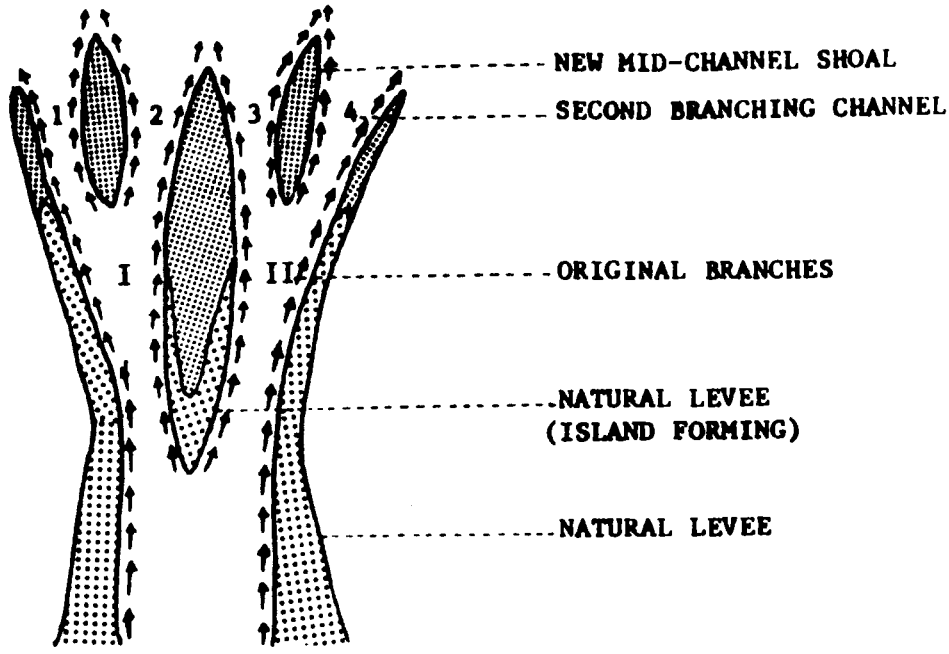

LATER STAGE OF CHANNEL SUBDIVISION

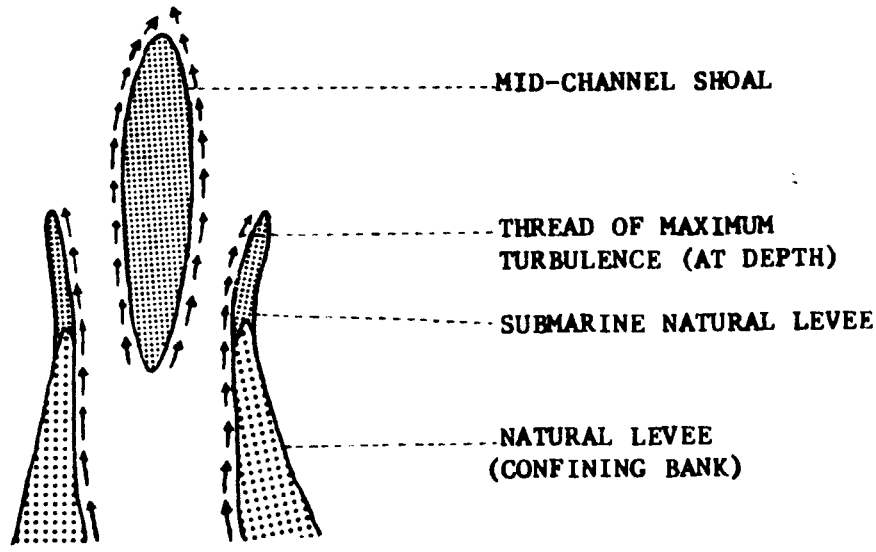

ORIGINAL BRANCHING OF A DELTA

Figure 5. Subdivision of river-mouth channels
(After Russell, 1967)

III. Assumptions and Hypotheses

3.1 Assumptions and Hypotheses:

The depositional regime of a channel mouth can reasonably be assumed to be governed by the water discharge and sediment transport conditions there. Bates (1953) related the depositional regime directly to jet diffusion which was thought to depend on the relative density difference between the river and basin water. Extending Bates' ideas, this study uses a small-scale laboratory experiment which has been designed to study delta morphology in a variety of discharge and sediment transport conditions.

This experimental study is a simple process-response model of delta formation. The process elements include water discharge (and thus the flow velocity and flow depth) as the independent variable representing the flow scale as energy factor, and rate of sediment transport as the material supply factor. The response element (the resultant yield) is the delta morphology, which is considered as the dependent variable. All other process elements such as channel slope, channel width, sediment properties, water density, water temperature, basin energy conditions (waves, tides, and currents), and basin geometry and

slope are assumed to be constant throughout the experiment. Experiments were performed in a homopycnal inflow situation. River sediments ranging from sand to fine silt were used; sediment properties were assumed to be unaltered between the runs. A series of runs were made to form deltas under different flow regimes and sediment transport conditions.

An analysis of the variation in discharge and in sediment transport rate in forming a series of deltas, even in a situation where most of the physical parameters are relatively constant, may provide altogether different ideas into the depositional regimes than those proposed by Bates. Accordingly the following hypotheses are tendered:

1. Delta morphology does not conform to the axial jet diffusion model.
2. Delta morphometry is functionally related to the changing flow scale and rate of sediment transport conditions.
3. The submerged natural levees, shoals, distributaries and the small-scale bed-forms are superficial features, characterized by the flow pattern and mechanics of sediment movement developed atop the delta paltform because of the mutual interaction between the flow and form.
4. Variations in the distribution of the grain size and the internal structure of the deltas are indicative of flow scale and sediment transport mechanisms prior to the deposition.

5. Shifting and structural deformation of the deltas are closely related to the intensity and scale of turbulence that forms within the main forward flow.

These hypotheses stress the interdependency and interaction of processes and forms; an intricate association conditioned by the changing flow scale and sediment transport conditions.

IV. Experimental Procedure

4.1 The Equipment

The present study is a small-scale experiment under laboratory conditions. A flume system consisting of a basin, rectangular open channel and hopper, was used to build several deltas in a variety of water discharge and sediment transport conditions (Figure 6). It was constructed in the geomorphology laboratory at Simon Fraser University. The design and engineering aspects of the flume are discussed in some detail in Appendix A.

4.1.1 The flume channel

The flume used in the experiment was a 100 cm long, 10.2 cm wide and 10 cm deep rectangular open-channel. Its sides and bottom were capped with very thin metallic sheets. To maintain unidirectional flow and to eliminate water loss, the upper end of the channel was closed. Tap-water, from two water-main outlets available inside the laboratory, was conveyed to the channel head through flexible hoses. In order to diffuse the initially high inertia of the flow, adjustable baffles were

placed at the flume entrance.

The entrance flume was supported by a block of wood and held fixed by weight supports (bricks) over and across the channel side-walls. This arrangement helped in maintaining the channel slope at a constant value of 0.002 and reducing the overall vibration of the flume system. The flume-channel mouth was joined with the basin at a 10 cm negative step between the channel bed and basin bottom (Figure 6).

4.1.2 The flume basin

A 300 cm long, 120 cm wide, and 33 cm deep flume basin was used in the experiment to accommodate the delta sediments. From the entrance flume mouth, for a distance of 240 cm, the basin-bottom was raised by 10 cm by fixing foam slabs to the basin floor. Foam, being permeable in nature, permitted rapid drainage of water after a run, leaving the delta in a relatively dry state for measurement and sampling. The foam surface was marked with a 5 cm x 5 cm grid (48 x 24) which provided a locational reference for all measurements inside the basin.

The water level of the basin corresponding to channel depth was maintained by a 22 cm high weir at a distance of 280 cm from the channel mouth. During the run, water spilled over the weir and was drained out through two pipes connected at the basin bottom. In addition, eight pipe-connections were made to remove

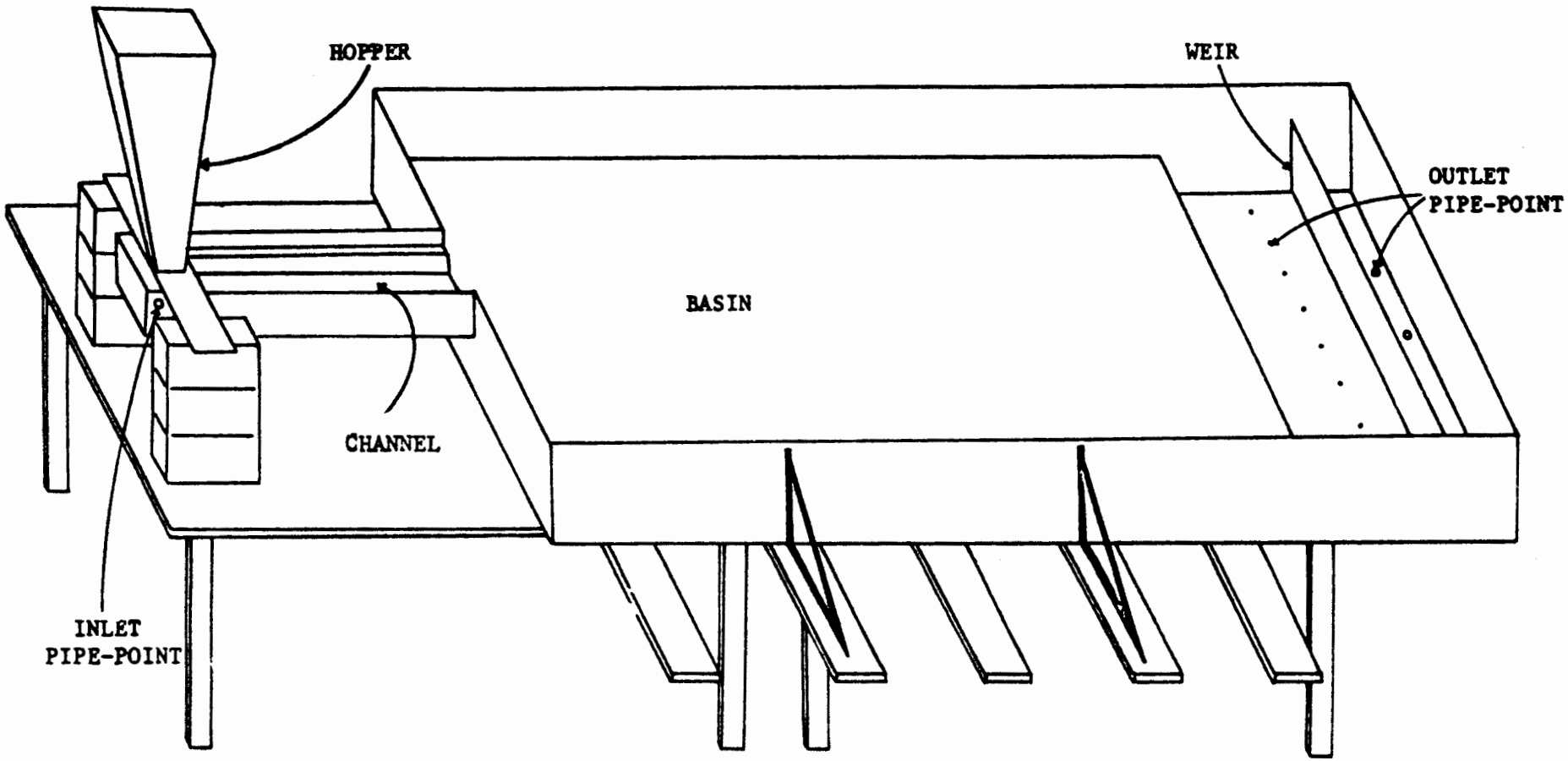

Figure 6. Diagrammatic representation of the flume system

water from the basin after a run; these were attached to the basin bottom at the weir (Figure 6).

4.1.3 The hopper

A 65 cm high hopper with a circular hole (dia. 3.4 cm) at the bottom, was used to add sediment to the flume system. The hopper was located near the head water so as to facilitate better mixing of the sediments at the basin entrance. A metal plate with six holes was used to regulate the sediment-feed into the flume. River sediments with mean grain-size of 0.365 mm were used in the experiment. Sediments were, in most cases, oven-dried and recycled.

4.2 The Measurement Instruments

To investigate the hypotheses, quantitative information concerning velocity-field and discharge, morphometry and structure of the deltas, and sediment size distribution characteristics was recorded. Other measurements such as slope aspects and water temperature were also recorded throughout the experiment. In addition, notes, sketches and photographs covering certain aspects of the experiment were made and, for the most part, treated qualitatively.

4.2.1 Velocity-field and discharge measurement

Although there are a number of basically different methods available for measuring the flow velocity of water, there are situations where, for one reason or another, the choice is limited to a few. The basis for making a specific selection is determined by the required precision, cost and technicalities, and the physical dimensions of the flow field. Because of the short channel reach adopted here, and of the shallow flow-depth and overall need to measure velocity at points, a Pitot static tube was used to determine the velocity variable.

When a Pitot static tube is immersed at a required flow depth, a differential water rise is indicated by the two connected heads of the tube (for detailed discussion, see Appendix B). One of these heads is known as total head (sum of the pressure-head and velocity-head) and the other is the pressure-head. The difference in water rise between the heads of the Pitot tube is the velocity-head and is represented by h. The velocity, V, is calculated from the relation: $V = \sqrt{2gh}$, where g is acceleration due to gravity (980 cm/sec).

Computation of the flow velocity of the channel was made through the determination of the velocity-head at ten locations across the channel width. The two-point method, measuring the heads at 0.2 and 0.8 of the floor depth from the surface water, was adopted to determine the velocity head. The average

velocity, V, was determined by taking the arithmetic mean of the velocities at the ten locations.

The discharge was computed by employing the equation, Q = VA, where V represents the average velocity and A is the cross-sectional area (depth x width) of the channel.

Using the Pitot static tube, the velocity at different locations of the jet flow was calculated. The measurement locations were made along the longitudinal, lateral and vertical (normal to centre-line) directions, and are discussed in Appendix B.

4.2.2 Morphology and internal structure

Employing a 35 mm camera (Pentax-MX), extensive photo-coverage was made to record the delta morphology, the nature of bed-forms, and any other features produced by the flow. The side and frontal slopes of the delta were measured with an Abney level. Then a slow process of delta dissection began. The dissection was carefully done using a knife to expose a longitudinal section (along the central line) as well as a lateral section (one half at a time). This has provided the basis for mapping the whole delta, showing areal extent of the topset, foreset and bottomset beds. In addition, measurement of thickness of the accreted deposits was made using a graduated ruler. All records and measurements were referred to the grid

network. This procedure is discussed further in Appendix B.

4.3.3 Sediment sampling and grain-size analysis

Samples of sediment were taken at different locations along the central line with a tea-spoon. The samples were obtained with the dissection of the longitudinal section covering topset, foreset and bottomset materials. They were wrapped in paper using codes and dried at room temperature.

Sediment samples were weighed on an electronic balance (calibrated in grams to read to the fourth decimal place), and passed through the visual-accumulation tube located inside the laboratory for determining the sediment-size distribution. The size analysis was based on a stratified sedimentation system in which a sample (weighing 4 gm to 7 gm) was introduced at the top of the transparent settling tube containing tap-water. A manually operated pen was used to trace the height of the sediment, accumulating in the contracted section at the bottom of the tube, on a chart which moved at a uniform speed. The procedure is discussed in some detail in Appendix C.

4.3 The Experimental Procedure

Throughout the experiment, two-factor interactions were performed in order to examine their influence on delta deposition. The factors were discharge and rate of sediment

transport. The discharge was varied from 295 cm^3 /sec to 1377 cm^3 /sec. Within this range, a selection of five discharges were made. Two of these discharges were in the supercritical flow stage, two others in the subcritical flow stage, while the fifth one was in the transitional regime. Treatment of the six sediment transport rates, ranging from 4.67 gm/sec to 42.50 gm/sec, was made at a constant total supply of 5.1×10^4 gm sediment in each run.

Thirty runs were made which combined five discharge and six sediment transport conditions. Because of a high proportion of sediment load per unit volume of water-discharge, two runs are excluded in the present study. That is, only 28 test runs are included in the present study. The runs were numbered from 1 to 28, and grouped into five series (A to E). Series were identified by a constant discharge condition with variation in the sediment transport rates between runs. For example, in series A, six runs were made at a constant discharge of 1377.00 cm^3 /sec treating six different sediment transport rates. The same format was followed in the succeeding series of runs.

The simultaneous arrangement of the two variables, namely the discharge and sediment transport rates, was treated once in every run. In other words, replication or repeats of any of the runs was not considered in the experiment.

During the experiment, the basin was initially filled with tap-water to the desired level. A time lapse was allowed to

bring the basin water to a relatively quiet stage by stopping tap flow. Water temperature in the flume was recorded. With the reopening of the tap flow, a time lapse was again allowed to form a definite flow pattern in the basin. When a persisting flow pattern was found to exist, flow in the channel was adjusted to a selected discharge by the regulatory device at the tap-points. Measurements of velocity-field were obtained for this sediment-free flow condition. Then sediment was fed to the flume entrance through a single opening of the hopper system. As soon as feeding of the total quantity (5.1×10^4 gm) which was constant in every run) had been completed, the channel flow was stopped by closing the taps and the bottom connection-pipes were opened to remove the basin water. In order to maintain relatively uniform flow from the tap-points, all experimental runs were performed after 10 o'clock in the evening, when head variation was minimal.

After removing water from the flume basin, a time lapse was allowed to bring deposits to a relatively dry state. Following this, the measurements and records of the deltaic deposition were made as discussed in the preceding section.

V. Presentation and Analysis of the Data

5.1 Hydraulic Geometry of Flow Expansion and Delta Formation

The present chapter outlines an analysis of the sedimentation pattern observed in the different phases of the experiment. Because of the limited range of flow conditions and the nature of flume material, the analysis is restricted in scope. Throughout the experiment certain common trends in the flow field and flow structure were observed to persist regardless of discharge conditions; these are presented below.

Tables 1 and 2 (grid references are shown in figure 7) show the distribution of velocities along the longitudinal, lateral, and vertical axes of the jets. Throughout the experiment the flow-velocity was determined in the sediment-free flow conditions. The data strongly suggest that the pattern of jet diffusion is three-dimensional (axial) and subject to boundary effects. An overall dynamic similarity is also evident from the same table. This implies that the flow field and flow structure of the jets, in a wide range of discharge conditions, are geometrically similar. Figures 8a and 8b illustrate the generalized picture of jet expansion which closely represents most of the flow geometries observed to form in the present

Table 1

Velocity distributions of the jet

Longitudinal and lateral directions

Grid References	Series-A cm/sec	Series-B cm/sec	Series-C cm/sec	Series-D cm/sec	Series-E cm/sec
M/0	100.95	52.38	43.15	72.07	83.41
M/4	100.95	52.38	43.15	72.07	83.41
L/4	70.70	35.69	29.70	50.48	57.72
K/4	00.00	00.00	00.00	00.00	00.00
M/7	100.95	51.44	42.00	72.07	83.41
L/7	60.22	31.30	24.25	43.15	49.50
K/7	9.90	***	***	***	***
J/7	0.00	0.00	0.00	0.00	0.00
M/11	82.82	42.00	34.29	58.57	67.87
L/11	57.72	29.70	24.25	39.60	46.43
K/11	38.34	19.80	14.00	24.25	31.30
J/11	***	***	***	***	***
I/11	0.00	0.00	0.00	0.00	0.00
M/15	76.68	39.60	31.30	54.22	62.61
L/15	55.12	28.00	19.80	38.34	45.36
K/15	35.69	17.15	14.00	24.25	29.70
J/15	19.79	9.90	***	14.00	17.15
I/15	***	***	***	***	***
H/15	0.00	0.00	0.00	0.00	0.00
M/20	58.56	29.70	24.25	40.82	48.50
L/20	51.05	26.19	17.15	35.69	42.50
K/20	39.60	19.80	14.00	26.19	31.30
J/20	29.70	14.00	9.90	19.80	22.14
I/20	19.80	9.90	***	14.00	17.15
H/20	9.90	***	***	***	***
G/20	0.00	0.00	0.00	0.00	0.00
M/25	50.48	24.23	19.80	35.69	40.82
K/25	39.60	17.15	17.15	28.00	32.83
I/25	22.16	9.90	***	14.00	17.15
G/25	17.14	***	***	9.90	14.00
E/25	0.00	0.00	0.00	0.00	0.00

(Continued on next page)

Table 1 (continued)

Velocity distributions of the jet

Longitudinal and lateral directions

Grid References	Series-A cm/sec	Series-B cm/sec	Series-C cm/sec	Series-D cm/sec	Series-E cm/sec
M/30	46.43	22.16	19.80	32.83	38.34
K/30	39.60	17.15	14.00	26.19	32.83
I/30	32.83	14.00	9.90	22.14	26.19
G/30	19.80	9.90	***	14.00	17.15
E/30	14.00	***	***	9.90	9.90
C/30	14.00	***	***	***	***
M/35	43.15	22.14	17.15	31.30	35.69
M/40	40.82	19.80	17.15	29.70	32.83
M/45	39.60	19.80	17.15	28.00	31.30

experiment.

Throughout the experiment the lateral expansion of the jet, through the free-flow region (not affected by the basin sides), was found to diverge at an angle of 16 +/- 3°. In other words, the jets appeared to spread laterally at an angle which increases with the distance from channel efflux section. This does not demonstrate satisfactory agreement with the analytical-experimental findings of Albertson et al (1950) and Bates (1953) who conceived a constant angle of jet spread. The likely reasons for this anomaly seems to lie in the conditions of finite volume of basin water considered in the present experiment.

The condition of finite volume of basin fluid was found to

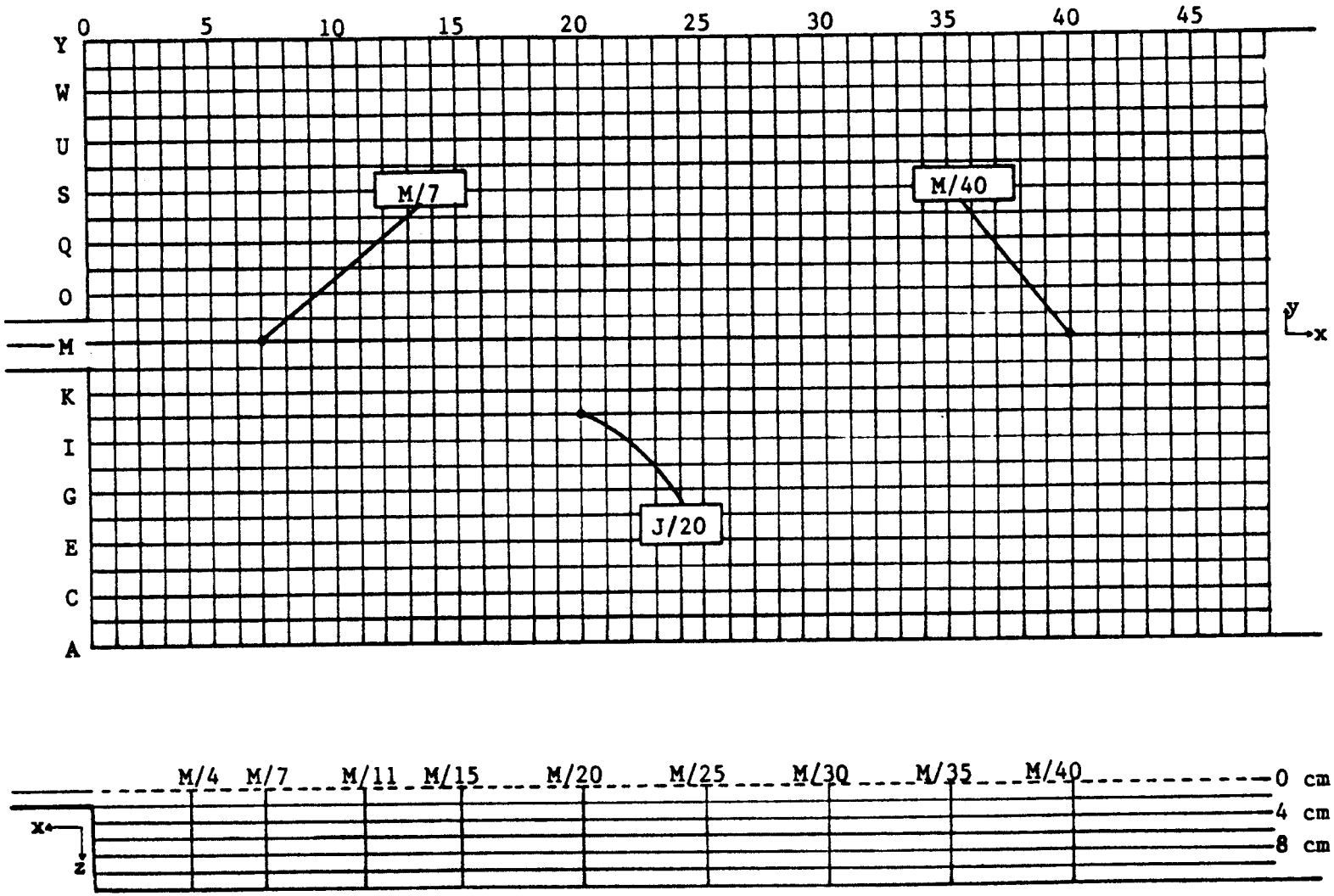

Figure 7: Diagrammatic representation of the grid-network

Table 2

Vertical Distributions of Velocities.

Grid Ref	Depth cm	Series-A cm/sec	Series-B cm/sec	Series-C cm/sec	Series-D cm/sec	Series-E cm/sec
	0.4	100.95	52.38	43.15	72.07	83.41
M/4	2.0	80.42	42.00	34.24	57.72	66.40
	4.0	26.19	14.00	9.90	17.14	19.80
	6.0	0.00	0.00	0.00	0.00	0.00
	0.4	100.95	51.44	42.00	72.07	83.41
	2.0	75.39	38.34	32.83	54.22	62.62
M/7	4.0	45.36	22.13	19.80	32.83	37.04
	6.0	14.00	9.90	***	9.90	9.90
	8.0	0.00	0.00	0.00	0.00	0.00
	0.4	82.82	42.00	34.29	58.57	67.87
	2.0	68.58	35.69	29.69	48.49	56.86
	4.0	50.48	29.19	22.13	35.69	40.82
M/11	6.0	34.29	17.14	14.00	24.24	28.00
	8.0	9.90	***	***	***	9.90
	10.0	0.00	0.00	0.00	0.00	0.00
	0.4	76.68	39.60	31.30	54.22	62.61
	2.0	50.47	26.19	22.13	35.69	40.82
M/15	4.0	35.69	19.79	17.14	26.19	29.69
	6.0	24.25	14.00	9.90	17.14	19.79
	8.0	14.00	***	***	9.90	9.90
	10.0	***	***	***	***	***
	0.4	58.56	29.70	24.25	40.82	48.50
	2.0	46.43	24.25	19.79	32.83	38.34
M/20	4.0	35.69	17.14	14.00	24.25	29.69
	6.0	26.19	14.00	9.90	19.79	22.13
	8.0	19.79	9.90	***	14.00	17.14
	10.0	9.90	***	***	***	***
	0.4	50.48	24.25	19.80	35.69	40.82
	2.0	40.81	22.13	17.14	29.69	34.29
M/25	4.0	31.30	17.14	14.00	22.13	24.25
	6.0	22.13	9.90	9.90	17.14	17.14
	8.0	14.00	***	***	9.90	9.90
	10.0	***	***	***	***	***

(Continued on next page)

Table 2 (continued)

Vertical Distributions of Velocities.

Grid Ref	Depth cm	Series-A cm/sec	Series-B cm/sec	Series-C cm/sec	Series-D cm/sec	Series-E cm/sec
	0.4	46.43	22.16	19.80	32.83	38.34
M/30	2.0	32.83	17.15	14.00	24.25	28.00
	6.0	17.14	9.90	***	9.90	14.00
	10.0	***	***	***	***	***
	0.4	43.15	22.14	17.15	31.30	35.69
M/35	2.0	28.00	14.00	9.90	19.79	22.13
	6.0	9.90	***	***	***	9.90
	10.0	***	***	***	***	***

be associated with the phenomenon of reverse circulation of flow. With the diffusion of the jet flow the fluid from the surrounding regions was observed in a process of continuous entrainment. Continuity considerations demand that this entrained fluid be replaced. These conditions generate a reverse flow circulation on either side of the expanding jet. Importantly, the entrainment of water into the jet was noticed to occur near the channel mouth which was being replaced or balanced by the water flow from the region where the free jet impinged upon the basin sides.

Figure 8a also demonstrates the limit of the zone of flow establishment. The longitudinal extent of this was measured to terminate at an approximate distance of 35 cm from the mouth of the channel. This means that the turbulent mixing from both sides has penetrated the centre-line at a distance which is equal to 3.40 times the channel width. Within this zone, a

well-defined central core, or the zone of no diffusion, was found to exist. At a low discharge, the core boundary was distinctly visible as an isosceles triangle separating this zone from the turbulent mixing of the zone of flow establishment. The zone of no diffusion, although present, was obscured by the surface undulations (standing waves) formed at a higher flow regime. The zone of no diffusion was described by Laursen and Toch (1959) and Jopling (1960, 1962) as the undisturbed part of the free boundary layer which overlies but is unaffected by the free-turbulence shear flow from below. It is evident from the table that the central core is marked by uneven velocity-distributions along the lateral axis, but along a straight-line path (parallel to the centreline) velocities are relatively constant. This seems to support the above view but invalidates the assumption of constant core-velocity as conceived by Bates (1953).

As noted in the experiment, the zone of flow establishment was replaced by one of flow expansion whose free boundary lines impinged upon the basin sides at a distance of 157 cm from the efflux-section. The velocity characteristics in this zone of established flow are shown in Figure 8a. The velocity at any section, normal to the jet axis, closely resembles a Gaussian curve whose standard deviation is a linear function of the distances from the channel mouth. Such trend of velocity distribution was roughly bounded by a line located at an

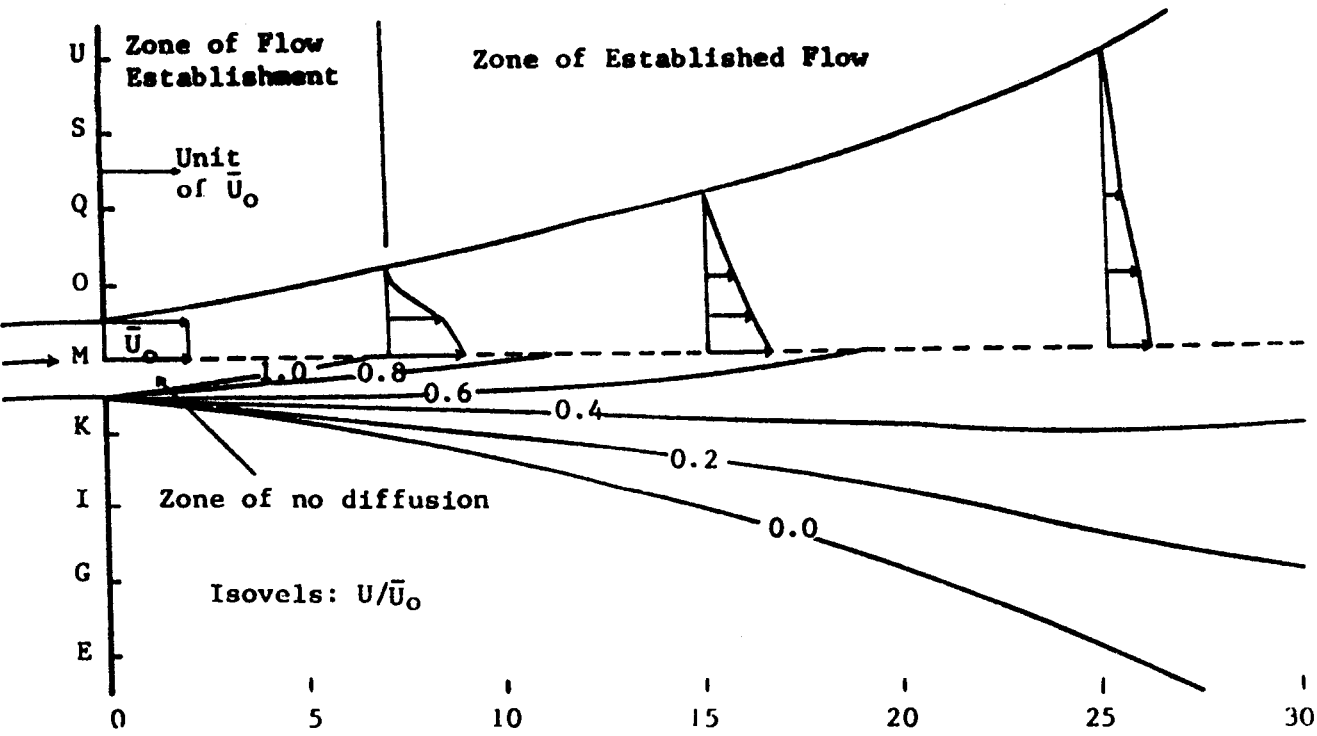

Figure 8a. Isovels and velocity structure of axial jet in plan view. Scale is 1 cm to 10 cm.

Figure 8b. Vertical velocity prifile of axial jet (along center-line). Scale is 1 cm to 10 cm.

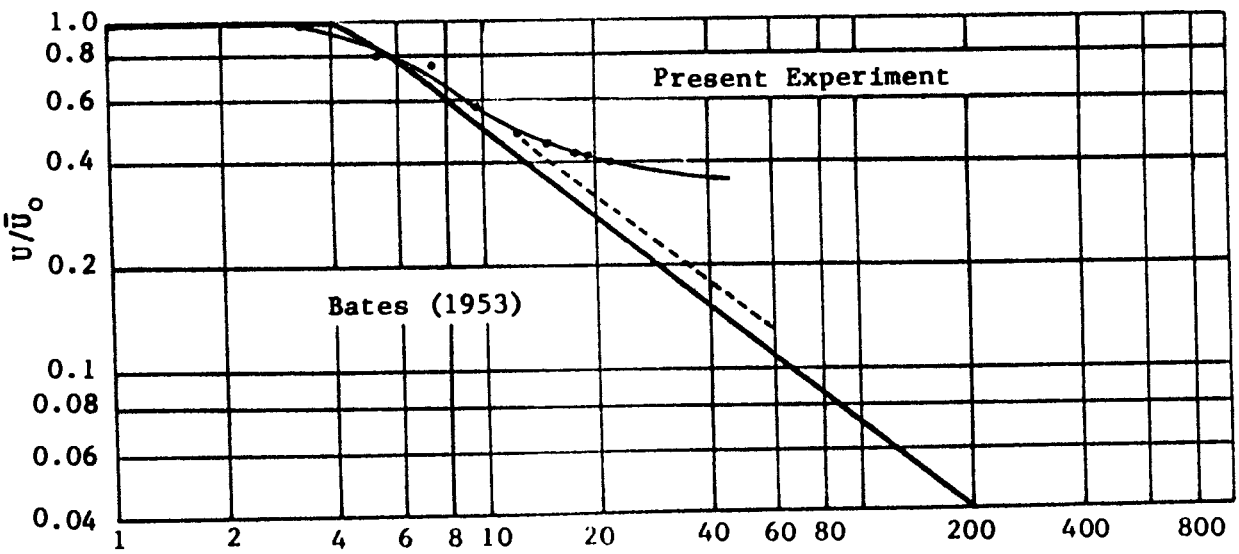

Figure 8c. Center-line velocity in axial jet.

approximate longitudinal distance of 157 cm off the channel outlet. Further down, the flow pattern took a different form whose velocity distribution is somehow comparable with that of a rectangular open-channel flow. Between the zone of flow establishment and established flow, Bates (1953) added a third zone of transition. The extent of this zone could not be defined in the present experiment. However, at the terminal point of the zone of flow establishment the formation of vortices and surface boiling were noticeably present.

Table 2 shows the velocity distribution along the Z-axis normal to the centre-line as measured at 2.00 cm depth-interval from the surface. The boundary layer, separating the region of vertical mixing from the surrounding fluid (Figure 8b) was estimated to slope down at an angle of 11 +/- 2°. The pattern seems to agree with Jopling's model of flow expansion related to leeside deposition of deltas (1960, 1962, 1964, 1965). The model describes that the locus of zero velocity, separating the zone of jet mixing from the backflow zone, dips at an angle of 12 +/- 1°. The locus of zero velocity or the boundary layer was found to fluctuate increasingly with the higher discharge conditions of the present experiment.

From the discussion it follows that the jet flows owe their existence to the condition of flow separation (Jopling 1960, 1962, 1964) which is strictly defined by the proximity of the rigid boundary conditions. This has been clearly observed in the

distribution of velocities along the centre-line as shown in table 1.

Figure 8c represents the dimensionless logarithmic plot of the centre-line velocity over the longitudinal distance which is shown as several times the channel width. The plot compares the theoretical findings (Albertson, 1950) with the present experimental results. The experimental plot shows a horizontal and sloping line which closely follows the theoretical trend of the free jet flow. This is, however, restricted to a limited longitudinal distance of about 125 cm (over 12 times the width of the channel) from the channel mouth. Beyond this distance, the plot demonstrates a significant departure from the line drawn from the theoretical consideration (broken lines in figure 8c) indicating that the rate of velocity decrease is relatively low. The explanation for this departure lies in the resistive effects imposed by the rigid boundary conditions. As a matter of fact, the basin boundaries not only inhibit the free expansion of the jets but also diffuse the flow in the region where the boundary layers of the expanding jet impinge upon the basin walls and floor. In turn, the diffused flow tends to move upward from the basin-bottom and laterally inward from the basin sides. These when coupled with the overall forward fluid movement (caused by flow inertia) bring a transitional flow condition affecting the distribution of flow velocity. As a result, a different pattern in the distribution of velocities emerged in

the flow field which appeared to adjust with the basin boundary conditions. This change of velocity, with distance from the channel mouth was considered unimportant in the present experiment of delta-building because the experimental runs were stopped well before this zone was reached by the main deltaic mass.

The preceding discussion, describing the hydraulic geometry of the jet diffusion, grossly represents the essential character of the flow expansion in the variety of discharge conditions adopted in the experiment. However, certain flow conditions, such as the formation of eddies and their effects are presented in the discussion of the series.

One of the central concerns of this study is whether the channel simply deposits its load as a result of energy dissipation by jet diffusion with the passive water of the basin. If it does, then the overall magnitude of the deltaic mass should be roughly correlative with the pattern of jet diffusion. On the other hand, if delta morphology is more than a passive product of the jet flow, the alien body of sediment deposits should reflect the process regime. Answers to these fundamental questions seem to lie in the understanding of sequential development of deltas as observed in the present experiment.

The granular boundary, introduced by the sediment mixing into the flow system, involves two major processes. One is the

process of transport describing the movement of sediment particles in the current, and the other one is the deposition which indicates termination of motion when the particles come to rest. The study further took cognizance of two mechanisms involved in the sediment transport. First, sediment particles moving along the bed, by rolling, sliding or skipping, constitute bedload. The causes of bed-load transport are usually attributed to the fluid forces of drag and lift on the particles. The particles travel with a velocity less than that of fluid and their weights are primarily carried by the solid channel-bed. Second, the sediments in suspension, known as suspended load, move with the fluid flow in such a way that the immersed weight of the particles is supported by the flow. This is known to be caused by the turbulent flow in the open-channel. The mechanism of sediment transport continues until the particles find positions of rest and become available for incorporation into the sedimentary sequences. The position of rest is a function of kinetic energy, sediment composition and grain size, and the boundary conditions. The interaction of these factors, as conceived by Sloss (1962), produces an equilibrium surface, base level, above which a particle cannot come to rest and below which deposition is possible. With this background information, the following observations were made in the flume experiment. The volumes of material carried in each kind of transport were noticed to vary depending on the input

conditions of the present experiment. Proportionately high bed-load transport was characterized by low discharge and high sediment supply rate. Conversely, high suspended load transport was characteristically associated with high discharge and low sediment input conditions. In spite of the variability in the mode of sediment transport the initial dispersal and deposition grossly correspond with the pattern of jet diffusion.

The photograph in plate 1a illustrates a fan-shape spread of sediment deposit. Much of its areal extent was derived from the suspended sediments carried with the flow current. The pattern of deposition seems to accord with the pattern of jet diffusion. The mechanism of the deposition may be explained by three basic considerations. First, the diffusion of free-jet flow is manifested with the entrainment of fluid from the surrounding regions causing flow volume to increase with distances from the channel efflux-section. The flow expansion, as required by the continuity equation, is counterbalanced by flow deceleration. In fact, data in Table 1 support this view. The inseparable and complementary phenomena of flow expansion and deceleration of the jet diffusion explain the progressive deconcentration of momentum, as described by Albertson et al. (1950), to be an integral property of free-jet diffusion. Second, suspended sediment-diffusion is considered as the equivalent of momentum diffusion (Ippen, 1971). This condition stipulates that the sediment dispersion tends to maintain the

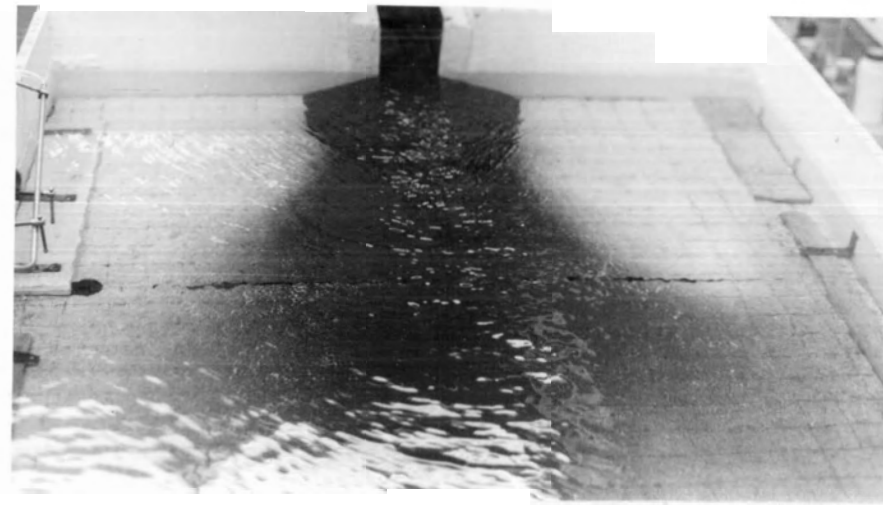

(a) Fan-shape spread of initial deposit.

(b) Intermediate stage of deltaic deposition.

(c) Delta formation at the end of a run.

PLATE 1. PHOTOGRAPHS ILLUSTRATING THE STAGES OF DELTA FORMATION.

concourse of the jet-diffusion pattern. Third, the deposition of the sediment particles, transported in suspension, normally occurs if the settling velocities of the particles exceed the vertical turbulent-velocity components. In summary, the direct manifestation of flow expansion and deceleration with jet diffusion necessarily represent losses of competence and capacity of current with distances from the channel efflux-section. These, in turn, activate the process of sedimentation through the sorting of sediment particles according to their heavier size grades. Similar or more elaborate views have been recorded by other researchers, including Jopling (1964). Jopling, in his model of lee-side deposition, has described the dispersion and subsequent deposit as an outcome of the differential settling-velocity of the suspended particles which is based on the occurrence of flow separation and flow divergence.

The same photograph also shows accumulation of relatively coarser sediment settled as a collective unit. The sudden discontinuity of the rigid boundary in the flow system appeared to be responsible for the dumping of sediment transported along the bed. This will imply that the bed-load transport is ineffective in the absence of a rigid bottom boundary. The sediments were observed to pile up as an upward accretion until traction occurred.

The photograph in plate 1b demonstrates an intermediate stage of delta-building. The deposition has expanded dimensionally. Concurrently the flow was observed to be more chaotic than before indicating an unstable state in the flow system. This appeared to be the turning point when the jet was subjected to the resistive effect of the vertical accretion. As a result, two fundamental changes were observed in the flow structure. First, there was a gradual increase in the lateral flaring of the flow followed by a decrease in flow-depth. Importantly, the lateral spread maintained a high angle of divergence and low measure of flow-depth with the low discharge and high sediment transport conditions. Second, the formation of eddies and bottom rollers became an integral part of the flow system. They were noticed to be consistently significant with high discharge conditions. Because they not only moulded the pattern of movement in which the forward flow looked like coiled-springs (von Karman vortex trials) but deflected the forward flows sideways. As a result, deltas tend to be asymmetrical in shape.

In the context of the present experiment, photo plate 1c represents the third rather than the final stage of delta formation. It demonstrates that a state of dynamic equilibrium has been reached in the mechanism of delta-building indicating an overall adjustment of process and form. The adjustment represents the interactions and interdependence of flow and

form. Because of the mutual interaction between flow and form the flow itself is altered in fundamental ways to form a different structure which barely resembles the jet flow. There seems to be a feedback effect between the flow and form which makes possible the development of different kinds of morphology in the deltaic environment. The efficacy of this interaction involving various processes depends in a complex manner upon the nature of flow regime and sediment transport conditions.

5.1.1 Series A

Table 3 lists the basic parametric information of Series A. The Series represents six test runs through which a constant rate of flow, 1377.00 cm^3 /sec. was passed. The runs were assumed identical in the sediment-free flow conditions. The rate of input of sediment was altered between runs. Table 2 identifies the rates with the runs. The same amount of sediment (5.1×10^4 gm.) was used in each run.

Figure 9a is the hydraulic geometry of the jet expansion, drawn on the basis of velocity data of Series A as in table 1. The figure is comparable with the generalized structural pattern of the jet diffusion, discussed in section 5.1. It was however, noticed that the boundary layers, bordering the expanding jet, were in a state of continuous fluctuation, indicating that the jet diffusion involves the statistical nature of the mixing

Table 3
Series A: Variation of Sediment Transport Rate

Parameters constant for each run

Channel depth (cm)	2.00
Channel width (cm)	10.20
Channel slope	0.002
Average velocity (cm/sec)	67.50
Water discharge (cm^3/sec)	1377.00
Froude Number	1.525
Basin depth (cm)	12.00
Sediment quantity ($x10^4$ gm)	5.10
Mean grain size (mm)	0.365
Water Temperature (°C)	13.80

Variables between runs	Run 1	Run 2	Run 3	Run 4	Run 5	Run 6
Time ($X10^3$ sec)	1.20	1.92	2.52	3.416	5.11	10.92
Sediment input rate (gm/sec)	42.50	26.56	20.24	14.93	10.00	4.67
Delta length:						
Max. X_{bs}^{T} (cm)	91.00	94.50	96.50	98.00	100.50	106.00
Max. X_{bs}^{F} (cm)	113.50	116.50	118.50	121.00	123.00	130.00
Delta width:						
Max. Y_{bs}^{T} (cm)	19.00	18.00	17.50	20.50	21.50	16.50
Max. Y_{bs}^{F} (cm)	48.50	45.00	43.50	49.50	52.00	47.00
Vertical accretion						
Max. ZT (cm)	9.80	9.50	9.10	8.80	8.50	8.10

X = longitudinal; Y = lateral; T_{bs} and F_{bs} indicate break of slope of topset and forset beds, respectively.

process. The zone of flow establishment was found to terminate at a distance of 37 cm from the channel mouth. Within this zone, the surface water appeared very undulating, analogous to standing waves usually formed at the transition of higher to lower regime flow. This phenomenon was to be expected with this Series because the average flow velocity of the channel was recorded as 67.50 cm per second, at which the Froude Number was in excess of one, denoting supercritical flow. Interestingly, such a wavy surface was observed to be bounded by the central-core of no diffusion, around which the surface water appeared only as boils. This was followed by the zone of established flow where sporadic formation of heterogenous eddies was noticed to develop on the proximal of the central-line forward flow.

In all runs, the average flow velocity of 67.50 cm/sec was found competent to move sediment particles into the basin. No particle was seen to creep or roll along the channel bed. It connotes that the sediment particles were transported either in suspension, or in transition between suspended-load and bed-load, or both combined.

As observed, the initial deposition occurred in two different ways. First, a fan-shaped thin carpet of deposit appeared to evolve gradually at the basin bottom, showing slight spread beyond the lateral boundaries of the jet flow. The fan-shaped deposit, presumably resulting from the sediment

carried in suspension, seems to be indicative of the jet diffusion pattern; and the depositional spread, exceeding the boundaries of the jet, may be attributed to the phenomenon of reverse circulation. Second, fairly coarse granular sediments were noticed to settle at the efflux-section of the flow, which subsequently took the shape of an elongated ridge showing axial declivity in the direction of the forward flow. The inclination showed some degree of variation in its steepness in between the runs. That is, runs with a higher sediment transport rate tended to develop a relatively steeper gradient, which eventually involved more frequent slumpings. Much of its material seems to have been derived from the particles carried in transition between bedload and suspended-load.

With the progress of the runs, the depositional ridge continued to increase in height with its concomitant advancement in the longitudinal direction. At some stage of the vertical accretion, the ridge-like deposit began to collapse by shear failure involving side slippages. As a result, the base of the deposit grew wider. In the subsequent stage, the exterior surface of the collapsed ridge gradually appeared to be rounded up, showing some degree of convex-curvature in the lateral direction. Concurrently, there was a marked tendency for the flow to develop eddies which eventually showed up as strong vortices superimposed on the main forward flow. This seems to be the turning point when the jet flow was subjected to the

resistive effects of the vertical accretion. This may be viewed in the following way. The growth of the deposit tended to constrict the flow, causing an increase in velocity and bed shear stress. Common to most of these considerations is the generation of the highly-turbulent flow, which is, in no way, representative of the free-turbulence shear flow of the jet diffusion.

A significant change in the general direction of sediment transport was also seen. Parts of the load were noticed to be propelled and moved towards the sides of the main flow. Such deviation suggests that the generation of intense turbulence due to growing interference arising from vertical accretion, involved the process of turbulent exchange expelling the sediment particles from the areas where the degree of turbulence was greatest, towards the areas of less turbulence. As a result, a flat-bed atop the axial-ridge slowly evolved, and over which the flow was found to develop a sinuous course. Following this, the submerged natural levees, on either side of the flow, gradually built up and eventually confined the flow into a single channel. Beyond the confinement and over the delta front, the current formed a distinct pattern of movement in which the forward flow looked like a coiled-spring representing a chain of eddies. Initially, the chain of eddies oscillated, but, subsequently, it continued to flow in a deflected course, causing drastic changes in the flow pattern, and so in the

depositional facets. Such a flow pattern was persistently present throughout the later part of each run.

Figure 9b represents the maps of the deltas showing the areal extent of the top-, fore-, and bottom-set beds. Each delta was produced in a given condition of sediment-input rate (table 3). The figure clearly demonstrates that the deltas are asymmetrical about their principal axes of deposition. Although there are differences in detail or in absolute magnitude, the deltas of this series developed the same kinds of significant features which may be characterized by nearly identical values of any given statistical measure of morphology. Some of these patterns or forms are catalogued below.

Broadly, the deltas of this series are elongated deposits, built-up through rapid advances, and are thought to be due to the high inertia flow. However, between runs, the delta-progradation showed a differential growth in the linear measurements of their morphometries. Table 3 and figure 9b list the measures of maximum length, width and vertical accretion of the different parts of the deltaic deposits. An interesting trend in the relations between these parameters is clearly evident. As read from Run 1 to Run 6, there is an increasing length in the longitudinal extent of the deltas, which appears to be accompanied by somewhat compensatory decreases in the measures of the lateral and vertical accretion. Major variations of these measurements, as well as their intricate relations,

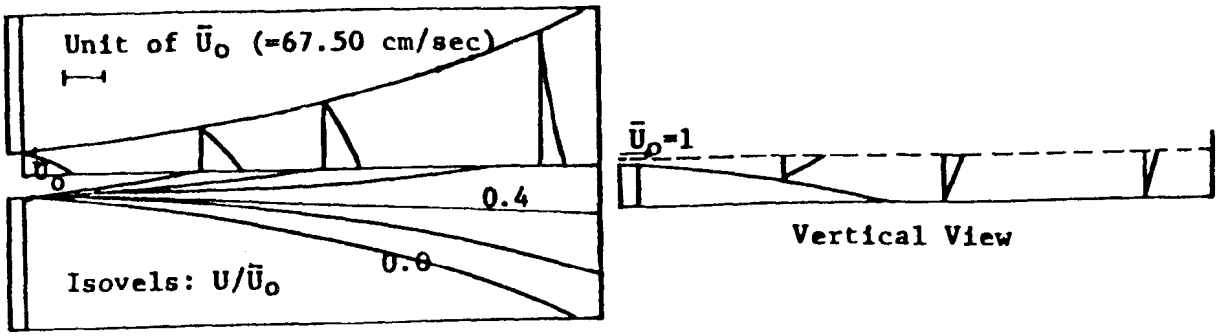

Figure 9a. Hydraulic Geometry of Axial Jet Expansion - Series A.

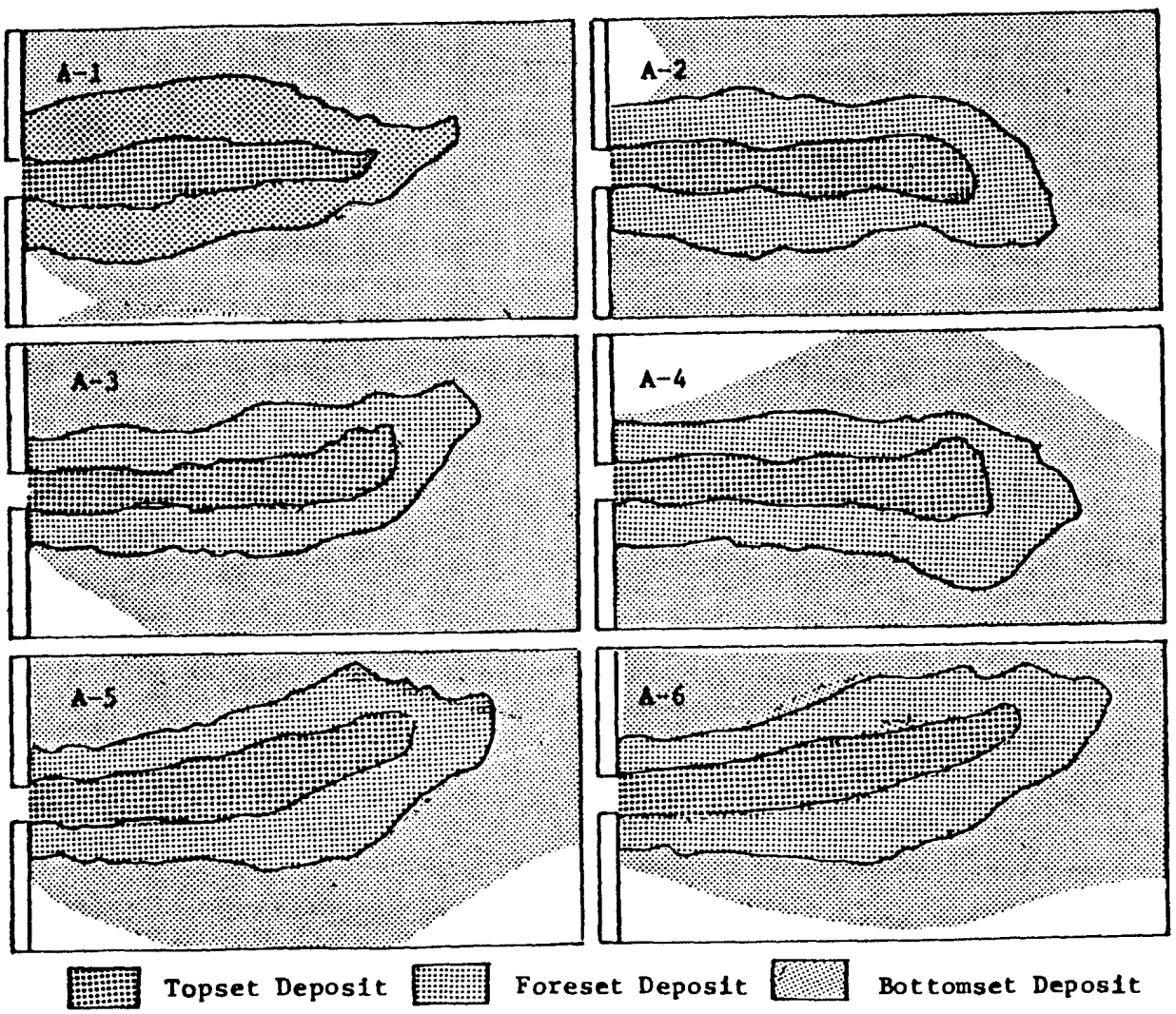

Figure 9b. Maps of the Deltas showing Top-, Fore- and Bottom-set Deposits. Scale is 1cm to 20cm.

could be attributed to the differential rate of sediment transport used in different runs. Although the effect of the sediment load in the flow system is not clearly understood, it is highly probable that the competence or capacity of the flow decreases with the increasing amount of sediment load, This is because a substantial quantity of energy is always expended in transporting the load, bringing changes in the availability of kinetic energy (working force). This change, coupled with the particles' settling velocity, explains the mechanism of short or long-distance travel, and thus the vertical and longitudinal deposition. Certain deviations to this mode of transport and subsequent deposition were observed in Runs 4, 5, and 6, where the relative increases in the longitudinal lengths do not represent compensatory decreases in the widths of the deltas (table 3). In one way or the other, the spiral motion of the flow which develops over the delta-front to various degrees, seems to be responsible for the widening of some parts of the deposits.

The discrete formation of the submerged natural levees showed differential growth in between runs. The vertical height of the levee-walls was greater in the runs with high sediment transport showing little longitudinal development. The reverse is true with the runs having a low rate of sediment transport. There was no breach of the natural levees, nor at any point did the flow bifurcate. It indicates that the formation of the

distributary-system was absent in the series, and that the flow was confined to a single channel. However, an elongated deposit (ridge-like), extending some distance along mid-channel line from the channel-efflux section, was found in runs 1, 2, and 3. Some of these features are shown in photo-plate 2,and are discussed in detail in the later section of this chapter.

Perhaps the most spectacular phenomenon, observed in the series, was the formation of strong eddies over the delta head. The interaction of the frictional and inertial forces on the flow is thought to have generated these eddies. As water passes over the delta platform, its velocity is greatly reduced by the bottom-boundary resistance. The surface water, which has much greater inertia due to its high speed, tends to maintain a downstream movement, forcing the slower moving fluid near the bottom to also move. The pressure thus created causes the water to flow upward, and to maintain continuity, the water continues to move inward, inducing spiral motion in the flow. When strong enough it causes scour-pools, and moves away the materials along its periphery, resulting in deposition elsewhere. The formation of the spiral flow superimposed on the main forward flow is so delicate that slight obstruction from one side or the other will deflect the vortices sideways. As a result, a drastic change in the direction of flow movement, as well as in the pattern of velocity distribution in the total flow system, is inevitable. Photoplate 2 clearly illustrates the effects of the spiral

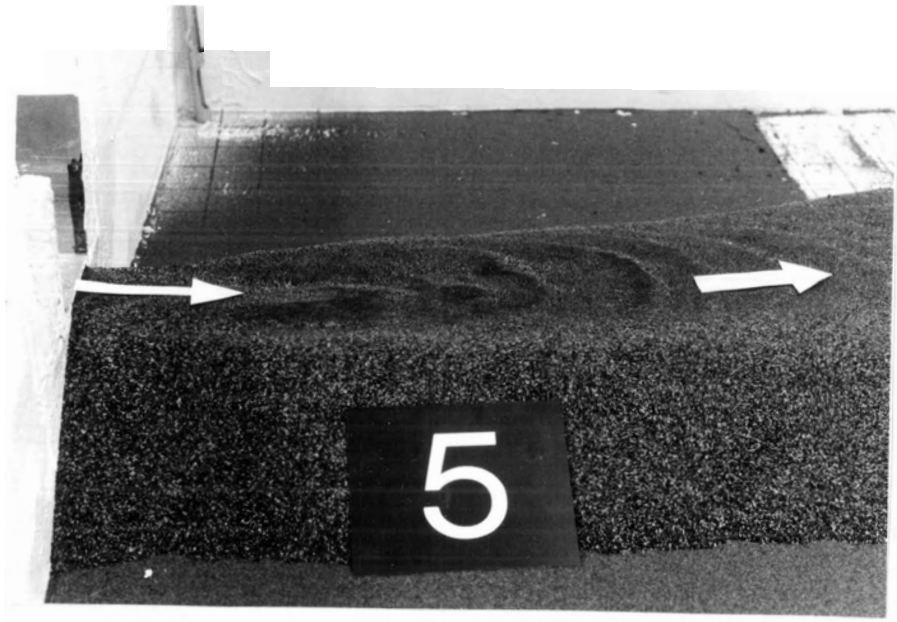

(a) Mid-channel bar and submerged natural levees.

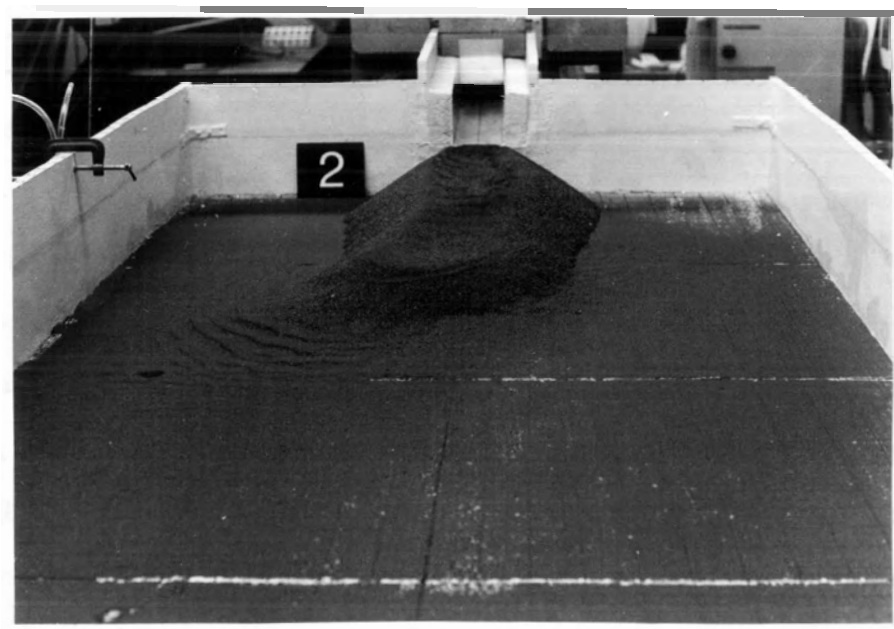

(b) Sandwave and ripple formation.

PLATE 2. PHOTOGRAPHS SHOW THE FORMATION OF LONGITUDINAL BAR, NATURAL LEVEES AND SANDWAVE. THE FORMS ARE TYPICAL OF THE DELTAS BUILT IN SERIES A.

motion of the flow, making the overall configuration of the deltas asymmetrical in shape, forming a series of semi-circular deposits analogous to sandwaves. None of these occurrences can be adequately described by the axial jet diffusion process noted as existing in sediment-free flow conditions.

5.1.2 Series B

Unlike Series A, a discharge of 495.70 cm^3 /sec was held constant throughout the runs of this series. The flow was at subcritical stage (Froude Number of less than one) whose average velocity, 36.00 cm/sec. was determined in the sediment-free flow conditions. The series represents five test-runs, each having an identical sediment-input rate to that of series A. One run was dropped because the discharge (495.70 cm^3 /sec) was found to be incompetent to transport the sediment supplied at the rate of 42.50 gm/sec. Table 4 lists the measures of the variables of the series.

Figure 10a is the flow geometry of the axial jet of the series, demonstrating satisfactory agreement with the generalized structural pattern of jet expansion discussed in section 5.1. As with Series A, a minor difference was noted when compared with the pattern of jet expansion. The expanding jet of this series showed a slight increase in the angle of its lateral spread. The longitudinal limit of the zone of flow establishment

Table 4

Series A: Variation of Sediment Transport Rate

Parameters constant for each run

Channel depth (cm)	1.35
Channel width (cm)	10.20
Channel slope	0.002
Average velocity (cm/sec)	36.00
Water discharge (cm^3/sec)	495.72
Froude Number	0.9897
Basin depth (cm)	11.35
Sediment quantity ($x10^4$gm)	5.10
Mean grain size (mm)	0.365
Water Temperature (^{0}C)	13.80

Variables between runs	Run 1	Run 2	Run 3	Run 4	Run 5
Time ($x10^3$ sec)	1.92	2.52	3.416	5.11	10.92
Sediment input rate (gm/sec)	26.56	20.24	14.93	10.00	4.67
Delta length:					
Max. XT (cm) bs	64.80	67.00	68.50	70.00	72.00
Max. XF (cm) bs	81.00	83.50	85.80	87.50	89.50
Delta width:					
Max. YT (cm) bs	33.00	31.00	30.00	28.50	27.00
Max. YF (cm) bs	65.00	63.00	61.50	60.50	59.00
Vertical accretion					
Max. ZT (cm)	11.00	11.00	10.90	10.85	10.85

was measured at a distance of 33 cm from the efflux-section. The central core or the zone of no diffusion was suggested by some kind of water line forming along the periphery of the zone. The boundary layer or the locus-line of zero velocity, separating the vertical mixing zone of the jet from the surrounding water, was estimated to be an angle of less than 10°. The overall surface flow of the expanding jet was found to be relatively calm.

At the beginning of the sediment mix, the given flow was found incapable of transporting all sediment particles quickly into the flume basin. That is, parts of the load were settling down along the channel floor, which eventually raised the channel bed by an average measure of 0.5 cm. This caused an upward shift in the water-level of the channel, but the rise was relatively small, suggesting a decrease in the flow depth. An increase in flow velocity must follow the decrease in flow depth. The reason for the increase of flow velocity may be seen in the equation Q = v.w.d. It appears from the observations that the mechanism of sediment movement of the series involved both bed-load and suspended-load transport. It is also important to note that a significant portion of the total load was transported through the formation of migratory ripples on the newly built channel-bed.

The occurrence of the initial deposition, regardless of differential rates of sediment transport on the runs, was

observed to involve two fundamental modes of settling. First, the finer sediments carried in suspesnsion tended to settle as a discrete unit, which eventually led to the formation of a fan-shape deposit on the basin floor showing conformal relation with the geometry of the expanding jet in plane form. This observation indicates that the mechanics of deposition is a consequence of the jet diffusion process, where effective sorting of the sediment is possible because of the particles' differential settling velocity. A similar observation was also reported by Jopling (1954, 1965) in his study of the lee-side deposition of the laboratory deltas. The author described the sorting mechanism as a result of selective transport due to differential settling velocity of the suspended particles caused by flow expansion, depending on the flow separation. It may be noted here that the deposit so formed eventually turns into a bottom-set bed when ovberridden and buried by the depositional layers of the coarser sediments.

Second, fairly coarse granular sediment, transported mostly as bed-load, was observed to settle as a collective unit, building a pile at the base of the efflux-section. With the continued addition of the load the pile tended to grow upward, with concomitant widening of its base through periodic slippages. At some stage of the upward growth a mutual interaction between the jet flow and the apex of the pile developed. A localized tendency for the sediment particles to

move in random directions seemed to have occurred, suggesting a variable velocity field had been created. However, this unsteadiness lasted only for a while. In the meantime, the top of the pile was observed to be extending its area, making a flat-bed for the flow, over which a portion of the load was being transported by ripple movement. On the other hand, the presence of the flat-bed which was extending its area slowly, caused the flow to develop a divergent pattern. This divergent pattern of flow appeared to be responsible for the transportation of sediments, particularly the bed load fraction, to the periphery of the deposit to form metastable wedges, which periodically slipped down the foreset-slopes under the influence of gravity. Progradation of the deltas was found to continue in the same manner until the end of the runs.

Figure 10b represents the maps of the deltas produced at a constant discharge of 459.70 cm /sec, showing a high degree of symmetry about their principal axes of deposition. The trend indicates that the progradation of the deltas involves the same mechanism of formation, and thus could be atttributed to similar sets of physical principles. As shown in table 4 and figure 10b, concomitant with the decreasing order of the sediment-input rates, there was an inevitable increase in the longitudinal length of the deltas, followed by corresponding decreases in both lateral and vertical deposition. These inverse relations in the linear measurements of the morphometries of the deltas are

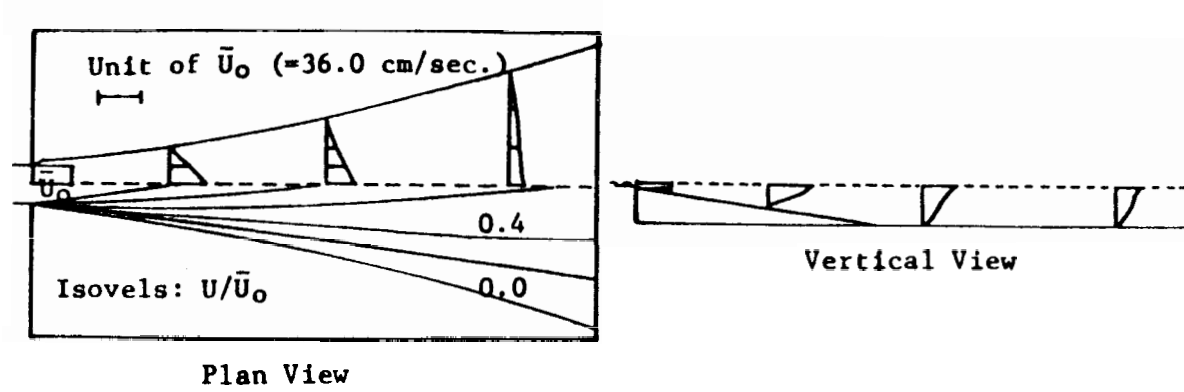

Figure 10a. Hydraulic Expansion of the Axial Jet in Series B.

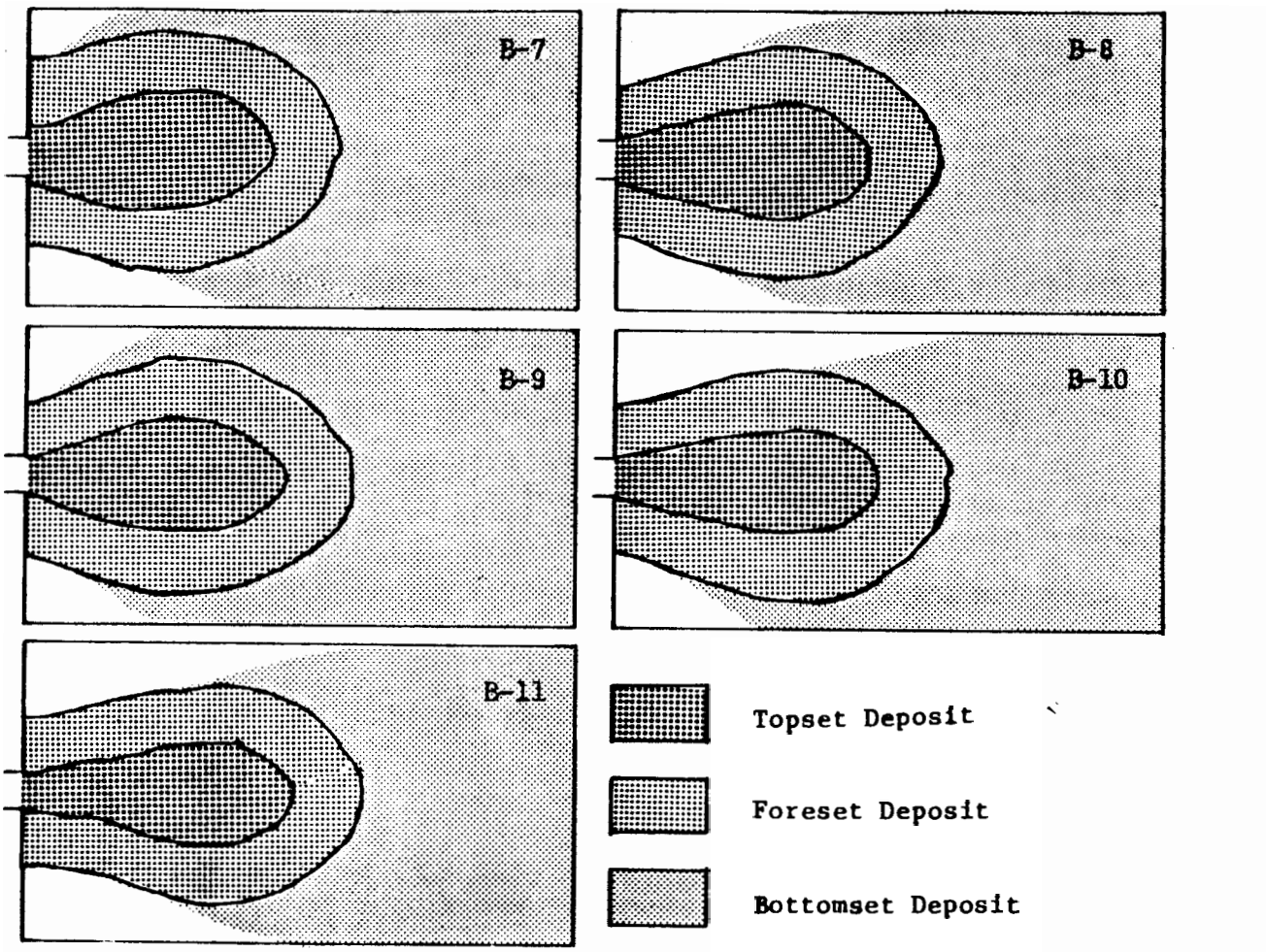

Figure 10b. Maps of the Deltas showing Areal Extent of Top-, Fore- and Bottom-set Deposits. Scale 1cm to 20cm.

thought to be due to the effects of the sediment transport rates. Conceivably, the high bed-load (assumed to be related to the high sediment input) causes rapid dumping of load and thereby offers instant resistance to the flow. Depending on the rapidity of this instant resistance, the flow tends to flare more divergently in one case than in the other, hence the lateral and vertical deposition. While comparing the deltas of series A and B, a marked difference in the pattern of their morphological formation is consistently seen. One way or the other, the difference is attributable to a single independent variable, namely the discharge.

Photo-plate 3 clearly illustrates that in this series the submerged natural levees were formed least discretely. Relatively undeveloped levees were observed to build-up to a proximal distance of only 10 cm from the efflux-section. The reasons seem to lie in the formation of mobile-beds analogous to sandwaves extending across the delta platform. The sandwaves, presumably formed under the direct influence of two-dimensional divergent flow and high bed-load transport, somehow prevent the formation of a turbulent-exchange process, and thus the levee formation.

Perhaps the most significant features that developed in the series were its distributary patterns. Using the classification of Coleman and Wright (1971), two of the four types of distributary patterns were noticeably formed: 1) There was the

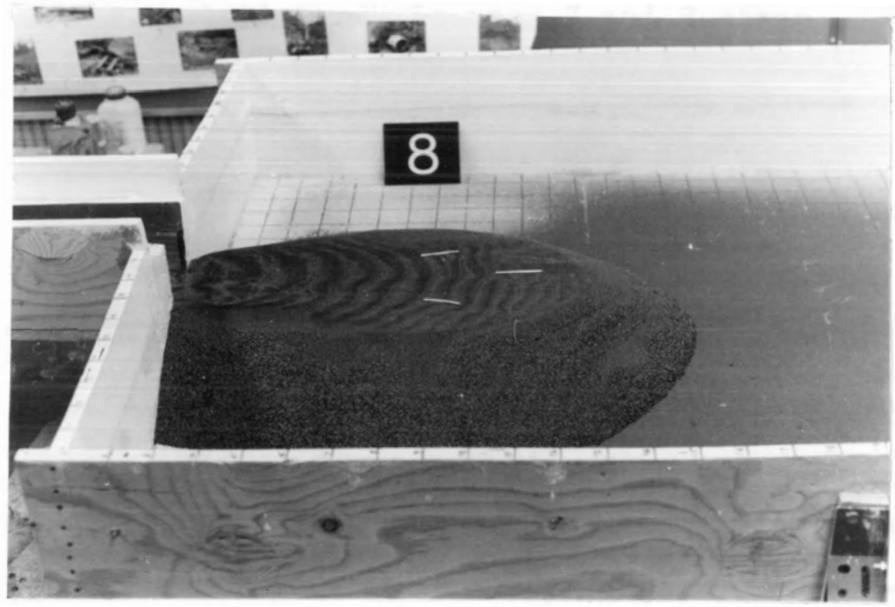

PLATE 3. A VIEW OF THE DISTRIBUTARY PATTERNS FORMED IN SERIES B. THE PATTERNS REPRESENT THE TYPE IN WHICH SPLITTING OCCURRED AT A SINGLE APEX.

type in which all splittings occurred at a single apex. (runs 7, 8, and 11 shown in photoplate 3) In runs 7 and 8 three distributaries formed, splitting at the same apex. The apex was measured and found to be located at an approximate distance of 14 cm from the efflux-section which is less than 1.5 time s the channel width. On the other hand, run 11 developed two distributaries bifurcating from the apex, located at an approximate distance of 17cm (more than 1.5 times the channel width) from the channel mouth. 2) There was the single type in which there was no bifurcation. Runs 9 and 10 showed such a formation. These are discussed more fully in the later section of this chapter.

5.1.3 Series C

Table 5 lists the parametric information of this series. The series consists of five runs conducted at a constant flow of 295.80 cm^3 /sec, representing the lowest discharge in the whole experiment. In the sediment-free flow conditions the average velocity and flow depth were recorded to be 29.00 cm/sec and 1.00 cm respectively. The flow was at the subcritical stage as indicated by the Froude Number. This series used the same sediment-input rates as in series B.

Figure 11 represents the hydraulic geometry of the axial jet of the series, showing close structural conformity with the

Table 5

Series C: Variation of Sediment Transport Rate

Parameters constant for each run

Channel depth (cm)	1.00
Channel width (cm)	10.20
Channel slope	0.002
Average velocity (cm/sec)	29.00
Water discharge (cm^3/sec)	295.80
Froude Number	0.9234
Basin depth (cm)	11.00
Sediment quantity ($x10^4$gm)	5.10
Mean grain size (mm)	0.365
Water Temperature (^oC)	13.80

Variables between runs	Run 1	Run 2	Run 3	Run 4	Run 5
Time ($x10^3$ sec)	1.92	2.52	3.416	5.11	10.92
Sediment input rate (gm/sec)	26.56	20.24	14.93	10.00	4.67
Delta length:					
Max. XT (cm) bs	54.20	56.50	58.00	59.80	62.00
Max. XF (cm) bs	69.00	71.30	73.00	75.50	78.00
Delta width:					
Max. YT (cm) bs	44.50	41.50	39.00	36.50	34.80
Max. YF (cm) bs	74.80	72.50	71.20	69.20	67.50
Vertical accretion					
Max. ZT (cm)	10.90	10.90	10.90	10.85	10.85

jet expansion of the other series. However, the jet was noted to be slightly expanding (laterally), in which the zone of flow establishment extended a relatively shorter longitudinal distance of 31 cm from the channel mouth. The overall surface flow appeared very calm.

Understandably, the average velocity, 29.00 cm/sec., was insufficient to transport all the sediment quickly into the flume basin. That is, parts of the load were found to settle, which eventually raised the channel bed by an approximate distance of 0.85 cm. An overall rise in the level of channel flow was also noticed, but the rise was comparatively small. This suggests that there was an increase in the flow velocity, presumably through the adjustment of the channel slope or the energy gradient. Although there was sporadic formation of bed-forms analogous to migratory ripples, most of the time the channel bed was in plane form. It appeared from the visual observations that the major portion of the load was transported by the mechanics of bed-load movements.

Like series B, the initial deposition occurred in two ways. The finer particles carried in suspension were noticed to settle as discrete units, eventually forming a thin carpet of fan-like deposit. Visually the shape of the deposit (in plan view) appeared to simulate jet expansion, suggesting that the initial sedimentation derived from the sediments in suspension could be correlated with the jet diffusion process. On the other hand,

the heavier grade size particles transported along the bed tended to settle as a collective unit, which eventually led to the formation of a pile upon the basin bottom. The rapid growth of the pile upward through vertical accretion gradually developed foreset-slopes, along which frequent slippages were observed to occur, extending the basal part of the deposit. At one stage of this upward growth a mutual interaction between the pile and the flow became clear where the top of the pile gradually developed into a a flat-bed over which the flow continued to flare, forming a two-dimensional divergent flow. The divergent flow continued to carry the sediment, forming metastable wedges at the periphery of the deposit which frequently slipped down the foreset slopes. Because of the homopycnal situations, the flow might have expanded in a three-dimensional form beyond the depositional periphery, but the assumption of three-dimensional expansion does not necessarily suggest the formation of jet flow. However, the progradation of the deltas was more or less related to the same process of sediment-input formation atop the depositional mass, involving irregular and frequent slumpings under the influence of gravitational pull.

Figure 11b represents the maps of the deltas produced in this series. The rounded-shape deltas are symmetrical about their axes of deposition and are thought to involve the same mechanics of formation as those in series B. Table 5 and figure

11b also demonstrate that with the increasing rate of sediment-input between runs, the increases in the longitudinal length of the deltas were, as a rule, related to the corresponding decreases in both vertical and lateral growth of the deposit. The relations in the linear measurements of the delta-configurations may be attributed to the effects of the differential rates of the sediment-input used in the runs.

Photo-plate 4 illustrates that the overall deposition has been considerably graded and extended laterally by accelerated sedimentation. At the later stage of this aggradation the natural levees were observed to form gradually on either side of the efflux-section, and they eventually narrowed down the divergent flow. Following this change, a secondary depositional platform began to evolve on the main delta platform. This, in the subsequent stage, appeared as a superficial deposit and is clearly seen in plate 4. Run 12 and 16 (plate 4) also show the breaching of the levee-walls, creating two short-range distributaries which occurred at the later stage of the development of the superficial deposit. However, there was no break of levee-walls in run 14; instead, the levees continued to grow, extending over the superficial deposit (Plate 4). Importantly, neither of these morphological features nor the overall configuration of the deltas could be adequately described by the jet diffusion process.

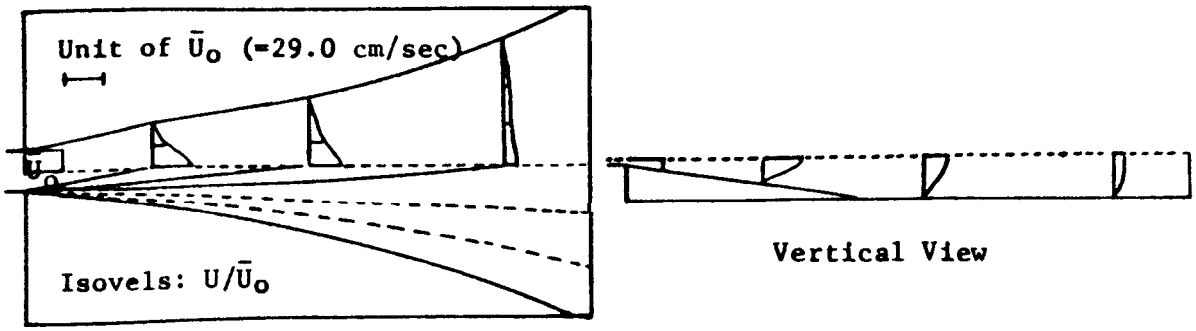

Figure 11a. Hydraulic Geometry of Axial Jet Expansion in Series C

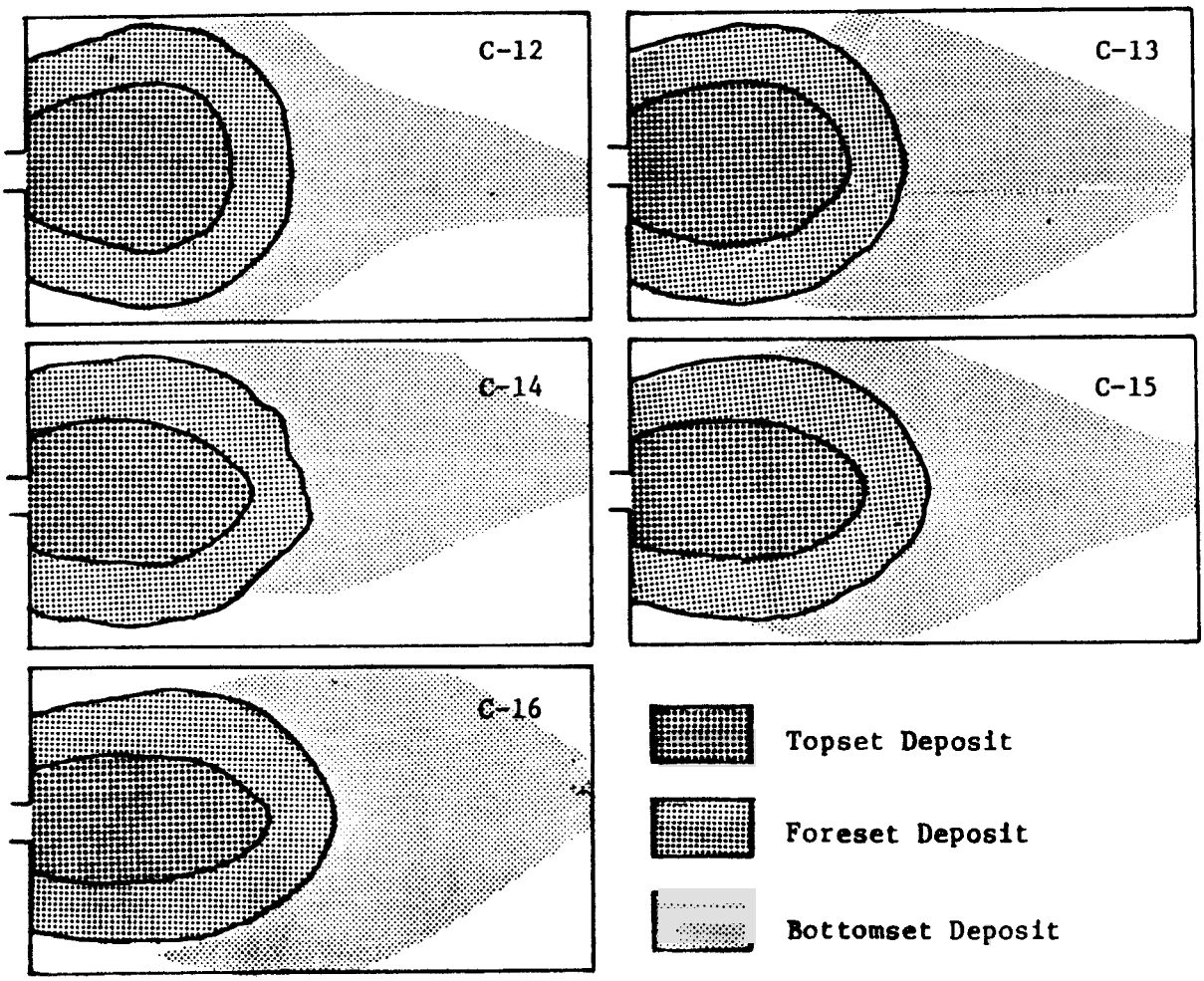

Figure 11b. Maps of the Deltas showing Areal Extent of Top-, Fore- and Bottom-set Deposits. Scale is 1cm to 20cm.

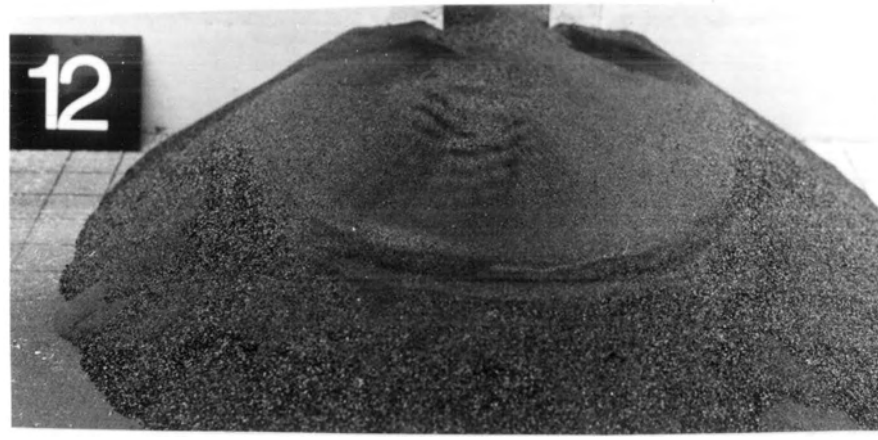

(a) A view of distributaries formed by breaching of the submerged natural levees.

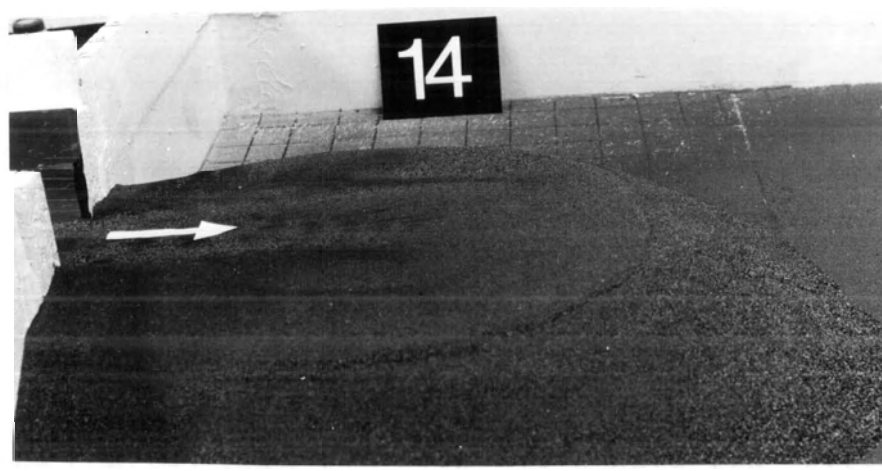

(b) Formation of a channel and natural levees atop the delta platform.

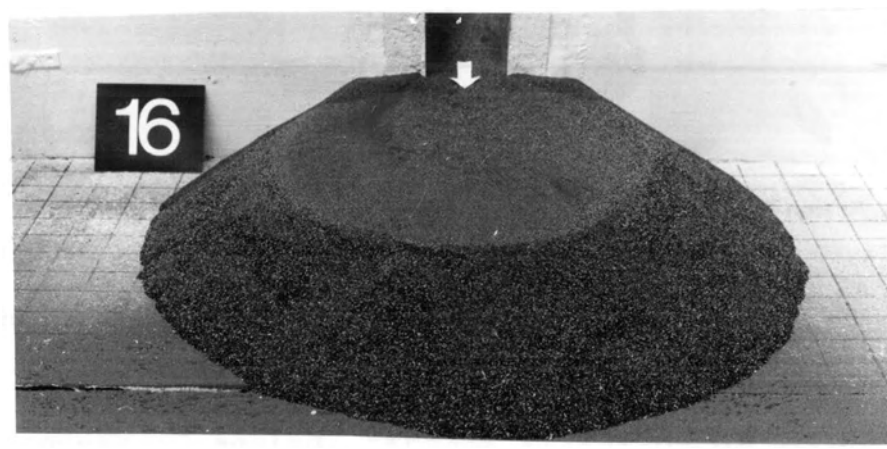

(c) Surficial bulge-deposit forming a circular-plan bar.

PLATE 4. PHOTOGRAPHS SHOW FORMATION OF DISTRIBUTARIES, NATURAL LEVEES AND BAR. THE FORMS ARE TYPICAL OF SERIES C.

5. 1. 4 Series D

The series, consisting of six runs, involved a constant discharge of 642.60 cm^3 /sec throughout the experiment. In the sediment-free flow conditions the average velocity and flow-depth were 42.00 cm/sec and 1.50 cm. respectively. The Froude Number was computed to be 1.0954, indicating that the flow was close to critical stage. Table 6 lists the measures of the variables of the series.

The geometry of the axial jet expansion is shown in figure 12a. The overall pattern of the flow expansion is roughly conformal with the jets of the other series. The zone of flow establishment was measured and extended over a longitudinal distance of 36 cm from the channel mouth. Within the zone, the surface of the central core was slightly undulating. Although no vortex motion was observed at the terminal point of the zone of no diffusion, the surface water appeared relatively turbulent.

The average flow velocity, 42.00 cm/sec. was found competent to transport the major portion of the load quickly into the flume basin. In runs 17 and 18 parts of the materials were carried along the bed in the form of a mobile carpet of sediment, while in runs 21 and 22, the mid-channel bed was clearly exposed, suggesting that a substantial part of the load was in the process of moving, through saltation or skipping.

Table 6

Series D: Variation of Sediment Transport Rate

Parameters constant for each run

Channel depth (cm)	1.50
Channel width (cm)	10.20
Channel slope	0.002
Average velocity (cm/sec)	42.00
Water discharge (cm^3/sec)	642.60
Froude Number	1.0954
Basin depth (cm)	11.50
Sediment quantity ($x10^4$gm)	5.10
Mean grain size (mm)	0.365
Water Temperature (?C)	13.80

Variables between runs	Run 1	Run 2	Run 3	Run 4	Run 5	Run 6
Time ($x10^3$ sec)	1.20	1.92	2.52	3.416	5.11	10.92
Sediment input rate (gm/sec)	42.50	26.56	20.24	14.93	10.00	4.67
Delta length:						
Max. XT (cm) bs	69.00	71.80	74.00	75.80	77.00	79.50
Max. XF (cm) bs	87.20	90.00	92.10	94.00	96.00	99.30
Delta width:						
Max. YT (cm) bs	27.50	25.50	24.00	22.50	21.00	19.80
Max. YF (cm) bs	60.50	58.00	56.50	54.50	53.00	52.20
Vertical accretion						
Max. ZT (cm)	10.40	10.40	10.20	10.10	9.90	9.85

The occurrence of initial deposition, as in the other series, involved two different modes of sedimentation. The sediment carried in suspension tended to settle in accordance with the diffusion pattern of the expanding jet. This was evident from the observed gradual formation of a fan-shaped deposit showing conformal, plan-form spreading. On the other hand, coarser sediment moving along the bed settled down collectively to form a pile. The pile appeared slightly elongated, displaying steeper declivity. Like any other runs of the previously described series, the outflow was eventually subjected to the resistive effects of the bottom boundary, raised through vertical accretion. At this stage, a marked tendency for the flow to develop secondary motion, creating vortices, was clearly noticed. Because of the vortex-actions, part of the load from the depositional surface was occasionally uplifted, swirled, and thrown toward the sides. This helped the lateral growth of the deposition and eventually led to the formation of indistinct, submerged natural levees. It is important to note that the flow over the delta surface was relatively divergent, suggesting that the flow was less competent, thus imposing a truncating effect on the depositional bed.

Figure 12b represents the maps of the deltas of Series A. By and large they were symmetrical about their principal axes of deposition. Besides minor differences in the detailed

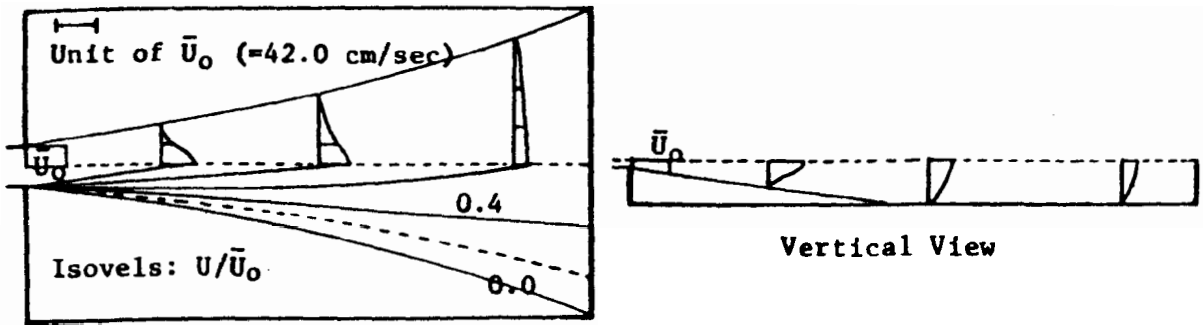

Figure 12a. Hydraulic Geometry of Axial Jet Expansion - Series D.

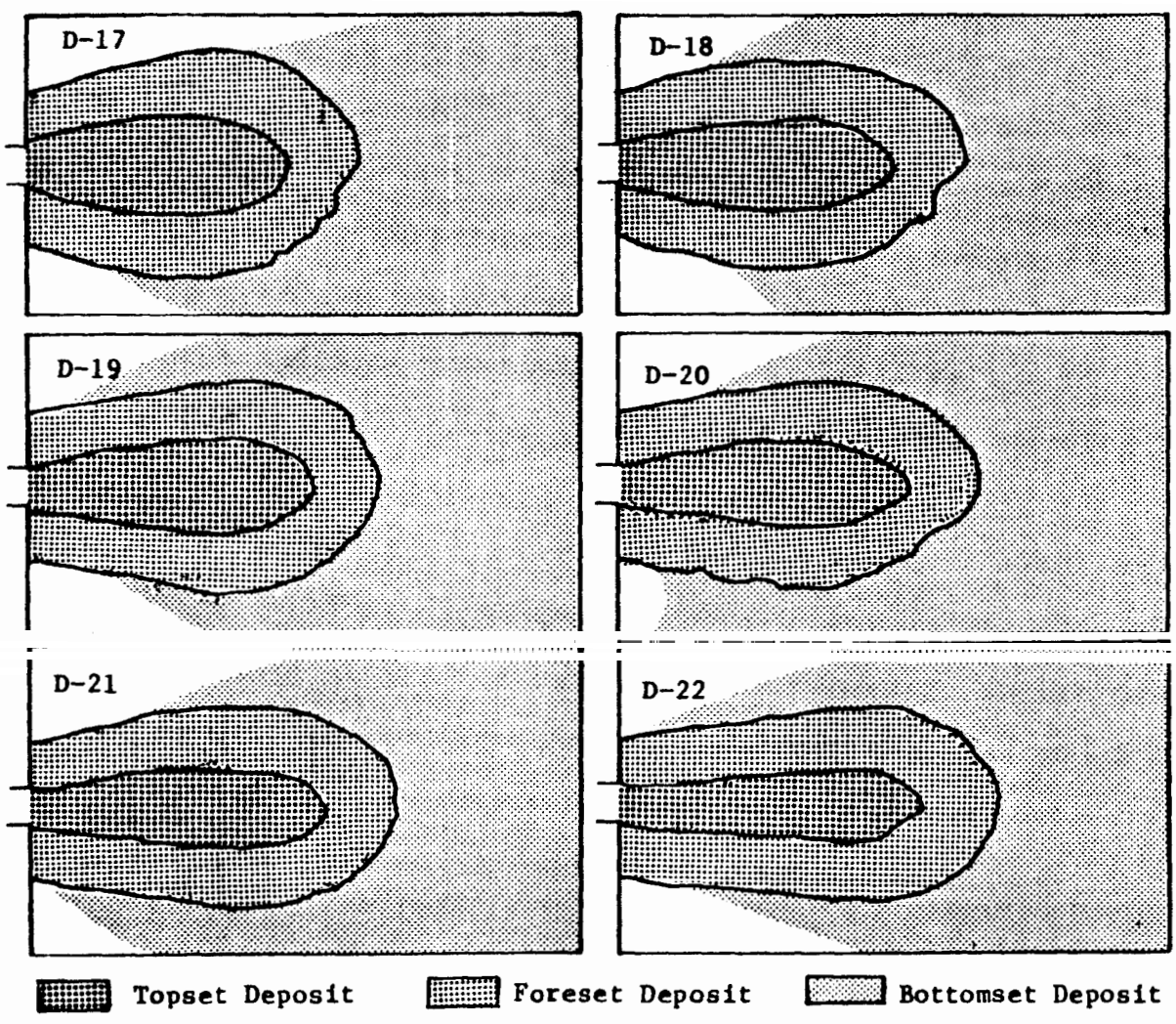

Figure 12b. Maps showing Areal Extent of Top-, Fore- and Bottom-set Deposits of Series D. Scale is 1cm to 20cm.

morphologies, progradation of the deltas displayed differential growth in the linear measurements of the morphometries. The measurements are listed in table 6 and demonstrate that the relative increase in one direction of the delta growth tended to be adjusted by a relative decrease in other directions. The compensatory adjustments or the differences in the measurements of the delta-configurations are thought to be due to the differential sediment-input rates used in the runs.

The morphological delta features were least developed in this series. Photo-plate 5 illustrates some of these features. Although formed, the submerged natural levees were small. The indistinctness of the levee formation was more pronounced in the runs with high sediment transport. That is, the formation of the natural levees in runs 17, 18, 19 was least developed, showing shadowy forms. But, some kind of broad-based and low-height shoaling were characteristically associated with these runs. On the other hand, the submerged natural levees of runs 20, 21, and 22 were relatively distinct (Photo-plate 5). However, no bar or shoal was seen to evolve in these runs; rather, some degree of concavity (laterally) along the flow-bed was clearly evident. In general, the depositional surface was characterized by the formation of irregular and low-built sandwaves. Almost in the middle of runs 17, 18, and 19 the formation of a strong vortex-system was observed. The vortices were noted to move more or less, along the centre-line. They seemed to be responsible

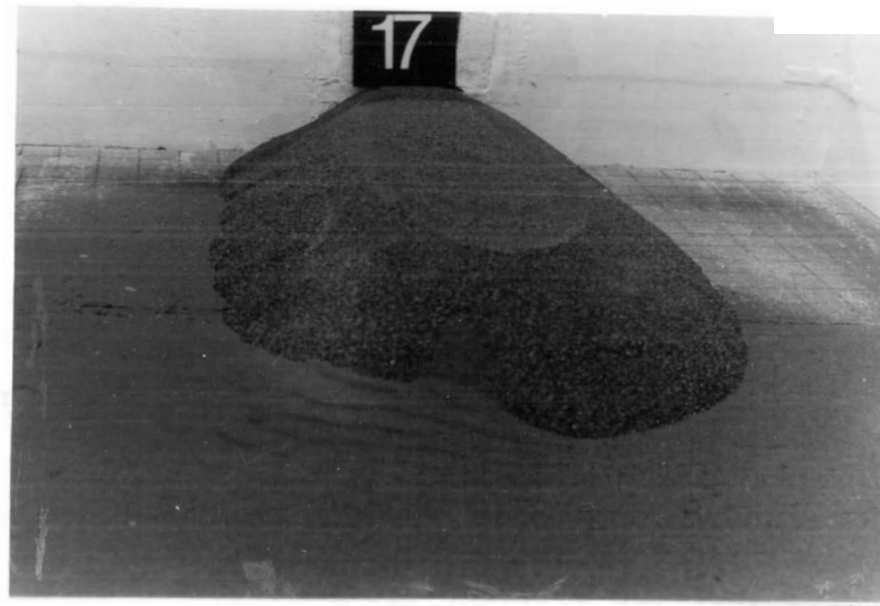

(a) A view of sandwaves formation, partly buried under the foreset deposit.

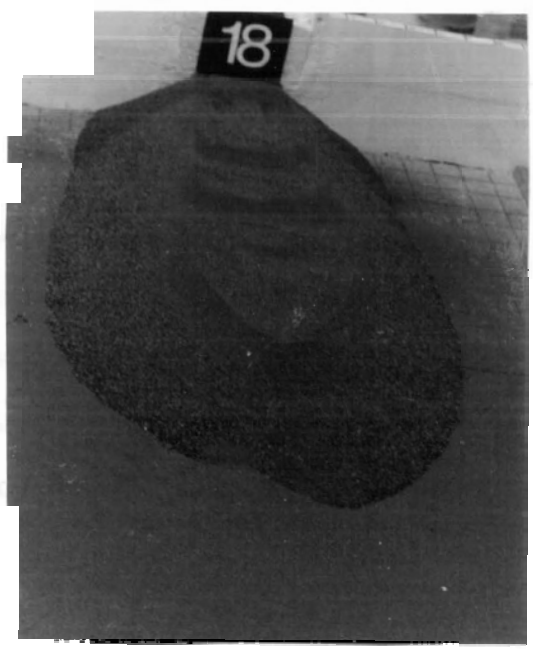

(b) Typical shoal formation.

(c) Natural levees and sandwaves.

PLATE 5. PHOTOGRAPHS ILLUSTRATING DELTA FORM - TYPICAL OF SERIES D.

for the formation of sandwaves, as seen in photo-plate 5 in partially buried form.

5.1.5 Series E

Table 7 lists the parametric information of Series E. The series represents six test runs through which a constant rate of flow, 901.10 cm^3 /sec. was passed. In the sediment-free flow system the average velocity and flow-depth of the flume channel were recorded as 50.48 cm/sec and 1.75 cm. respectively. The Froude Number was computed to be 1.2189 indicating upper regime flow in the channel.

Figure 13 represents the hydraulic geometry of the axial jet expansion drawn on the basis of velocity data listed in tables 1 and 2. As observed in the experiment, the zone of flow establishment was terminating at an approximate longitudinal distance of 36 cm from the efflux-section. The central core of the zone was marked by surface undulations. At the terminus of the zone of no diffusion, the surface water was observed to be forming boils. By and large, the character and behaviour of the jet were comparable with the jet pattern of Series A.

The average velocity, 50.48 cm/sec. was found competent to transport all sediment into the flume basin. Part of the load was observed to creep along the sides of the channel bed, forming bands of mobile sediment. It appeared that the higher

Table 7

Series E: Variation of Sediment Transport Rate

Parameters constant for each run

Channel depth (cm)	1.75
Channel width (cm)	10.20
Channel slope	0.002
Average velocity (cm/sec)	50.48
Water discharge (cm^3/sec)	901.07
Froude Number	1.2189
Basin depth (cm)	11.75
Sediment quantity ($x10^4$ gm)	5.10
Mean grain size (mm)	0.365
Water Temperature (^{0}C)	13.80

Variables between runs	Run 1	Run 2	Run 3	Run 4	Run 5	Run 6
Time ($x10^3$ sec)	1.20	1.92	2.52	3.416	5.11	10.92
Sediment input rate (gm/sec)	42.50	26.56	20.24	14.93	10.00	4.67
Delta length:						
Max. XT (cm) bs	78.00	80.50	82.50	84.10	86.40	90.00
Max. XF (cm) bs	97.50	100.20	102.00	104.00	106.30	108.80
Delta width:						
Max. YT (cm) bs	21.50	20.00	19.50	18.60	19.00	20.20
Max. YF (cm) bs	53.00	51.50	51.00	48.00	48.10	46.80
Vertical accretion:						
Max. ZT (cm)	10.10	10.05	10.05	9.85	9.60	9.45

the sediment-input rate, the wider was the band. The other part of the sediment was carried in suspension as well as through saltation or skipping. In other words, the series involved both bed-load and suspended-load transport mechanics.

From the beginning to the end, the pattern of sediment dispersal and deposition of the series appeared very much like series D, although they differed widely in terms of the discharge variable. The initial deposition occurred in two ways. First, a fan-shaped carpet of finer sediments appeared on the basin bottom. Second, coarser sediments moving along the channel bed settled collectively to form an elongated pile. At a stage of the upward growth, the accreted form tended to constrict the flow, resulting in the intensification of the turbulence activities of the flow components. Following this development, a flat-bed atop the depositional surface evolved, over which the flow seemed to diverge. The degree of divergence was, however, less than that of series D.

Figure 13b represents the maps of the deltas produced in series E. Like Series D, the depositional pattern of the series was symmetrical about the principal axis of deposition. However, the linear measurements of the morphometries showed that the deltas of this series were of the relatively advancing type (table 7). It seems, as a rule, that the relative progradation of the deltas in one direction was being compensated for by the relative decrease in the other direction. Such figurative

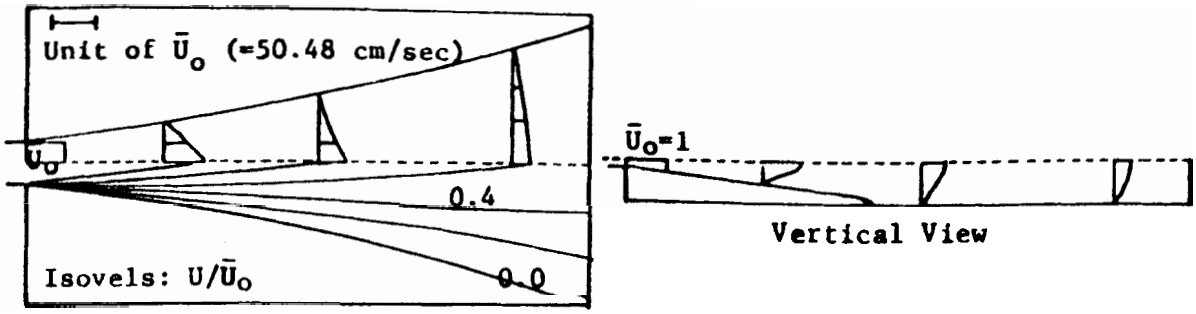

Figure 13a. Hydraulic Geometry of Jet Expansion - Series E.

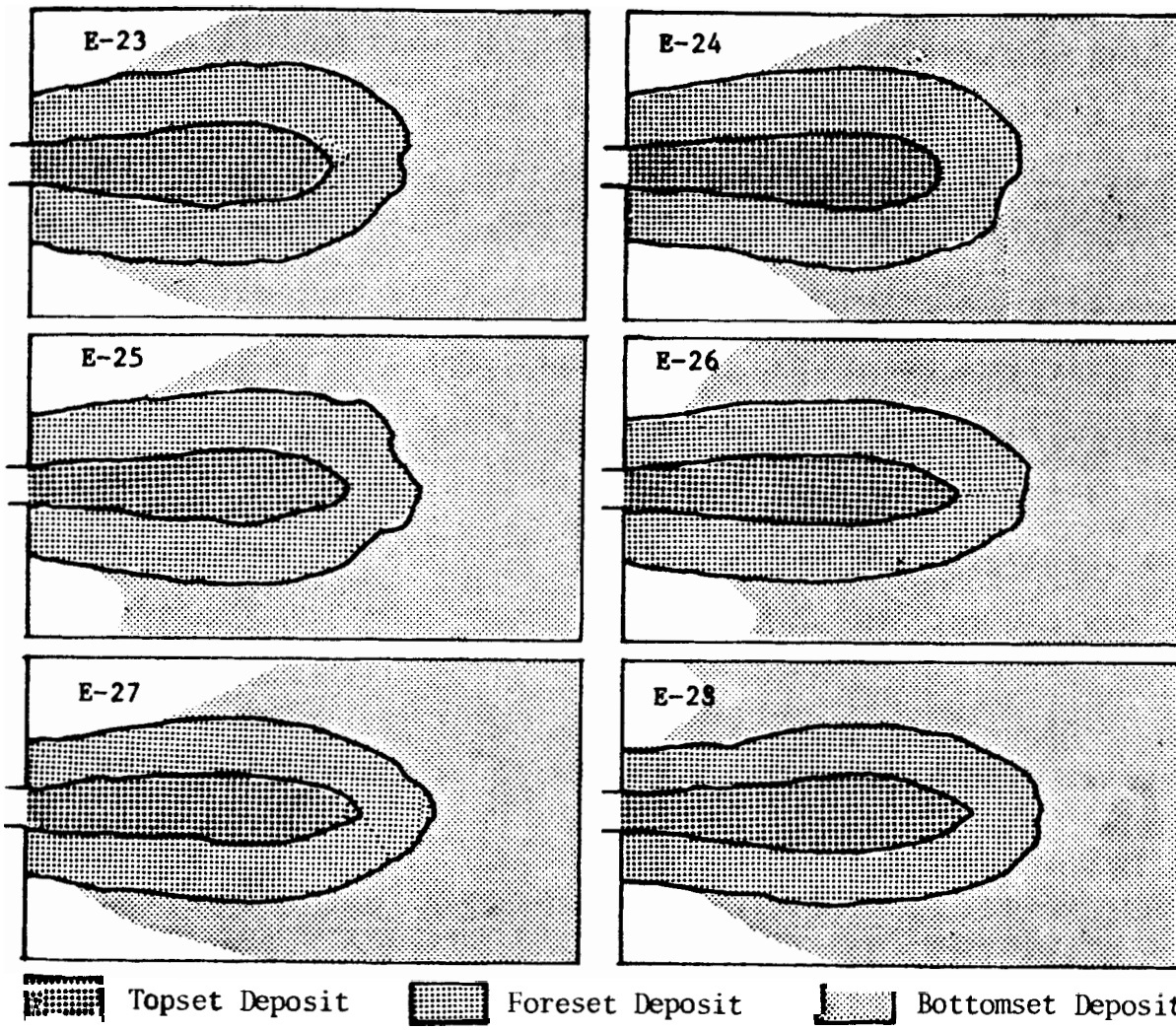

Figure 13b. Maps showing Areal Extent of Top-, Fore- and Bottom-set Deposits of the Series E. Scale is 1cm to 20cm.

adjustments to the deltas are thought to have been contributed by the differential rates of sediment transport.

The morphological delta features are shown in photo-plate 6. The submerged natural levees of the deltas were low-built, but continuous. They were more distinct in the runs with low discharge of sediment transport. That is, run 28 formed natural levees more discretely than did run 23. There was no tendency to form some kind of shoal in runs 26, 27, 28: rather, the delta surface of these runs displayed a concave channel-bed across the lateral axis. However, very shallow-built shoals were found to evolve in runs 23, 24, and 25. Branching or bifurcation of the main flow was observed to be absent throughout the experiment. As in series D, relatively symmetrical sandwaves were built in runs 23, 24, and 25, and some of the partially exposed sandwaves are seen in photo-plate 5. Importantly, most of these features, as well as the overall configuration of the deltas, cannot be adequately described in terms of the axial jet flow pattern of the experiment.

5.2 Effects of the velocity variable and the rate of sediment transport on the dimensional growth of deltas

In this section the use of velocity as the variable in place of discharge is thought to be logical because of two considerations. One, the velocity variable, most commonly the

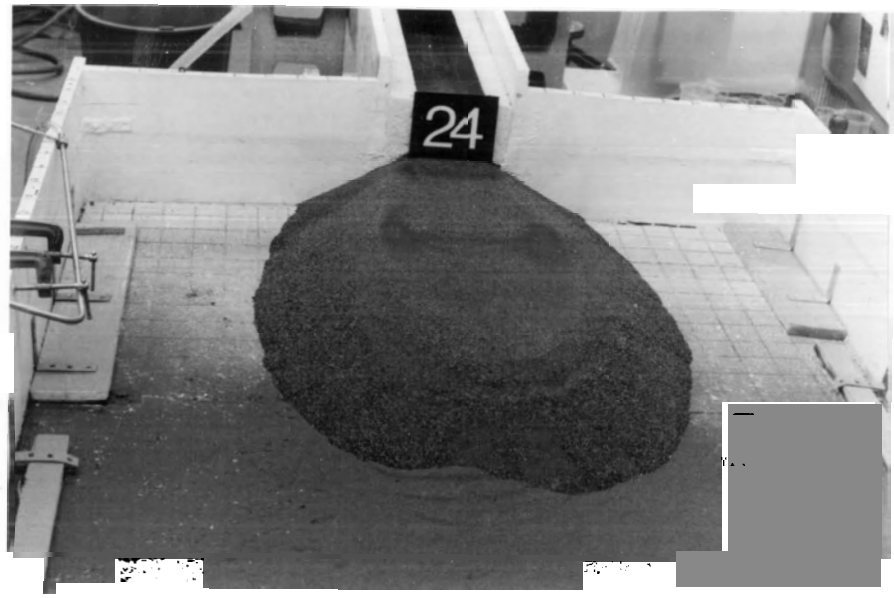

(a) Formation of low-relief and wide-based shoals.

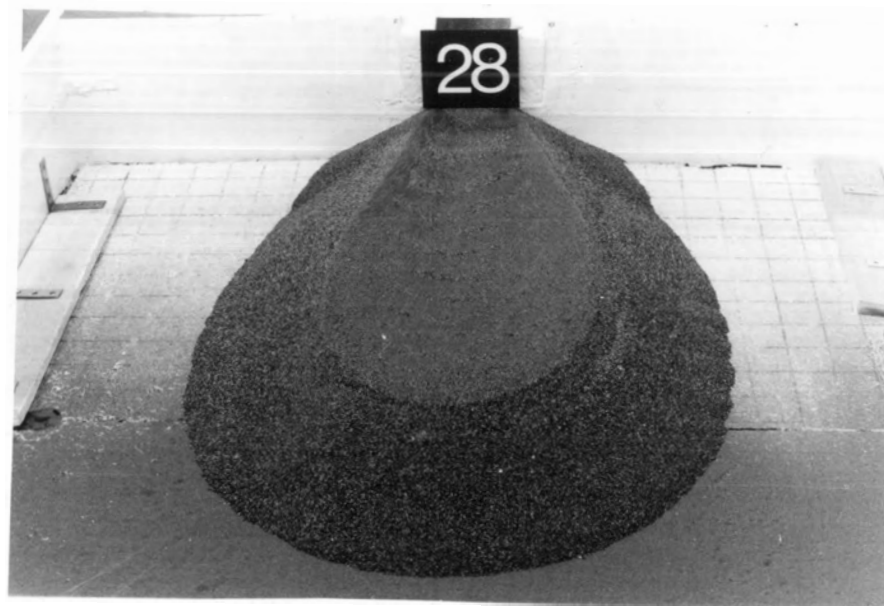

(b) Formation of submerged natural levees.

PLATE 6. PHOTOGRAPHS ILLUSTRATE THE MORPHOLOGICAL DELTA PATTERNS BUILT IN SERIES E.

average velocity, is a power function of discharge (Leopold and Maddock, 1953), and the other, velocity, is an index to the dynamics of transport and deposition. The dimensional delta growth is represented here by the deltaic component in terms of the maximum length, width, and vertical deposition measured at the terminal coordinate in the direction parallel to their respective axes.

From the preceding section it is already apparent that the morphological delta pattern developed very differently in different discharge and sediment transport conditions. But, the observed linear measures of the delta morphometries suggest that the dimensional growth, both in magnitude and direction, of the deltaic deposits are functions of the volume and character of the flow, and sediment load transport. It is desirable to formalize these relations as follows. For a given sediment discharge, an increase in flow velocity causes a relative increase in longitudinal length, with concomitant decreases in both vertical and lateral growth of the deltaic mass. Conversely, at a given discharge variable, an increase in sediment load tends to retard the longitudinal length, and is effectively related to increases in width and vertical accretion of the delta formation. In the following subsections, these are discussed in some detail.

5.2.1 Longitudinal delta length versus average velocity

Figure 14 is the semi-logarithmic plot, shown in two parts, of the average velocity against the maximum delta length. Plot A relates the measurements of the maximum delta length extending over to the break of slope of the foreset bed, and plot B is representative of the maximum length measured at the terminus of the topset bed. In the figure, the Y-axis is in linear scale showing delta length as the dependent variable, and the x-axis represents average velocity on the logarithmic scale. The data forming the basis of these plots are presented in the discussion of the series in section 5.1.

The straight lines in the graphs (Figure 14) are parallel, and most of the points lie within a narrow limit of scatter. The graphical representation of the straight lines in the figure clearly demonstrates a functional relationship between the velocity variable and delta lengths. However, the relationship is in semi-logarithmic form and can be expressed as $Y = m.\log X + C$, where Y and X represent delta length and average velocity, and m and c are slope and intercept, respectively.

The trend of the straight lines as well as the calculated values of m of the plot A and B (mean values being 125.35 and 109.80 respectively) illustrate positive slopes, indicating that an increase in the velocity variable is accompanied by a relative increase in delta length. Because average velocity is

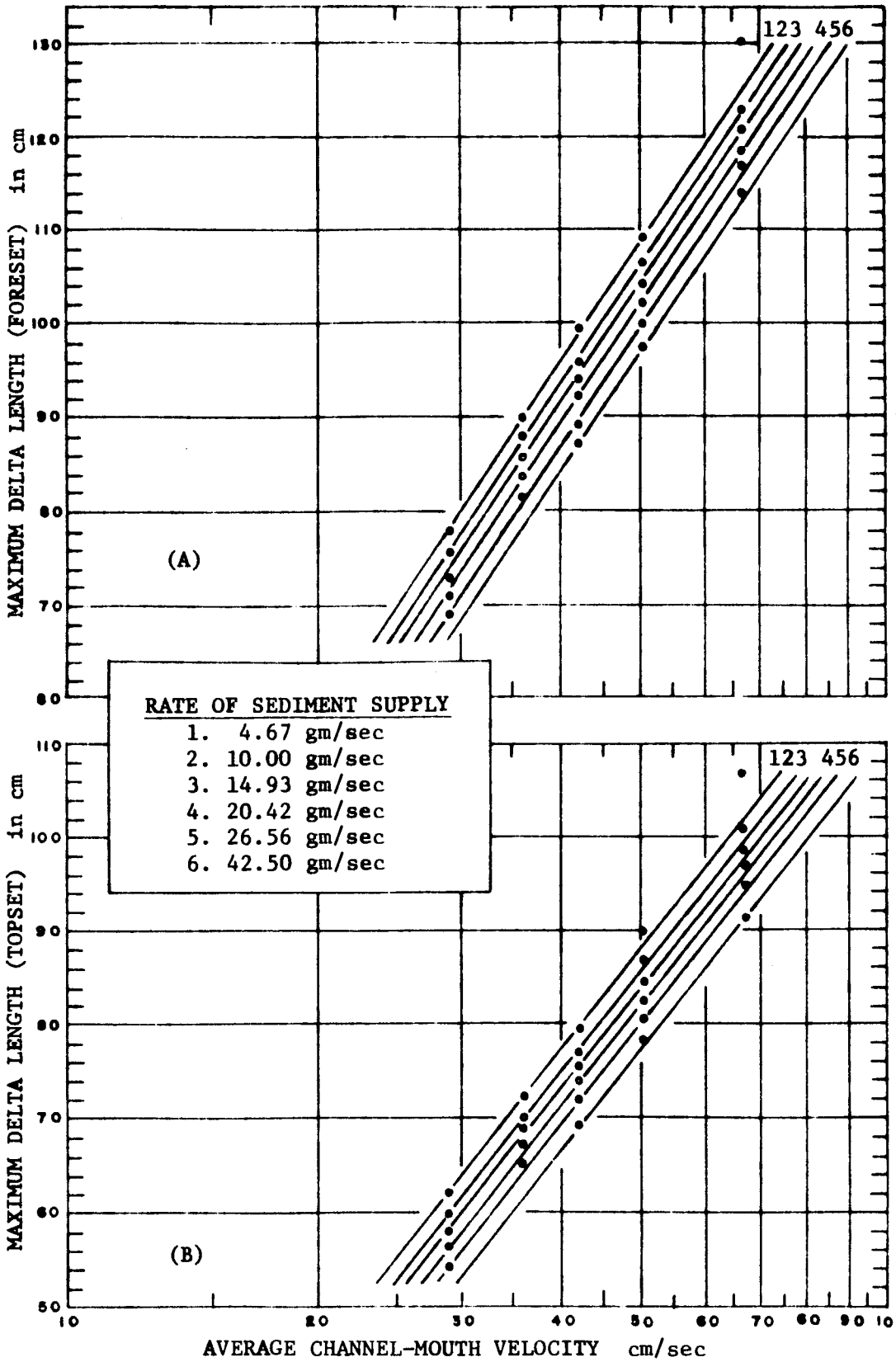

Figure 14. Relation between Average Channel Velocity and Maximum Delta Length.

directly proportional to log X, the average velocity varies several orders of magnitude in order to change the delta length by a relatively small measure. Conceptually, the relation is regarded as an attribute of the flow power, that is, the rate at which the flow performs work. For a steady and uniform flow, flow power is generally described as a product of the mean velocity and boundary shear stress. However, in turbulent flow there is an addition of the internal resistance factor (to shear stress) which is related to the structure and intensity of turbulence formation. The flow strength is also viewed in a way which provides the rate of energy expenditure involving external and internal frictional losses. Despite these conceptualizations, the average velocity seems to be providing significant relations in the present experimental conditions of delta formation.

The graphs also reveal a few other characteristics. One of them concerns spacing between the straight lines (Figure 14) suggesting the involvement of a certain other variable in the experimental situations. Conceivably, the known variable in this case is the differential rate of sediment transport. In fact, each of the straight lines in the graphs represents a constant rate of sediment input. The departure of some of the points from the straight lines is also seen in the plots (Figure 14). Most likely they are related to the generation of secondary motion within the main forward flow, resulting from the interaction

between form and high inertia flow.

5.2.2 Longitudinal length of the deltas versus sediment-input

Figure 15 shows the logarithmic plots of the maximum delta length against the sediment transport rates. The vertical scale is proportional to the logarithm of delta length and the horizontal scale is the log of sediment input rate. The figure illustrates two different graphs measuring the maximum delta length with reference to the terminal coordinates of the foreset and topset beds, respectively. The data forming the basis of these plots are listed in table 3-7.

As is evident from figure 15, the general alignment of the plotted points has given a straight line relation between the delta length and sediment transport rate. The straight line relation can be expressed in the functional form, Log Y = m. Log X + C, whereby X and Y represent sediment rate and delta length, respectively.

The above expression clearly demonstrates that the delta length is a simple power function of the sediment transport rate. It must be remembered that the generalization is restricted to the present experimental situation. As seen in the graphs (Figure 15), the slope (m) is obviously negative. It stipulates that the relationship is in inverse form. That is, at a given condition, delta length increases with the decreasing

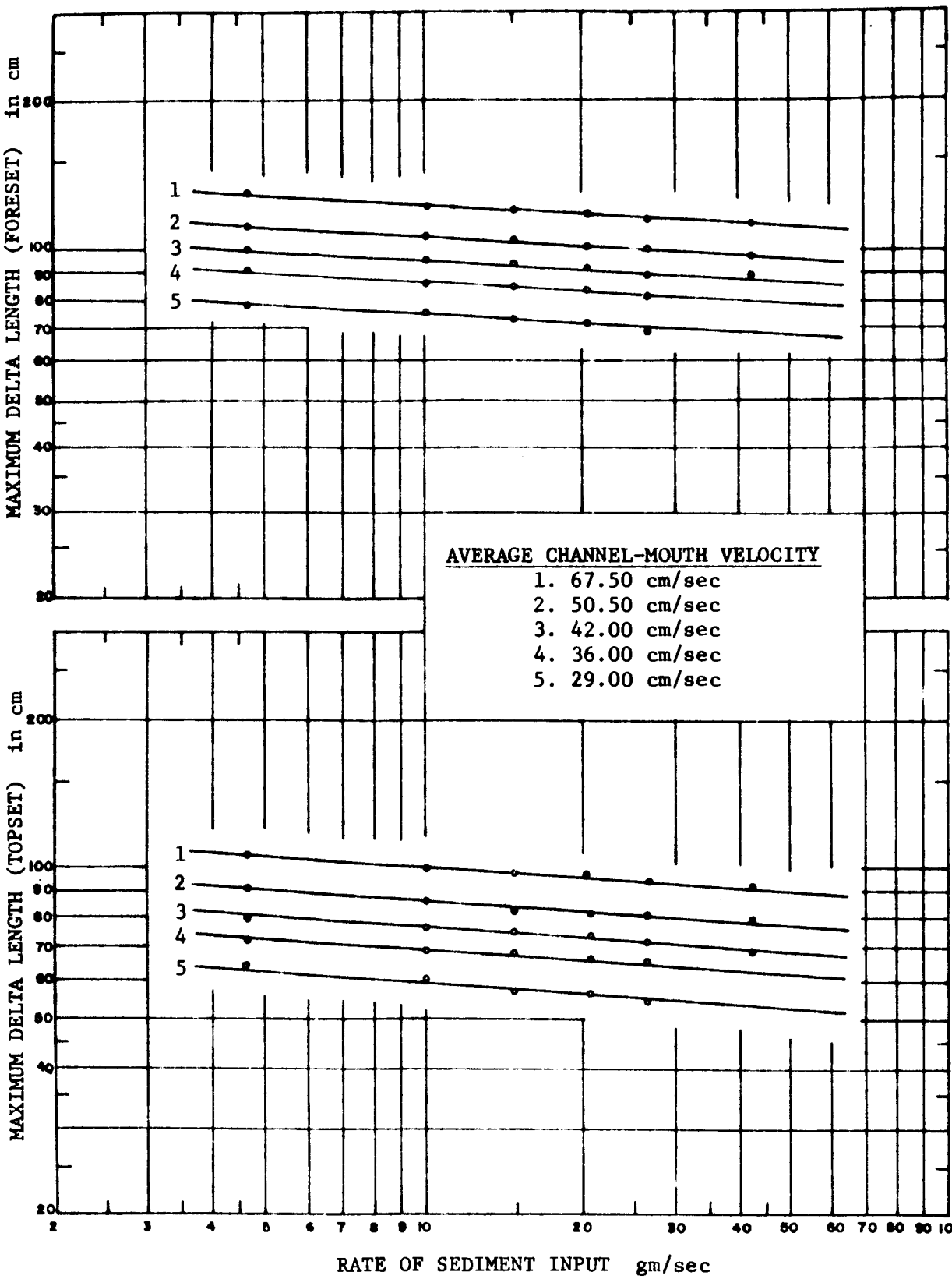

Figure 15. Relation between Rate of Sediment Supply and Max. Delta Length.

sediment transport rate in the form of a power function. The other way to say this is that the increase in load transport tends to retard the longitudinal length of the deltaic deposit, suggesting that the transporting ability of the flow in the longitudinal direction is somehow reduced by the increased rate of sediment transport. Although the effects of sediment load on the flow are not clearly understood, it is generally thought that a part of the kinetic energy is consumed in the transportation of the load (Mackin, 1943). Chow (1959) suggested that the energy expenditure is only due to the bed-load transport. These apportioned energy losses most likely cause lowering of the competence of the flow, which in turn assists the rapid dumping of the load at the channel mouth, thereby forming a pile. The upward growth of the pile at some stage tends to constrict the flow. If the flow is sufficiently strong, it continues to maintain its course in the convergent pattern, causing the depositional mass to advance quickly. On the other hand, if the current is not strong enough, the flow gradually flares when opposed by the vertical accretion, forming a divergent pattern over the delta platform. The divergent flow was observed to cause sediment wedges at the periphery of the depositional platform, involving frequent slumpings to prograde the delta.

The straight lines in figure 15 are clearly parallel suggesting different values of the intercepts. In other words,

the spacing between the straight lines in figure 14 directly indicates that certain other variables are involved in the experimental situations. Understandably, the primary variable in this context is the discharge factor. In fact, the line at the top of the graphs represents a constant discharge of 1377.00 cm^3 /sec per second while the bottom line represents the lowest rate of flow, which is equal to 295.80 cm^3 /sec.

5.2.3 Relation between the maximum delta length and width,

Figure 16 is the graphical representation of the maximum delta length against its corresponding maximum width. The data forming the basis of these plots are shown in table 3-7. The figure has two graphs, each representing the respective length and width related to the terminus of the foreset and topset beds. Although there is a considerable scatter of points, a curvilinear graph has been fitted. The purpose of this attempt is to provide a rough generalization in the compensatory adjustment of the length and width of the deltas.

Despite the scatter about the curves, the graphs clearly demonstrate that when delta length increases, its width decreases. It suggests a balancing tendency in the linear expansion of the deltaic deposition. The relative increase in longitudinal length, and the compensatory decrease in the width of the deltas are primarily a function of the volume and

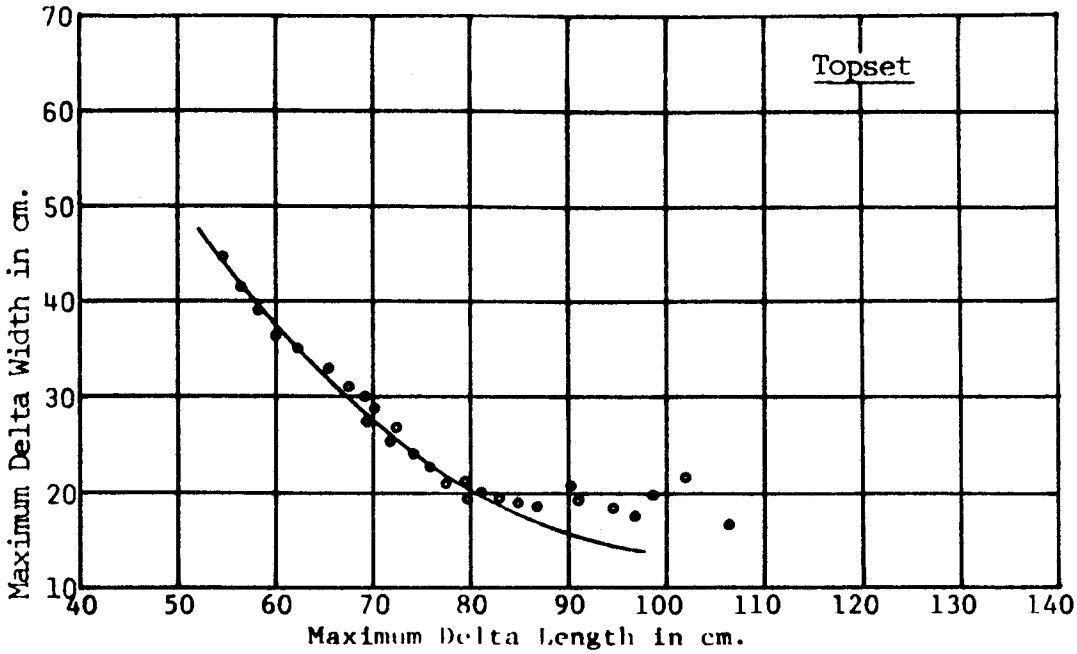

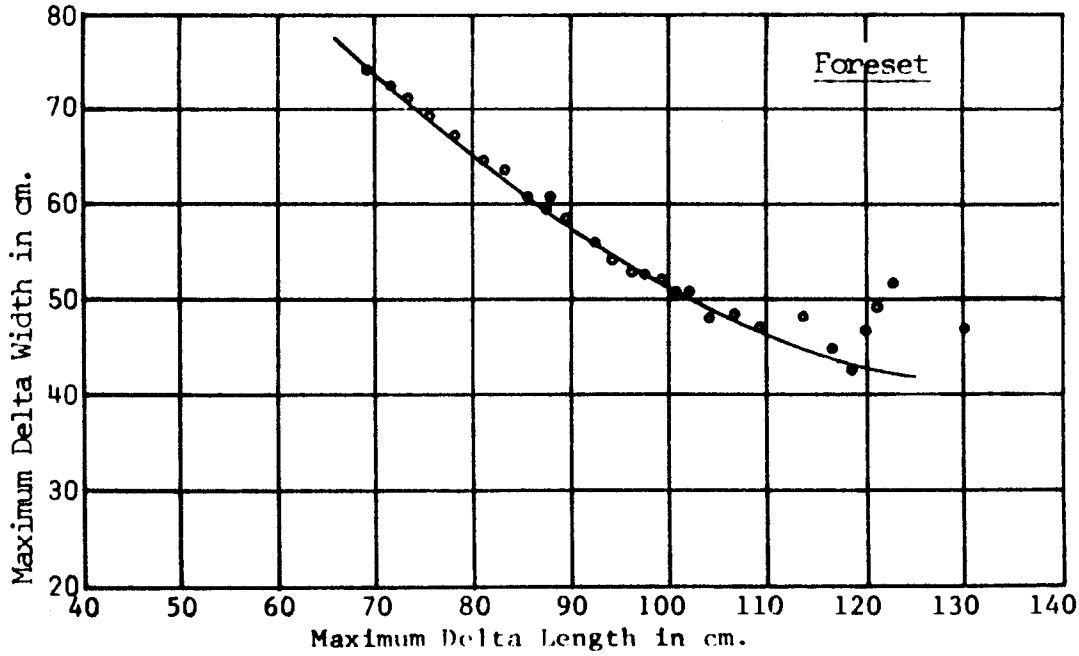

Figure 16. Relation between Maximum Length and Width of the Deltas.

character of the flow, and to some extent the volume of sediment load carried per unit of flow discharge. Broadly, at high discharge and low sediment load transport, delta progradation advances quickly, and is caused by the convergent flow passing over the delta platform. On the other hand, at low discharge and high sediment transport, the lateral progradation of the deltas is highly significant and is thought to be caused by the divergent flow pattern which involves frequent slumpings.

5.2.4 Relation between the vertical accretion and the length of the deltas

Figure 17 is the plot of the maximum longitudinal length (extended to the terminus of the topset bed) against the corresponding maximum vertical growth of the deltas. The maximum height of the vertical accretion was carefully measured to exclude all small bed-forms (ripples, sandwaves) and the natural levees. The data forming the basis of the plot are listed in table 3-7. It is important to remember that all deltas were produced at a constant quantity (5.1×10^4 gm) of sediment-fed.

The plots in figure 17 demonstrate that as delta length increases, the vertical height of the upward growth correspondingly decreases. It stipulates that a rapidly advancing delta develops a low measure of upward growth. As a rapidly advancing delta is primarily a function of high inertia

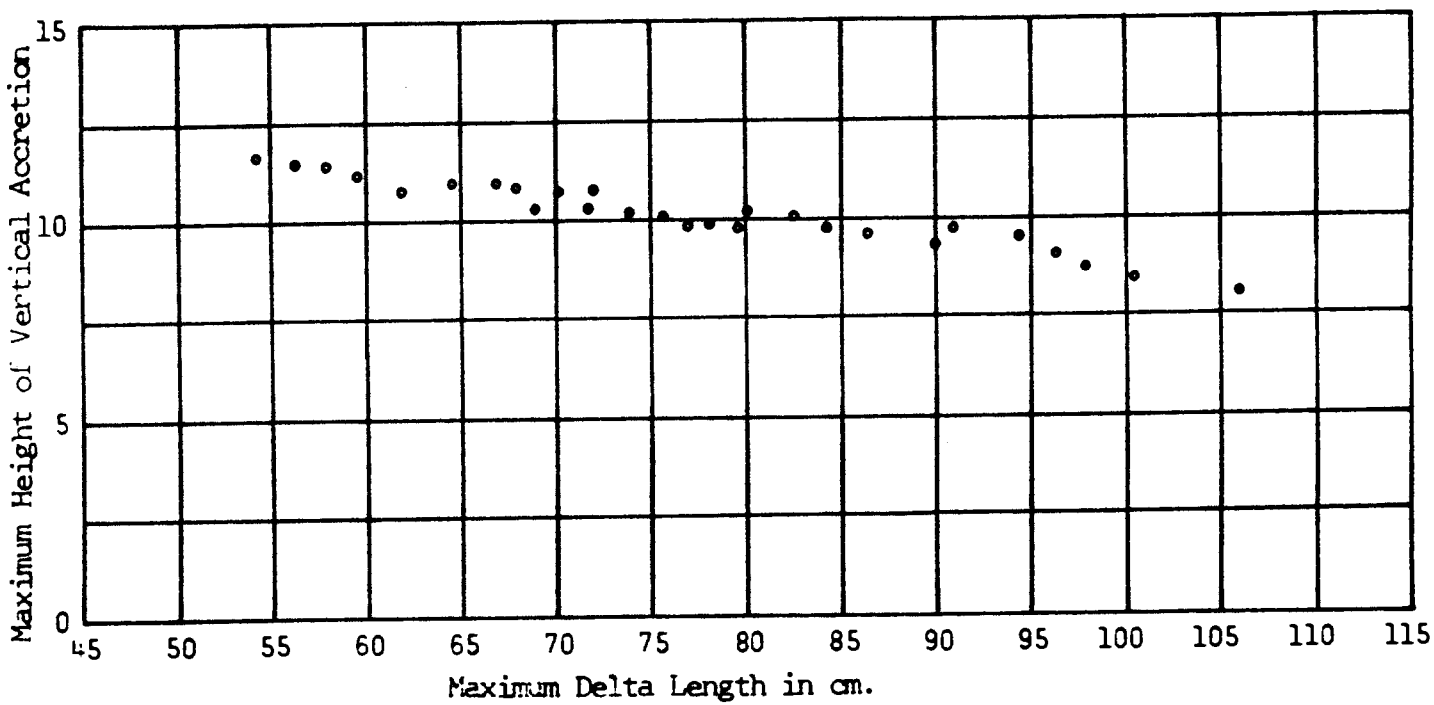

Figure 17. Relation between Maximum Vertical Accretion and Longitudinal Delta Length. V.E.= x 2

flow, and to some extent low sediment load transport, it follows that low discharge and high sediment transport conditions effectively promote higher upward growth of the deltas. This was clearly noticed throughout the experiment.

The afore-described relation is clearly illustrated in figure 18 where each graph representing a run of a series is roughly indicative of the general trend of the vertical accretion along the longitudinal length of the deltas. The relation may appear very simple, but its implication seems to provide a useful basis in the interpretation of the sedimentation problem at the channel mouth. As observed in the experiment, the low discharge and, to some extent, the high transport rate tended to increase the overall vertical accretion through rapid dumping of the sediment load at the efflux section. There appeared a limit of upward growth at which vertical accretion was no longer possible. The limit was described by Sloss (1962) to be an equilibrium surface (base level), which is presumably determined by the interaction of the volume and character of flow, the quantity and properties of the transported load, and the boundary conditions. Because of these, the relative levelling of the depositional surface was always higher when the flow discharge was very low and the rate of sediment transport high. Since the water level of the basin was assumed to be constant throughout the experiment, the relative increase in the vertical height of the upward growth connotes a

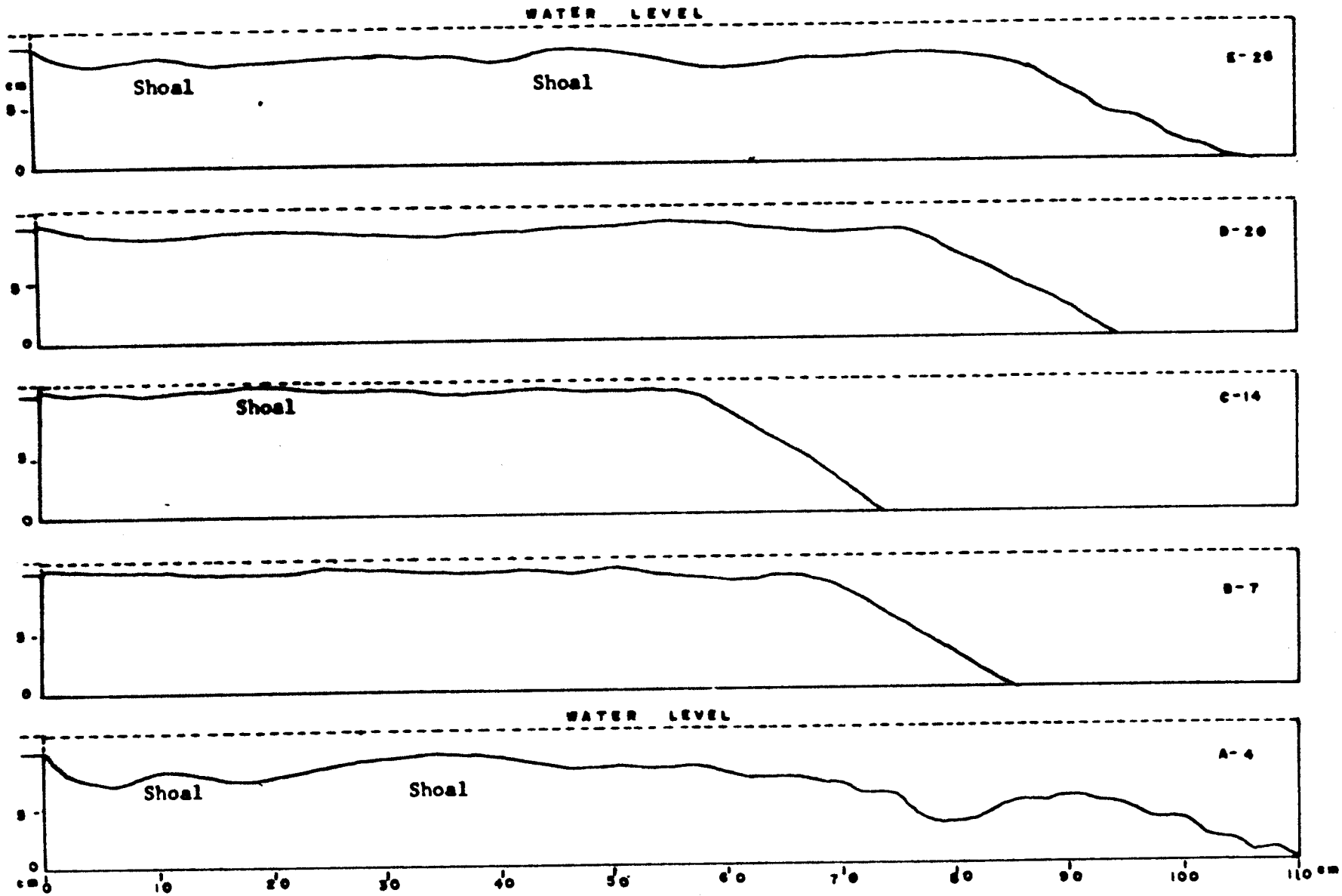

Figure 18. Longitudinal Profile along the Center-Line of the Deltaic Depositions.

decrease in flow depth over the depositional surface.

5.3 The morphological features and the structure of the deltas

It has been noted in the previous sections that the overall development of the delta-morphometry is greatly controlled by discharge and, to some extent, by the sediment transport conditions. In the present section, an attempt is made to describe the superficial morphologies and internal structure of the deltas, and the causes of their variations and distributions.

The morphological delta feature may be very differently developed in different discharge and sediment transport conditions. But, the features generally reflect the totality of the flow indicating that they are effectively controlled by the volume and intensity of the outflow passing over the primary deltaic deposit. Importantly, the features were noted to form at some stage of the delta progradation and were characteristically related to the nature of the convergent or divergent flow pattern forming over the deposition. The degree to which the moving water converged or diverged seemed to be determined by the mutual interaction between the flow and the accreted depositional form of the upward growth.

The usual picture of the delta structure comprising the topset, foreset, and bottomset beds, classically described by

Gilbert (1885), was noted to form distinctly throughout the experiment. But the structural designs of the beds were found to differ according to the flow and sediment transport conditions. In the following subsections these are discussed in some detail.

5.3.1 The submerged natural levees

The submerged natural levee is one of the most common depositional features of delta morphology. Not all series showed its discrete formation, nor were the natural levees built up with equal dimension in the runs. By and large, series with high discharge conditions tended to form discrete natural levees, suggesting that the greater volume and higher intensity of the outflow are significantly related to the formation of the natural levees over the primary deltaic deposit. Figure 19 demonstrates the dimensional growth of the natural levees of the five runs showing cross-section along the longitudinal distances of 5, 25, 45. 65, 85 and 105 cm from the channel mouth. Each run represented a particular series, indicating identical parametric conditions except for the discharge variable. In fact, run 6 of series A and run 16 of series C (A-6 and C-16 in figure 18) are representative of the highest and lowest discharges, respectively.

The formation of the submerged natural levees appeared to be directly related to the nature of the flow pattern that

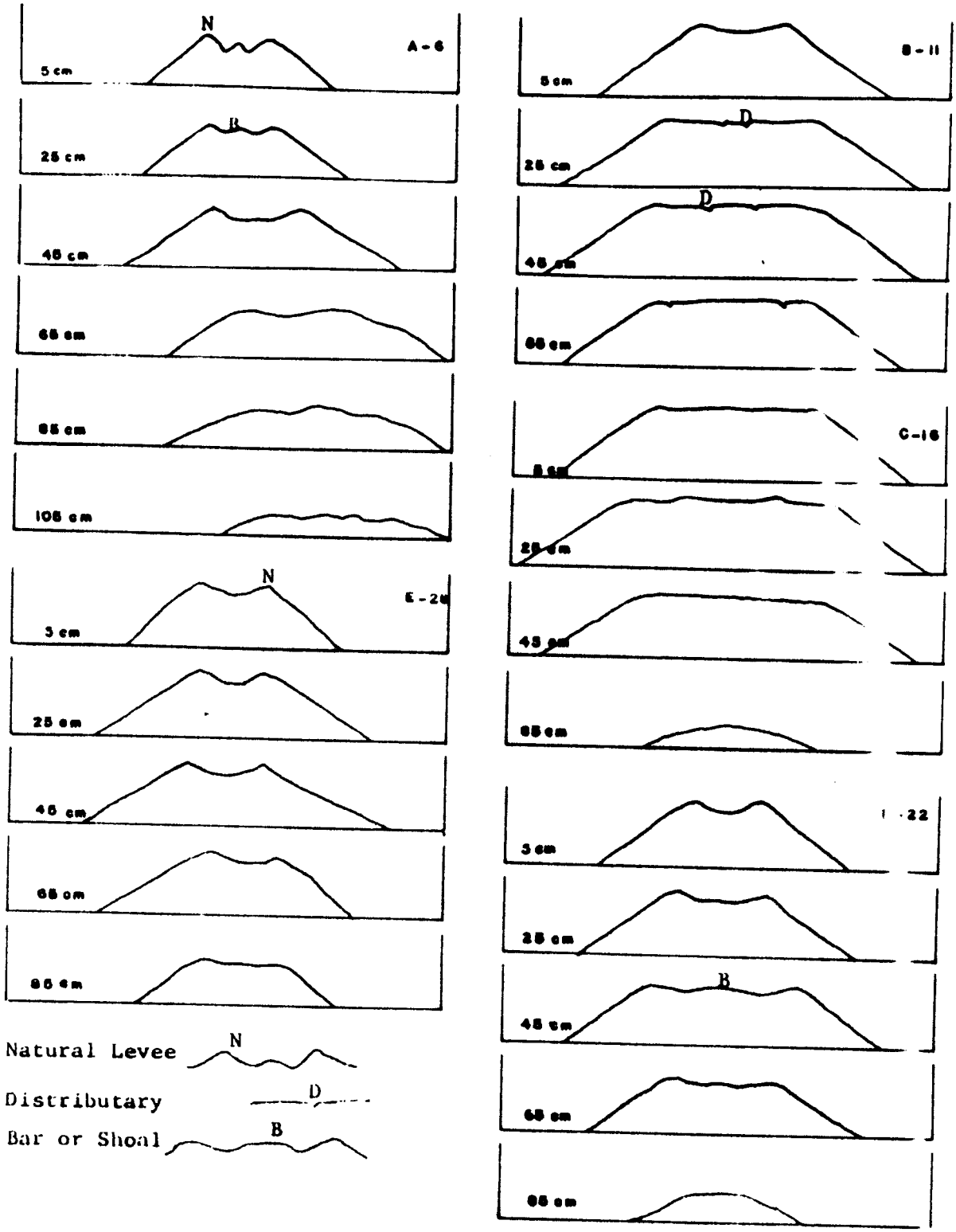

Figure 19. Cross-Sectional Profile of the Deltas at the selected Distances from the Channel-Mouth. Scale is 1cm to 10cm.

developed over the primary deltaic deposition. The flow pattern may be described as being of the convergent and divergent type, and is thought to be a consequence of the mutual interaction between the flow and the vertical accreted form of the deltas. Broadly, the divergent flow pattern over the deposition occurred at low flow discharge and high bed-load transport conditions. These conditions involve dumping of sediment load at the efflux section, promoting rapid upward accretion. Eventually, the vertical deposition tends to constrict the flow. Depending on the competency of the current, the flow tends to diverge or flare-up when it fails to truncate or erode the surface of the deposition. The divergent flow seemed to form a radiating pattern forming streamlines as recognized by the radiating pattern of sediment movement shown in the photo plate 7. As the direct result of this radiating flow pattern, wedges of sediment tended to form around the periphery of the depositional surface involving frequent slumpings. The frequent slumpings seemed to prevent levee formation, but were related to the widening of the delta progradation.

On the other hand, at high discharge the flow pattern tended to remain relatively convergent, suggesting that the flow was hydrodynamically more competent. The relatively high inertia flow when subjected to the resistive effects of the primary depositional form generates intense turbulence which often causes rotatory motion in the forward flow. Depending upon the

PLATE 7. A VIEW OF THE RADIATING PATTERN OF BED-LOAD MOVEMENT. THE PATTERN IS INDICATIVE OF THE STREAMLINES OF THE DIVERGENT FLOW.

scale and intensity of turbulence the process of transfer of water particles, and thus of the sediment particles, according to their heavier grade-size takes place. As a result, the particles move away from the threads of maximum turbulent interchange to settle where the degree of turbulence is less. The turbulence caused by the interaction of the flow and form seemed to propel the sediment load with intense upward and transverse components, eventually leading to the formation of the natural levees. Photo-plate 8 illustrates some of the natural levees formed at the given input conditions adopted in the runs.

5.3.2 Shoals, bars and the micro-bed forms

Broadly, the formation of the shoals and bars may be attributed to localized conditions of overloaded flow. That is the flow, for one reason or the other, fails to move the available load, which causes aggradation, forming shoals and bars on the flow-bed. The rate of aggradation is, however, dependent upon the flow velocity as well as on the amount of load entering the region. In the present experiment, most of the runs produced shoaling of one kind or the other. Some of them were very well-defined. Photo-plate 9 illustrates a typical shoal or the bar formation produced under different parametric conditions of the series. They represent various shapes and

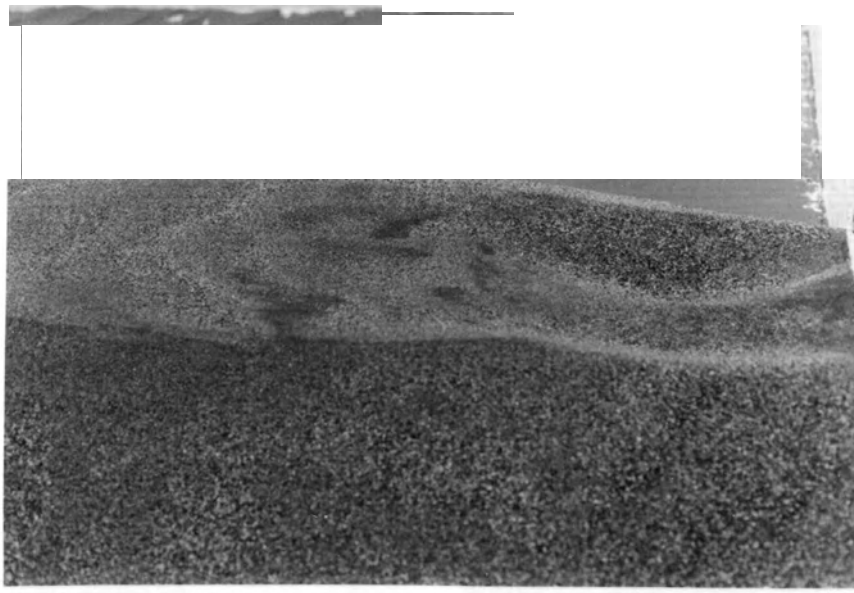

(a) A view of the submerged natural levees. The forms are typical of Series A.

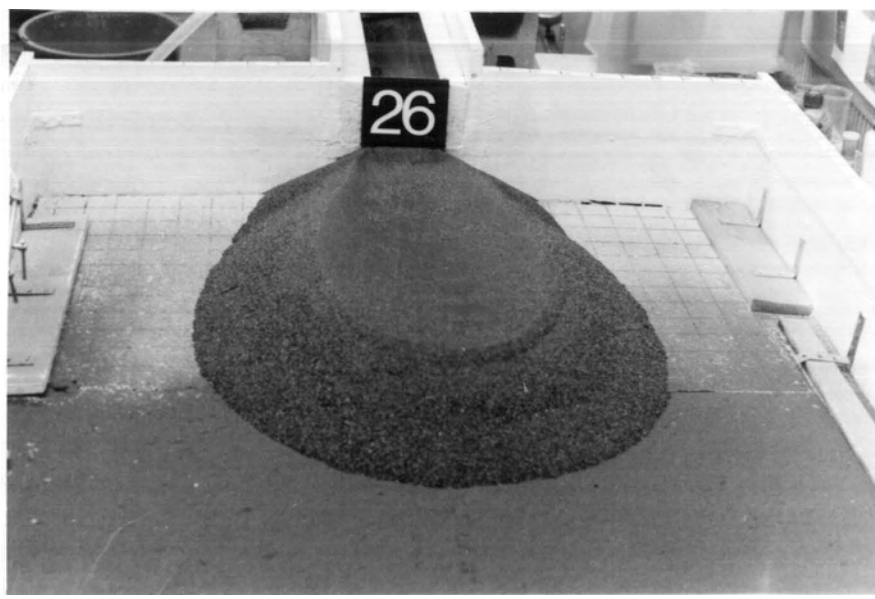

(b) A view of the low-relief natural levees of Series E.

PLATE 8. PHOTOGRAPHS ILLUSTRATE THE FORMATION OF SUBMERGED NATURAL LEVEES UNDER DIFFERENT INPUT CONDITIONS OF THE SERIES A AND SERIES E.

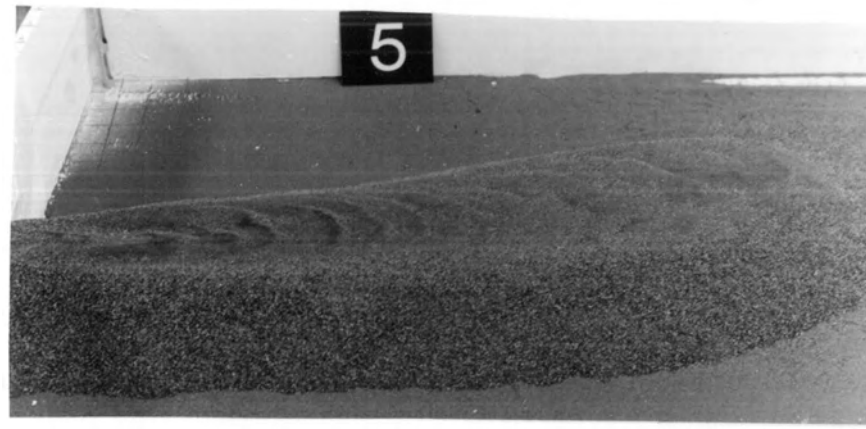

(a) A longitudinal bar and natural levees.

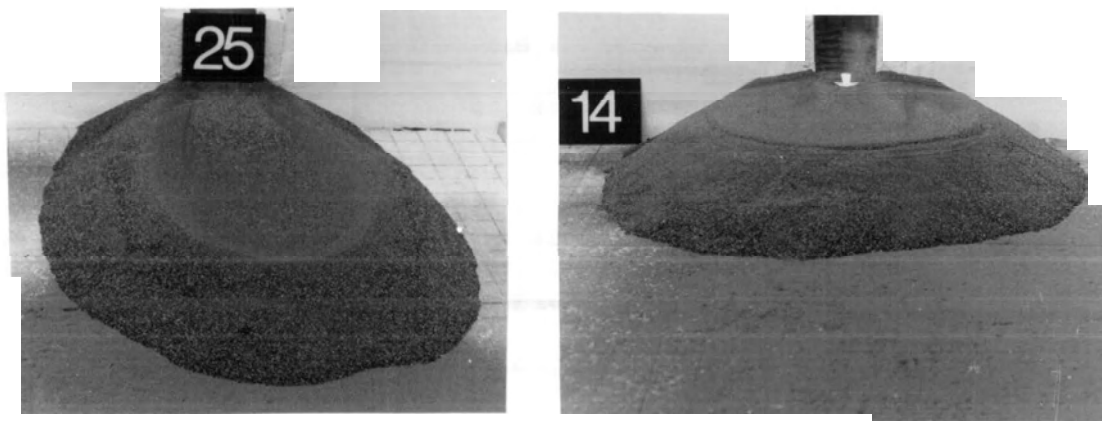

(b) A typical formation of the circular-plan bars.

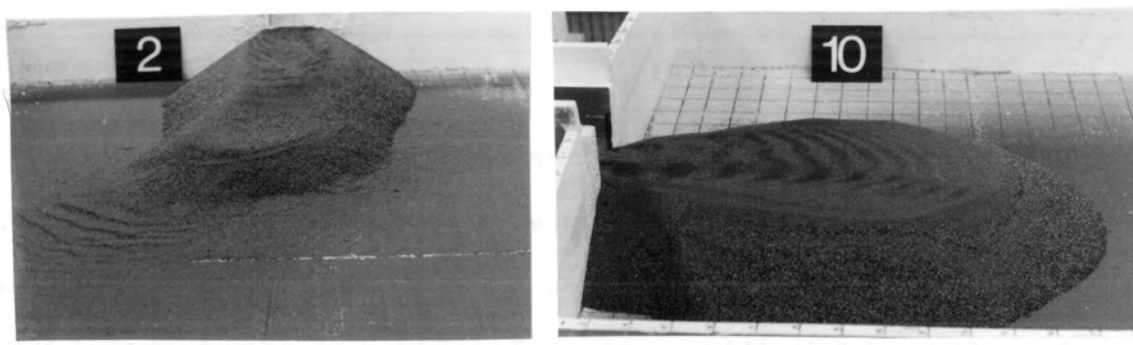

(c) Formation of surficial bed-forms and sandwaves.

PLATE 9. PHOTOGRAPHS ILLUSTRATING DIFFERENT SURFICIAL BED-FORMS.

sizes, showing random spatial distributions in their formation. Figures 18 and 19 show their dimensional growth and locations along the longitudinal and transverse cross-sections.

There seemed to be some direct relation between the pattern of outflow spread over the delta and the morphologies of shoals. In other words, depending on the degree of convergent or divergent flow-pattern, shoals and bars are elongated or rounded in shape. The actual mechanism was not apparent in the experiment. However, there was a strong feeling that two different modes were involved in the mechanics of bar formation. They are as follows.

The longitudinal bar, as in series A, was seemingly created by the relatively convergent flow passing over the delta platform. The high inertia flow, when opposed by the bottom boundary conditions developed through vertical accretion, generates intense turbulence, and eventually creates natural levees involving a turbulent exchange process. When the natural levees are discretely formed, the secondary motion of the flow tends to intensify as a result of wall-drag. This seems to involve some kind of truncating or scouring effects along both sides of the main forward flow, creating two threads of maximum turbulence. As a result, part of the sediment is propelled with upward components and carried in the middle of the flow where aggradation occurs to form symmetric shoals or longitudinal bars. On the other hand, when the pattern of outflow spreading

is relatively divergent, localized deceleration of velocity as well as an increase in the proportion of the bed load take place, which eventually results in the deposition of bed load to form broad concentric delta bars. An exception to these mechanisms of bar formation was noted in the runs of series B. In fact, no discrete shoal was found to form. Instead, a series of crescentic sandwaves were found to occur covering the entire delta surface, as shown in photo-plate 3. They are known to evolve in response to the local flow and sediment-transport conditions in such a way as to provide adjustments of the resistance to flow. The formation of these sandwaves appeared to prevent shoal formation.

Despite the adaption of two clear-cut flow regimes in the flume channel, the bed-forms that evolved on the delta surface were broadly crescentic sandwaves and flat or plane beds. Some of these are shown in photo-plate 8. All series B produced a most spectacular formation of sandwaves. They evolved in response to the local flow and bed-load transport conditions so as to ensure continuity of flow and bed-load movement. Their crescent shape appearance seems to suggest the magnitude and direction of the flow velocity over the delta plain. Most of the series showed their formation at one time or the other. But, series C recorded more of the plane bed than of any other forms. In series D and E, both flat-bed as well as sandwaves were noticed to appear and reappear with time.

Perhaps the most spectacular features, forming ahead of the delta-front and on the bottomset bed, were the crescent-shape depositions which may be described as sandwaves with greater amplitude. They built up in a series with gentle upstream slopes and steep downstream slopes. They were invariably formed in series A (photo-plate 9c) which had greater amplitude than those associated with series D or E.

Although the exact mechanism of formation was not apparent, it seemed clear that there was a direct connection between these large sandwaves and the flow of rotatory motion. As discussed earlier, the spiral motion of water, forming vortices superimposed on the main forward flow, occurs as a result of the resistive effects to flow by the bottom boundary conditions. The intensity of this spiral motion depends on the boundary shear stress caused by the interrelated variables of flow velocity and roughness elements including bed forms and bed material sizes. Because of a delicate balance between the rotatory vortex-system and the forward flow, an opposition from one side may change the direction of the forward flow. The experiment strongly suggested that the flow was mainly deflected to one side or the other owing to differential deposition along the sides of the flow. Whatever is the reason for the deflection of the forward flow, sandwaves of the observed kind were noticed to form in accordance with the direction of movement, and presumably the magnitude of the eddies forming in a chain. As observed, the

forward flows of series A, developed a deflected course and they continued to move until they impinged upon the basin-walls where the flow used to break and move in an opposite direction causing ripples or dunes to form along its path. The depositional pattern shown in plate 2 confirms the above observations.

5.3.3 Distributary patterns of the deltas

The distributary pattern is one of the most recognized salient features of deltas. Coleman and Wright (1971) grouped the distributary patterns into four primary types. Two of the four types were visually evident in the experiment. They are, 1) the single channel type in which there was no splitting, and 2) the type in which all splitting occurred at a single apex. A third type may be added to these in which short-length distributaries evolved by breaching the levee-walls. Photo-plate 9 illustrates the types of distributary patterns that developed in the present experiment.

Delta channel branching is generally attributed to shoal or bar formation causing splitting of the flow (Leighly, 1934; Axelsson, 1967). Welder (1955, 1959) stressed the important role of crevasse formation in the development of multiple channels. From the standpoint of the present experiment, the branching of the distributary patterns seemed to depend on localized damming effects resulting from depositional obstructions of one kind or

the other.

As noted in the preceding subsection, the morphology of the bars and other bed-forms depends on the nature and degree of flow divergence. The degree of divergence is determined by the interactions of flow and form, which are greatly dependent on the discharge and the mechanics of sediment movement. As observed in the experiment, the shape, size and channel splitting seemed to be directly related to the nature and degree of flow spreading over the delta platform.

As noted in the experiment, the formation of a distributary pattern was best developed in series B where the flow split into two or three branches, forming symmetrical forks (photo-plate 10). The splitting was observed to occur at a single apex located about 15 cm off the channel mouth. The distributaries were shallow and often short-lived, and their appearance and reappearance are quite spectacular. It was strongly felt that splitting was caused by the local damming actions related to the formation of the crescentic sandwaves. In series C, similar damming effects, caused by the broad bar forming in close proximity to the channel mouth, led to the breaching of the natural levee-walls. Following these breaches, two side-distributaries were seen to evolve (photo-plate 4). The variables that seemed to control the formation of this type of distributary pattern are low discharge and high sediment transport, involving a divergent flow pattern and considerable

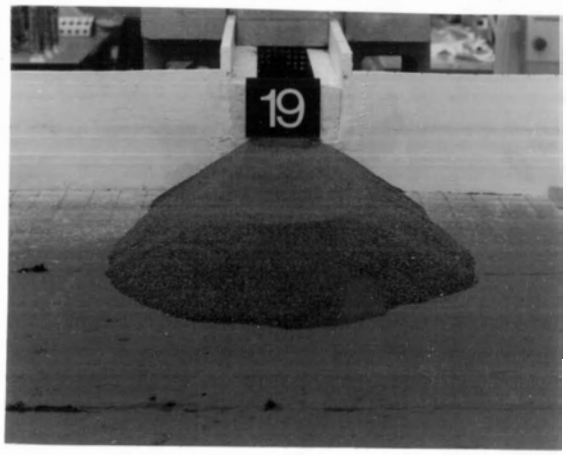

(a) A view of a wide and shallow channel, typical of Series D.

(b) Longitudinal bar and channel bifurcation - typically formed in Series A.

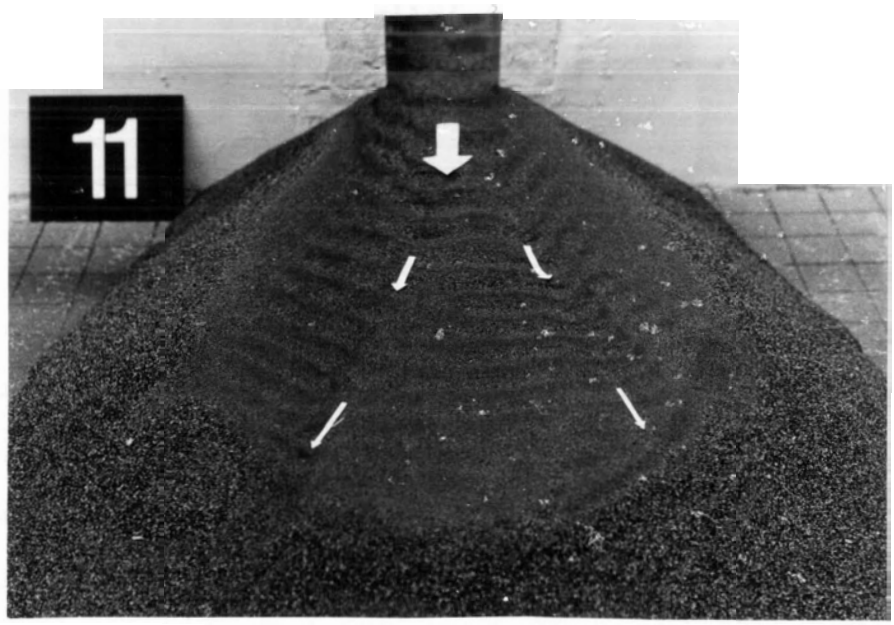

(c) Channel splitting - a common view in Series B.

PLATE 10 . PHOTOGRAPHS ILLUSTRATING PATTERNS OF DISTRIBUTARY FORMATION.

bed-load transport.

Despite the formation of a mid-channel bar or longitudinal shoal in series A, there appeared no tendency for the flow to bifurcate into two well-defined currents. Rather, flow tended to pass through a single channel confined by the well-defined natural levees. Photo-plate 10b clearly illustrates two truncated channels along the longitudinal shoal, although the development of a bifurcated channel flow was not distinct. It seemed probable that because of a low profile, or a high flow-depth over the mid-channel bar, the bifurcation could not take place. It was, however, felt that variable discharge conditions could provide better options for the division of the flow into two distributaries.

From the above discussion it is already apparent that channel splitting is caused by the superficial bed-forms (bar, shoals, sandwaves), which are dependent on the volume and character, and sediment transport conditions. It is important to note that blocking and splitting of a flow are more rapid in relatively more divergent flow patterns in which the natural levees are either missing or poorly developed, and are related to the conditions of low discharge and high bed-load transport.

5.3.4 The internal structure of the deltas

The tripartite arrangements of topset, foreset and

bottomset beds, classically described by Gilbert (1885), were observed in the deposition of the small laboratory deltas. The topset beds forming over the steeply dipping foreset beds developed horizontal bedding. The foreset deposit resting on the bottomset bed showed distinct formation of cross-bedded structure. The bottomset bed, composed of finer sediments carried in suspension, did not develop any recognizable (visually) bedded layer. Some of these structural features are shown in photo-plate 11. The variability in structural settings of the deltas is thought to be a consequence of the various hydrodynamics and rheologic processes related to the different discharge and sediment transport conditions of the present experiment.

As discussed earlier, the finer sediment carried in suspension tended to settle as a discrete unit, forming a carpet of basin-bottom deposition. Deposition of this kind, when overridden and buried by the foreset beds, is termed bottomset beds. The settling of the suspended sediment is thought to be dependent upon the rate of flow deceleration and the particles' settling velocity.

The bottomset deposits of the runs showed varying dimensional growth suggesting differential transport of bed-load and suspended-load. By and large, deposition in series A was very thick, but asymmetrically formed. The asymmetric formation may be attribted to the deflected-flow pattern caused by the

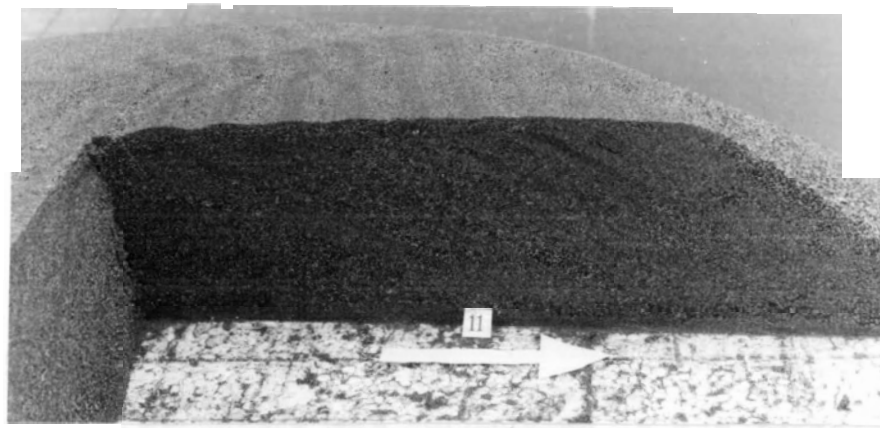

(a) A common view of internal structure of the deltas formed in Series B.

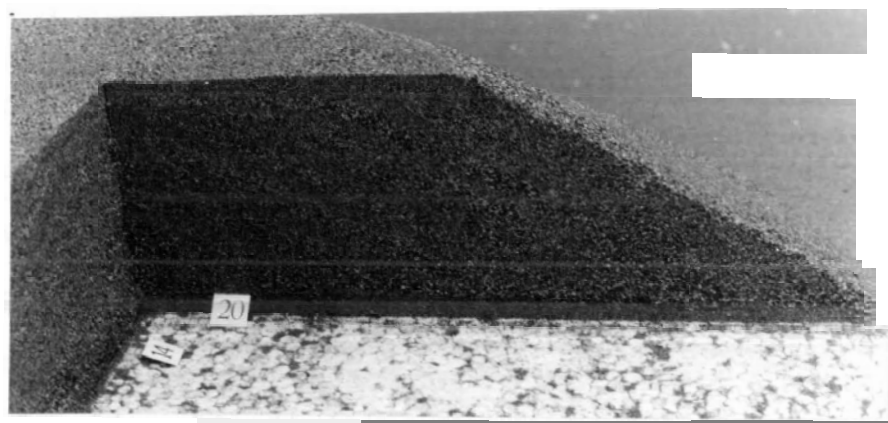

(b) Formation of topset, foreset and bottomset beds. The structural design is representative of the Series D.

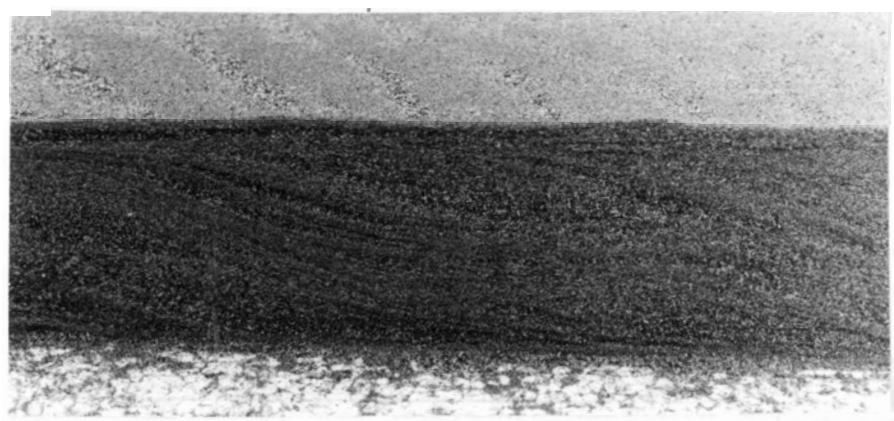

(c) Deformed or trough cross-bedded structure of foreset deposit, typically formed in run 27 of Series E.

PLATE 11 . PHOTOGRAPHS ILLUSTRATING THE INTERNAL STRUCTURE OF THE DELTAS.

interaction between high inertia flow and depositional form. The maximum thickness, 2.70 cm, of the bottomset deposit was found in runs 2 and 3, where sandwaves merged with bottomset beds. On the other hand, series C generally developed very thin bottomset beds in which the maximum thickness of 0.7 cm was measured in run 15. No bedded structure was recognized in the formation of the bottomset deposits. It is felt that a variable discharge may provide better environmental conditions for producing bedded structure.

The foreset beds contributed the gross structural organization of the present laboratory deltas. The coarser sediment moving along the bed tended to accumulate on the upper foreset slopes as metastable wedges. The wedges of sediment periodically collapsed by shear failure and, due to gravitational pull, slipped down to form cross-bedded units of foreset deposits. This has been the common observation throughout the experiment, except for series A, in which no cross-bedded structure was seen to form in the deltas. Photo-plate 11 represents some of these structures.

Jopling (1964) pointed out that the mechanics of cross-bedded structure can be adequately explained in terms of differential particle trajectory, pulses in trajectory behavior, segregational tendencies of the sediment particle along the transport surface, and dispersive pressure (Bagnold 1954, 1956). It stipulates that depending on the particles' differential

fall-velocity and flow deceleration, part of the suspended load settles on the delta front. The segregation and non-uniform distribution of sediment grain size along the upstream bed occur because of a particle's differential trajectory or dispersive pressure. However the sorting efficacy of finer and coarser sediments on the frontal slope of the deltas is described, there remains the fact that a substantial amount of finer sediment is necessary for the formation of a cross-bedded structure of the foreset beds. There seem to be three basic considerations which are directly related to the formation of cross-bedded structure on the deltas. They are, 1) the mechanics of both bed-load and suspended-load transport, involving the formation of bed-forms characteristically related to lower regime flow, 2) the phenomena of flow separation and expansion, leading to flow deceleration, and 3) the occurrence ofa divergent flow pattern, indexing the nature of interaction of flow and form. The efficacy of these responses may be attributed to the volume and character of flow-discharge, and the sediment input conditions.

As was evident from the visual observations, no traceable bedded structure was present in the deltas of series A, suggesting non-occurrence of flow separation. In fact, the surficial morphology, frontal slope (3 - 13) and the nature of the flow pattern that developed over the delta platform and delta front are supportive of the above view. On the other hand, the cross-bedded structure was clearly formed in all other runs,

indicating the occurrence of flow separation and bed-load transport. The phenomena of flow separation and bed-load transport can also be traced from the records of the frontal slopes and characteristic bed forms. In fact, the frontal slopes of series B, C, D and E were noted to be ranging within 28 to 31, 30 to 32 , 25 to 29 and 21 to 26 degrees, respectively.

The cross-bedded structure of the foreset deposit of the different deltas displayed marked differences in the angle of dip as well as the spacing of the alternate layers. By and large, series B, C and D developed parallel sets of beds, dipping at an angle of 27, and 24° (series average), respectively. On the other hand, the angle of dip of an individual bed was measured as varying from 16° to 22°, showing steeper slopes close to the channel mouth. The most spectacular cross-stratification was found in run 27 (photo-plate 11) of series E. The trough-like structure seemed to have originated from local scouring and fill. It suggests that for one reason or the other, the flow was not separated from the depositional boundary. As a result, the intensity of turbulent actions was greatly increased, leading to local scouring. In the subsequent stage the scour-pool was filled to form such a structure.

The topset beds were observed to form in all runs except series A. The photo-plate 11b illustrates the horizontal bedded structure of the topset deposits. From observations it appeared that the formation of the topset beds, representing the finer

grade-size of the bed-load, involved the process of segregation. Jopling (1964) described the process as a result of differential particle trajectory involving sorting of bed load caused by the localized conditions of flow divergence and convergence. Bagnold (1954, 1956) showed that for the inertial region of grain shear the normal dispersive pressure is proportional to the square of the diameter of the particle when other conditions remain the same. Because of this relationship, there is an inherent tendency for the larger particle to move toward the free surface (upward) where the zone of least shear strain prevails. Whatever is the explanation, there appeared a dominating effect of the coarser particles relative to finer sediments while moving along the bed. Importantly, the lower regime flow characterized by the formation of small bed-forms (Simon, Richardson and Nordin, 1965), or divergent flow pattern originating from the interaction between form and flow, are directly related to the development of the topset beds. On the other hand, no topset bed was observed to evolve in the deltas produced in series A. The reason seems to be due to the stripping of the topset desposit caused by the upper flow regime with a relatively convergent flow pattern. Perhaps the significant fact arises because the cross-bedded structure of the foreset deposit is directly dependent on the formation of the topset beds.

5.3.5 Variation in the sediment character and size-distribution

It was seen in the preceding section that formation of different beds in the structural design of the deltaic deposit is primarily controlled by the mechanics of sediment movement and mode of deposition; and the mechanics of sediment transport and deposition are directly related to the flow, and to the character and volume of sediment transport. It seems likely that sediment-size distribution of a given spatial-location of the deltas forming in response to different input conditions of the experiment will be different. In order to examine this, two sets of runs are arbitrarily chosen. Runs 4, 9, 14, 20, and 26, constituting the first set, involved a constant rate of sediment fed (14.93 gm/sec) but different discharge between the runs. On the other hand, runs 17, 18, 19, 20, 21, and 22, representing the second set, were performed at the constant discharge of 642.60 cm^3 /sec with differential rates of sediment-input between the runs.

The sediment parameters, considered in the discussion, are: grain-size (mean and median), sorting (standard deviation), skewness, and kurtosis. The forms suggested by Folk and Ward (1957) are adopted here, and are discussed in some detail in Appendix C.

The sediment was sampled from the topset, foreset, and bottomset deposits along the centre-line of the deltas. The

samples were analysed by using the vertical accumulation tube and percentiles (in phi-unit), and are listed in Appendix C. Certain limitations in the analysis of size-distribution need to be mentioned here. There has been some doubt about whether spot samples are representative of the material at a particular site. Because of thin formation of bottomset and topset beds, it is possible that part of the material from the foreset deposit has been sampled with the bottomset and topset sediment. Contamination, due to bad handling of the samples when part of the sediment from one sample might have entered into another, is another consideration. Despite these limitations, it will be seen that certain trends in sediment parameters appear to be related to the flow scale, and volume and character of the sediment supply.

Table 8 lists the sediment parameters of the topset, foreset, and bottomset deposits at different discharge conditions of the runs. Likewise, table 9 shows values of sediment parameters representing differential rates of sediment-input of the runs. Although the tables do not suggest strong relations between the variables and sediment parameters, there are indications in the overall trends of the data which may justify certain inferences. These are discussed below.

The mean or median grain size in the sediment sample is usually considered to be representative of all the grain sizes in that sample. Since mean and median grain size differ slightly

Table 8

Sediment size parameters of topset, foreset and bottomset deposits.

At a longitudinal distance of 25.00 cm from the channel-mouth

References		Mean Φ	Median Φ	Sorting	Skewness	Kurtosis
Run/4	Topset	1.9366	2.0150	.5133	-0.2036	1.1344
	Foreset	1.6100	1.6700	.4707	-0.2394	1.8504
	Bottomset	1.5450	1.5900	.5021	-0.1620	0.8988
	Topset	2.5250	2.5600	.4916	-0.1705	1.0708
	Foreset	1.6300	1.6950	.5330	-0.1723	0.8576
	Bottomset	2.1366	2.1600	.4805	-0.1791	1.0529
	Topset	2.3066	2.3250	.4634	-0.0303	1.1154
Run 14/	Foreset	1.7733	1.8450	.5497	-0.1900	0.9669
	Bottomset	0.9033	0.8450	.3666	+0.2634	1.1818
	Topset	2.2300	2.2900	.5430	-0.1870	1.1394
Run/20	Foreset	1.6916	1.7550	.5584	-0.1650	0.8913
	Bottomset	1.7733	1.7850	.4500	-0.0749	1.1119
	Topset	2.0516	2.1000	.4978	-0.1820	1.0230
Run 26	Foreset	1.6517	1.7300	.4577	-0.2354	0.8744
	Bottomset	1.7563	1.7850	.4444	-0.0920	1.0633

At a distance of 65.00 cm

	Topset	1.7566	1.7850	.4247	-0.0775	0.1780
Run/4	Foreset	1.5400	1.5600	.5369	-0.1745	1.1780
	Bottomset	1.9000	2.0150	.4571	-0.3226	0.9939
	Topset	2.3360	2.4150	.4739	-0.2537	1.1553
Run/9	Foreset	1.4500	1.5150	.6328	-0.0835	0.7957
	Bottomset	2.2350	2.2900	.4952	-0.2419	1.1366
	Topset	1.4837	1.5600	.5455	-0.2038	0.8097
Run/14	Foreset	1.6250	1.2900	.4936	+0.1073	1.0000
	Bottomset	2.6066	2.6300	.4363	-0.1250	1.0123
Run/20	Topset	2.1700	2.2200	.5169	-0.1072	1.0144
	Foreset	1.7683	1.8450	.5816	-0.1919	1.1891
	Bottomset	2.0900	2.1500	.5647	-0.2398	1.2770

(Continued on next page)

Table 8 (continued)

Sediment size parameters of topset, foreset and bottomset deposits.

	Topset	2.2400	2.2750	.3804	-0.1545	0.9690
Run/26	Foreset	1.4733	1.5150	.6349	-0.0644	0.7894
	Bottomset	2.8900	2.4800	.4278	+0.1766	0.6067

At a distance of 105.00 cm. Bottomset deposits only.

References	Mean Ø	Median Ø	Sorting	Skewness	Kurtosis
Run/4	2.0466	2.2100	.5974	-0.2736	1.1150
Run/9	2.8250	2.8600	.4234	-0.1084	1.1862
Run/14	3.1266	3.1500	.4409	-0.0879	0.9221
Run/20	2.2000	2.2600	.4924	-0.0962	1.0749
Run/26	2.5933	2.6200	.3933	-0.0848	0.9628

At a distance of 145 cm.

Run/4	2.5616	2.5850	.4909	-0.0511	1.0777
Run/9	3.0666	3.1000	.4015	-0.1189	1.1597
Run/14	3.3916	3.4400	.3490	-0.2376	1.1084
Run/20	2.7166	2.7300	.4560	-0.0089	1.0504
Run/26	2.8900	2.9100	.4288	-0.1766	0.6067

(tables 8 and 9), only mean value is used in the discussion. Data in tables 8 and 9 (shown in figure 20) clearly indicate that the foreset deposit is composed of coarser materials, while bottomset and topset deposits are made of relatively finer materials. This is to be expected, because foreset materials are primarily derived from the sediments moving along the bed, while the bottomset deposit is derived from the sediment carried in suspension. As noted earlier, because of dispersive pressure caused by particles in motion, a part of the finer sediment always moves under the shadow of the coarser bed-load transport. The finer materials, moving very close to the bed, ultimately

Table 9

Sediment size parameters of topset, foreset and bottomset deposits.

At a longitudinal distance of 25.00 cm from the channel-mouth

References	Mean Φ	Median Φ	Sorting	Skewness	Kurtosis
Topset	2.1133	2.1300	.5393	-0.0834	1.0661
Run 17 Foreset	1.6800	1.7550	.5452	-0.1947	1.9447
Bottomset	1.8816	1.9400	.4818	-0.1585	1.1039
Topset	2.1183	2.1600	.5978	-0.1488	1.0018
Run 18 Foreset	1.6300	1.6950	.5414	-0.1539	0.8589
Bottomset	1.5583	1.6150	.5051	-0.1543	0.8270
Topset	2.3583	2.3850	.4132	-0.1070	1.1743
Run 19 Foreset	1.8066	1.9100	.5145	-0.2383	0.0675
Bottomset	1.9516	2.0150	.4138	-0.2122	0.9690
Topset	2.2300	2.2900	.5430	-0.1870	1.1394
Run/20 Foreset	1.6916	1.7550	.5584	-0.1650	0.8913
Bottomset	1.7733	1.7850	.4500	-0.0749	1.1119
Topset	1.9733	2.0150	.5612	-0.1833	1.0765
Run 21 Foreset	1.8350	1.2350	.5441	-0.0752	1.5813
Bottomset	1.8350	1.9100	.5441	-0.2755	1.4813
Topset	1.8283	1.9400	.5748	-0.2705	0.7275
Run/22 Foreset	1.3683	1.3950	.6666	-0.0720	0.7850
Bottomset	1.9650	2.0450	.3734	-0.3072	0.9652
At a distance of 65.00 cm					
Topset	1.7900	1.8750	.5502	-0.1936	0.9509
Run/17 Foreset	1.6833	1.7300	.5691	-0.1081	0.9487
Bottomset	2.1983	2.1600	.5989	-0.2462	1.2110
Topset	1.8150	1.7300	.6120	-0.0860	1.0775
Run/18 Foreset	1.6866	1.7300	.5670	-0.1121	0.9335
Bottomset	2.1483	2.1950	.5039	-0.1866	1.0473
Run/19 Topset	2.2983	2.3600	.4408	-0.2464	1.0792
Foreset	1.7833	1.8750	.5497	-0.2338	0.9246
Bottomset	2.0866	2.1000	.5169	-0.1081	1.0739

(Continued on next page)

Table 9 (continued)

Sediment size parameters of topset, foreset and bottomset deposits.

References	Mean Φ	Median Φ	Sorting	Skewness	Kurtosis
Topset	2.1700	2.2200	.5169	-0.1072	1.0144
Run/20 Foreset	1.7683	1.8450	.5876	-0.1919	0.1891
Bottomset	2.0900	2.1500	.5647	-0.2398	1.2770
Topset	2.2200	2.2600	.4941	-0.0679	1.1680
Run/21 Foreset	1.3553	1.3400	.5729	-0.0430	0.7675
Bottomset	2.8266	2.1200	.6377	-0.5436	1.8876
Topset	2.0733	2.1200	.5342	-0.2018	1.9189
Run/22 Foreset	1.4833	1.5150	.5817	-0.1057	0.7908
Bottomset	2.0466	2.1000	.4474	-0.2246	1.9884
At a distance of 105.00 cm. Bottomset deposits only.					
Run/17	2.0650	2.2900	.4445	-0.0327	1.0438
Run/18	2.3200	2.3500	.3779	-0.1120	1.9975
Run/19	2.3016	2.3250	.3953	-0.0700	1.0679
Run/20	2.2000	2.2600	.4924	-0.0962	1.0749
Run/21	2.1883	2.2300	.3858	-0.1622	0.9250
Run/22	2.3667	2.3600	.4263	+0.0224	1.0587
At a distance of 145 cm.					
Run/17	2.8400	2.8200	.4783	-0.0274	1.1073
Run/18	2.6600	2.6800	.4282	-0.0288	0.9519
Run/19	2.6966	2.7100	.4218	-0.0324	1.9989
Run/20	2.7166	2.7300	.4560	-0.0089	1.0504
Run 21	2.6400	2.6300	.3811	+0.0255	0.9449
Run/22	2.4116	2.4400	.4109	-0.0866	1.0804

form the topset bed.

Figure 21A is a plot of average velocity against the mean grain-size (in phi-unit), in which topset, foreset, and bottomset deposits are separately shown. Although the relationship is not a strong one, the plots do indicate a negative trend between the average velocity and mean grain size

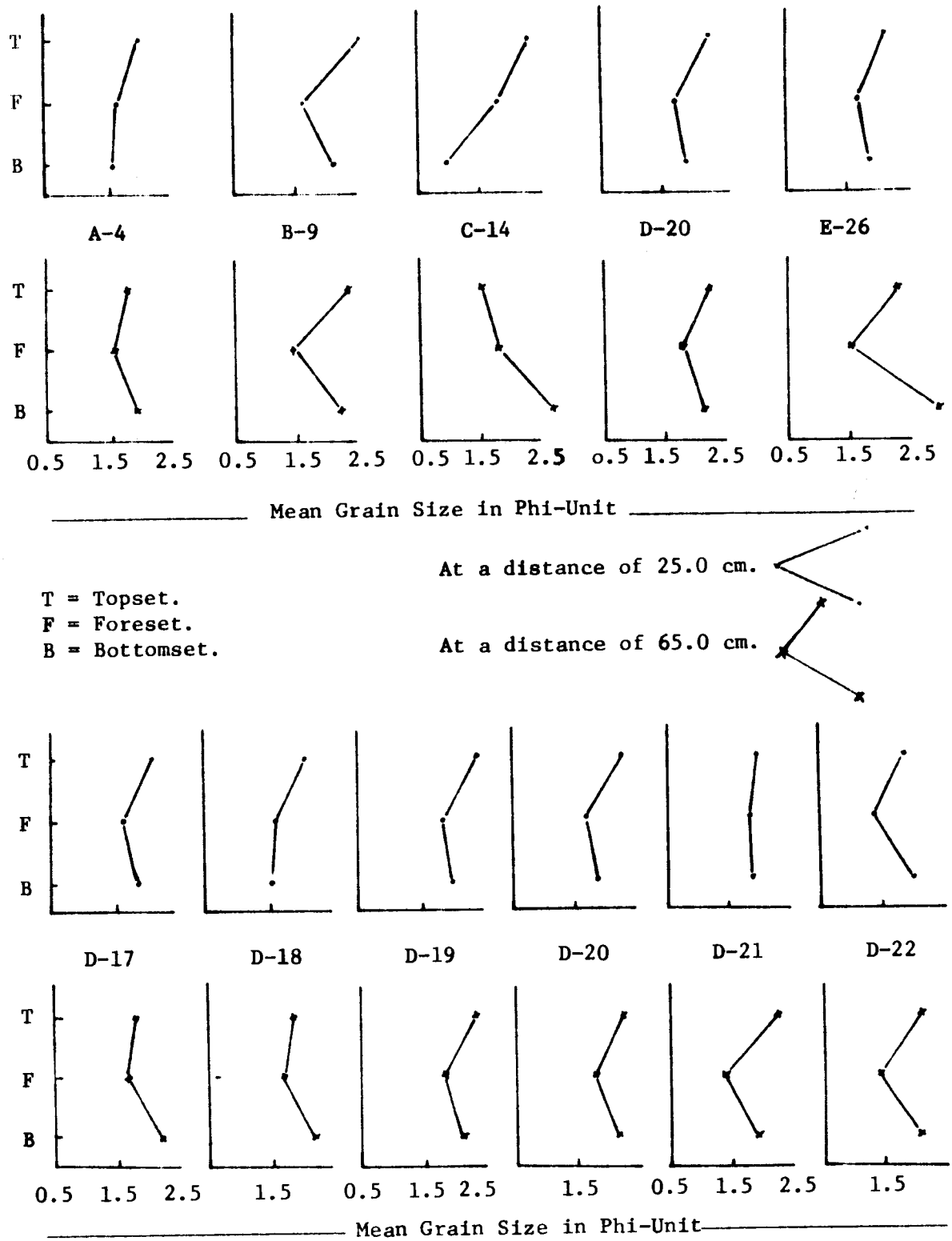

Figure 20. Variation of Mean Grain Size of Top-, Fore- and Bottom-set Deposits.

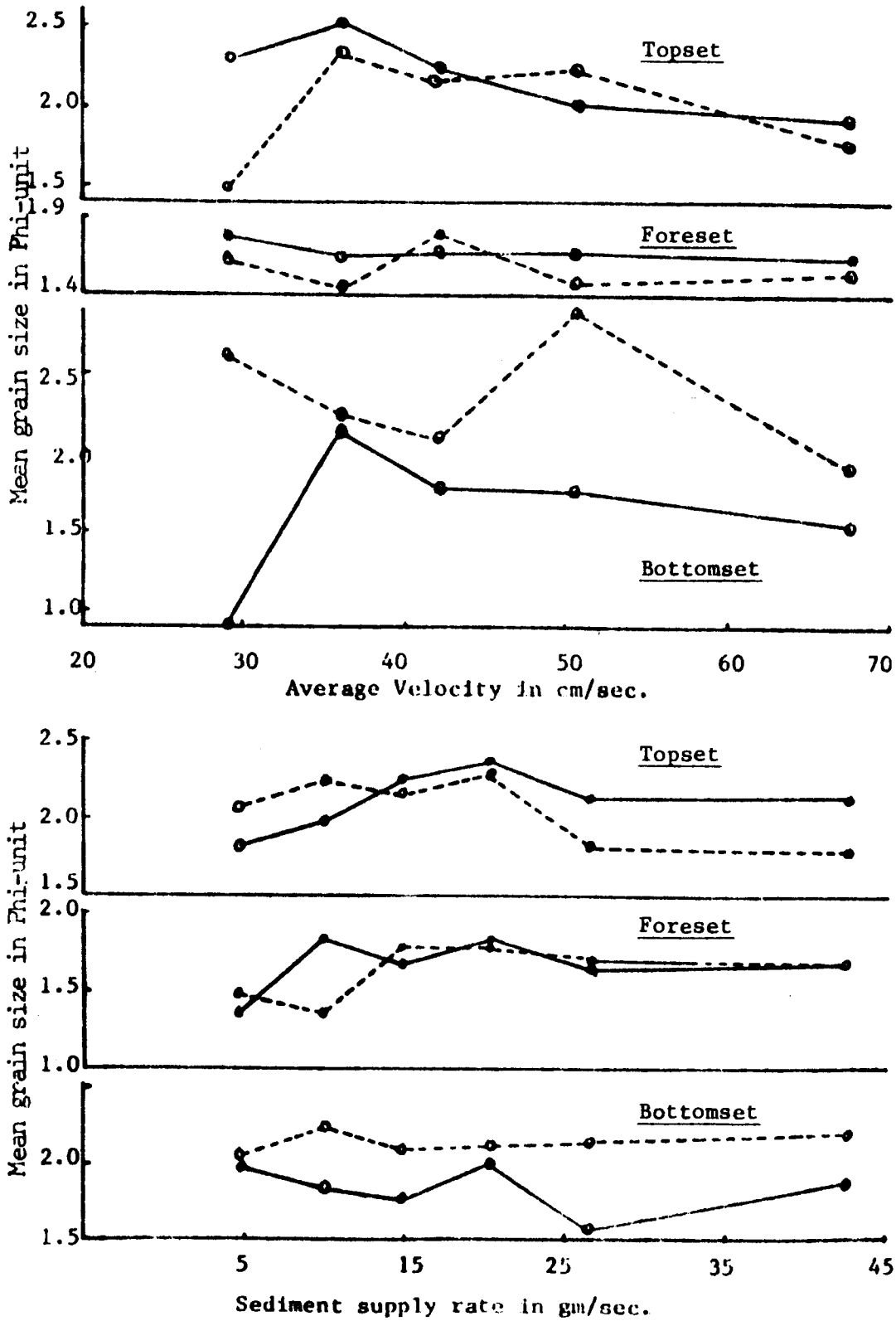

Figure 21. Relation among Mean Grain Size and Velocity and Sediment Input Rate.

(in phi-unit). That is, as velocity increases the actual mean grain diameter of the sediment deposited also increases. The phenomenon is simply a response to flow competence related to the discharge variable and the intensity of boundary shear. The relation between sediment-input rates and the mean grain-size (in phi-unit) is relatively insensitive. This is demonstrated in figure 21b. The figure indicates that the mean grain-size of sediment is less affected by the increasing or decreasing of sediment input rates.

Figure 21 further suggests (only indirectly) that the mean grain-size is not independent of distance from the channel mouth. There are indications in the graphs (Figure 20) that the mean grain-size of the topset materials increases with distance from the channel mouth. Such a tendency, however, is less obvious in the case of foreset-bed materials. However, mean grain-size of the bottomset deposit decreases with increasing distance from the channel mouth. The validity of this inference is supported by data listed in tables 8 and 9.

The degree of sorting in the sample is another aspect of sediment analysis, and is known to depend to a large extent on the method of transport of the sediment. Further, where the sediment is bimodal, the sorting is likely to be somewhat poorer than when it is unimodal. Folk and Ward (1957) suggested a verbal scale, used in the present study, to describe sorting. The coefficients of sorting are as follows:

under 0.35 very well sorted

0.35 - 0.50 well sorted

0.50 - 1.00 moderately sorted

1.00 - 2.00 poorly sorted

2.00 - 4.00 very poorly sorted

over 4.00 extremely poorly sorted

Tables 8 and 9 indicate that the sorting of the sampled materials falls within the range of well sorted to moderately sorted status. Foreset materials are predominantly moderately sorted, while bottomset materials are mostly well sorted. However, topset deposit shows a mixed tendency of the two. This is clearly illustrated in figure 22. Although the foreset deposit is composed of predominantly coarser materials carried along the bed, a part of the finer materials is always deposited on the foreset slope from the sediment in suspension and wedge-materials of the topset beds. This seems to explain the moderately sorted co-efficient of the foreset deposit. On the other hand, bottomset materials, derived principally from the sediments carried in suspension, involve the process of differential settling (Jopling, 1964) through which sorting improved.

The relation of the topset, foreset, and bottomset deposit sorting to average velocity and sediment-input rates is illustrated in figure 23. Although the relationship is not a strong one, the graphs (Figure 23a) do indicate that there is a

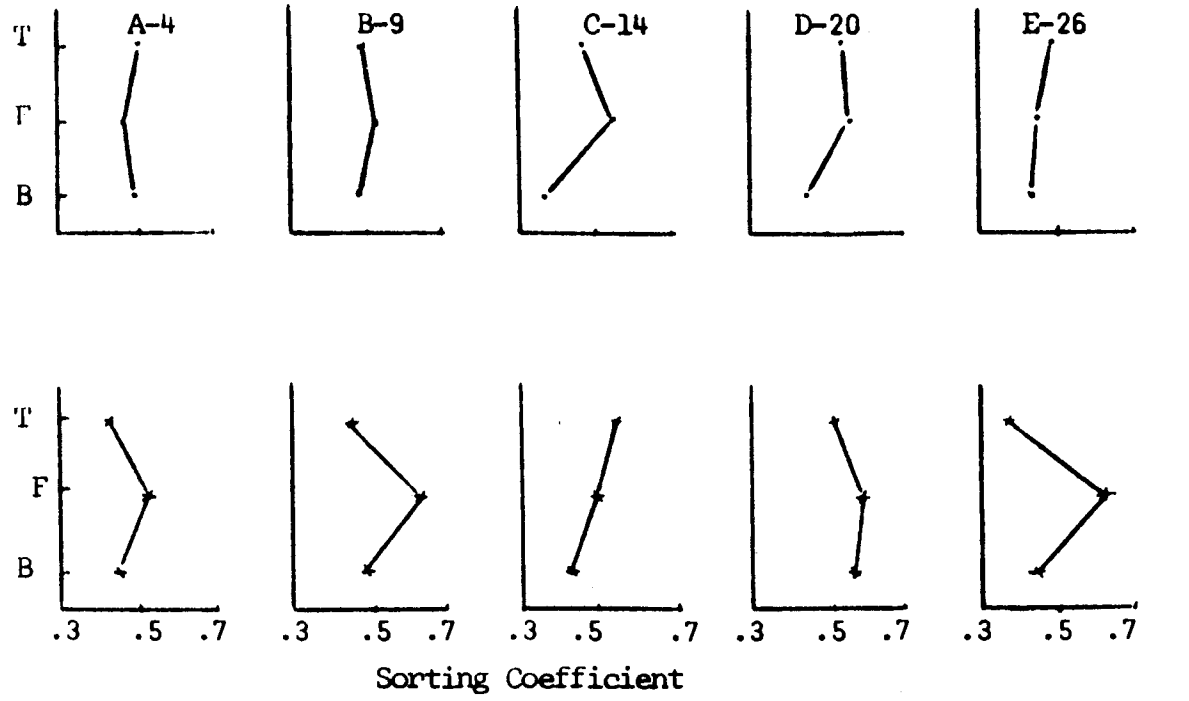

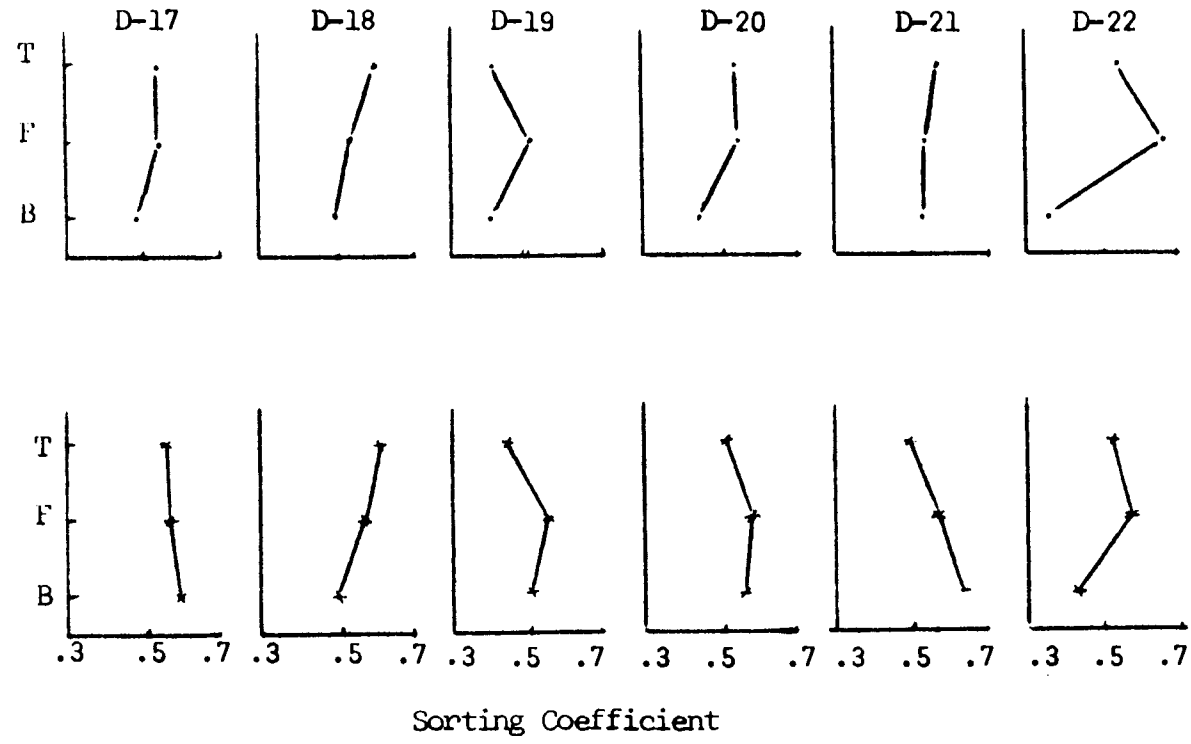

Figure 22. Variation in the sorting status of Top-, Fore- and Bottom-set Deposit.

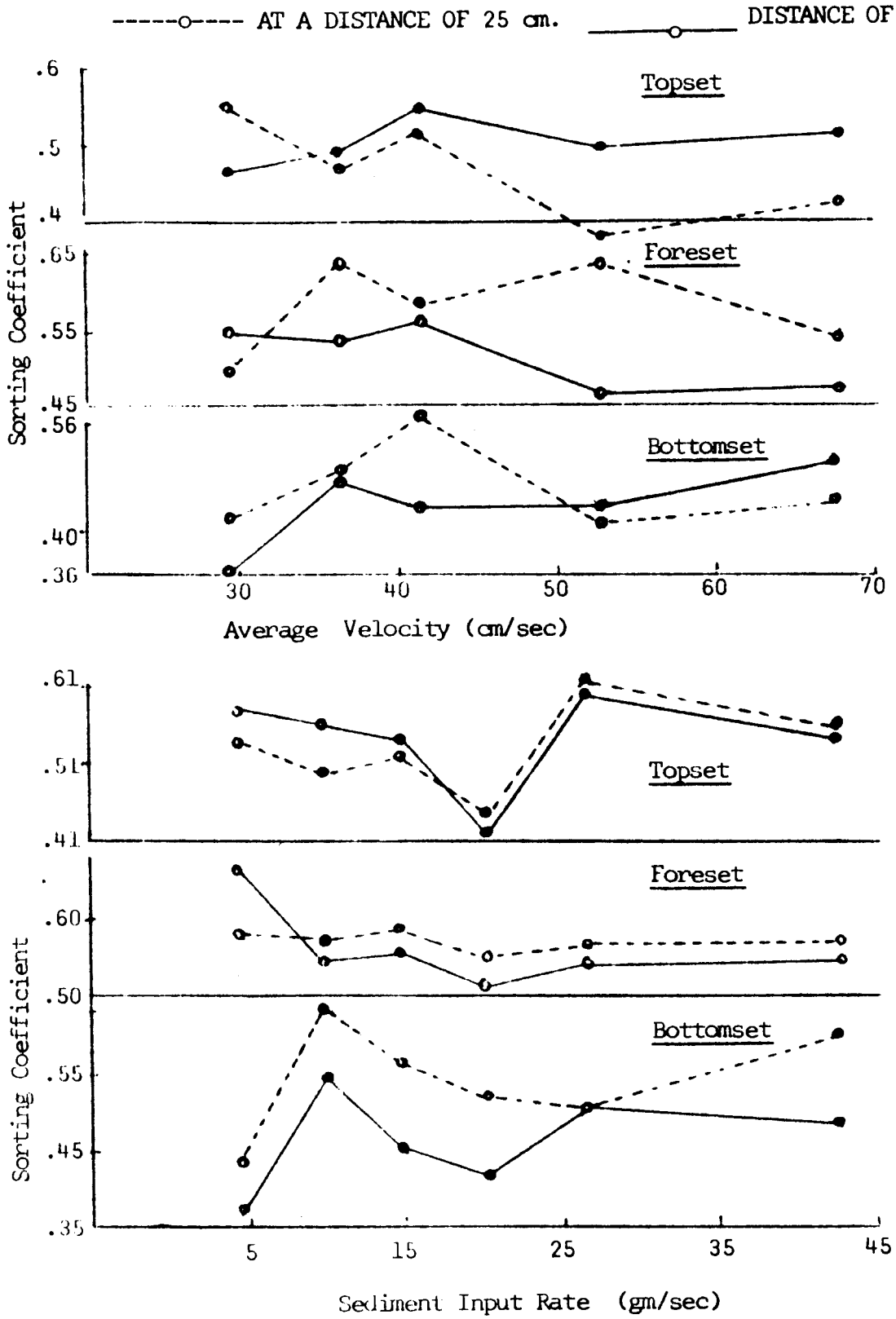

Figure 23. Relation between Sorting and Average Velocity and Sediment Supply Rate.

tendency for sorting to worsen when flow regime is transitional (42.00 cm/sec in the present study). It further suggests that sorting is better in the case of bottomset materials than in that of the foreset bed. Likewise, the effect of sediment-input rate on sorting status differs with the specified sediment-feeding rate. That is, there is a tendency for the materials to improve sorting when sediment-input rate is 20.24 gm/sec. Figure 23b also suggests that the sorting of the foreset materials improves with increasing sediment transport. This, to some extent, applies to both bottomset and topset materials.

Skewness measures the degree of asymmetry as well as the "tails" of the curve. Symmetrical curves have skewness of 0.00; those with excess fine materials (a tail to the right) have positive skewness and those with excess coarse material (a tail to the left) have negative skewness. The following verbal limits as suggested by Folk and Ward (1957), are adapted.

Skewness from: + 1.00 to + 0.30 strongly fine-skewed
+ 0.30 to + 0.10 fine skewed
+ 0.10 to - 0.10 near symmetrical
- 0.10 to - 0.30 coarse-skewed
- 0.30 to - 1.00 strongly coarse-skewed

Data in tables 8 and 9 (shown in figure 24) indicate that the top-, fore-, and bottom-set materials are predominantly negatively skewed; that is, the sediment samples have an excess of coarse materials. The skewness limits are mostly from near

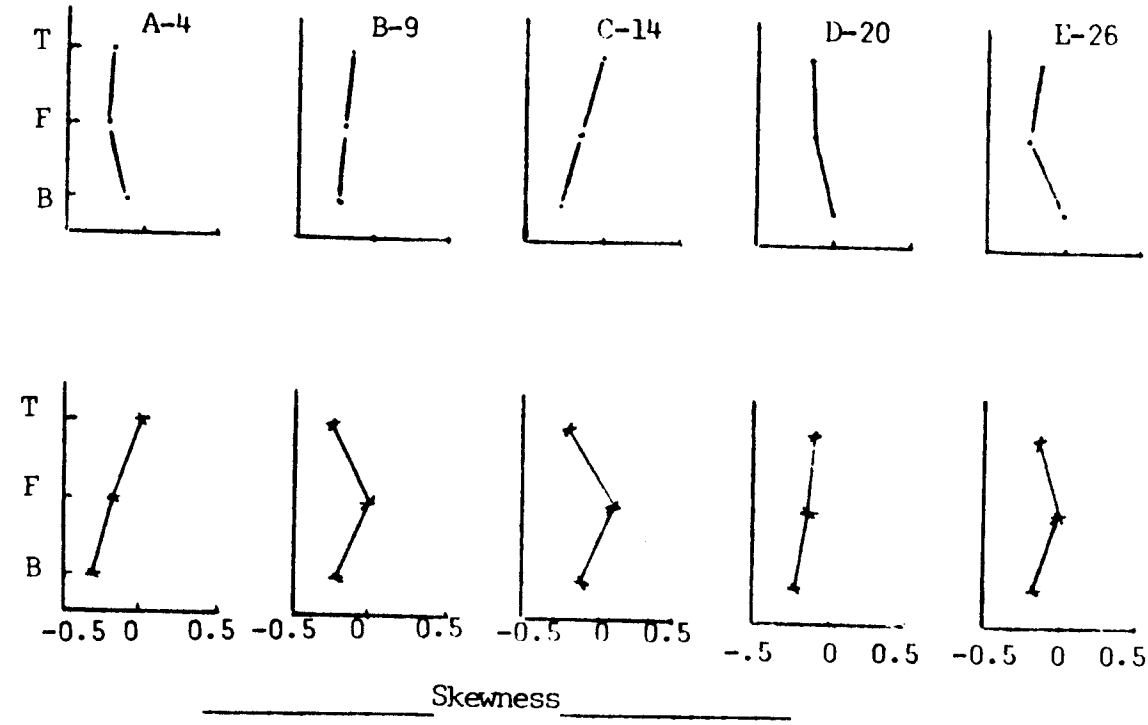

Figure 24a. Skewness of Top-, Fore- and Bottom-set Deposit.

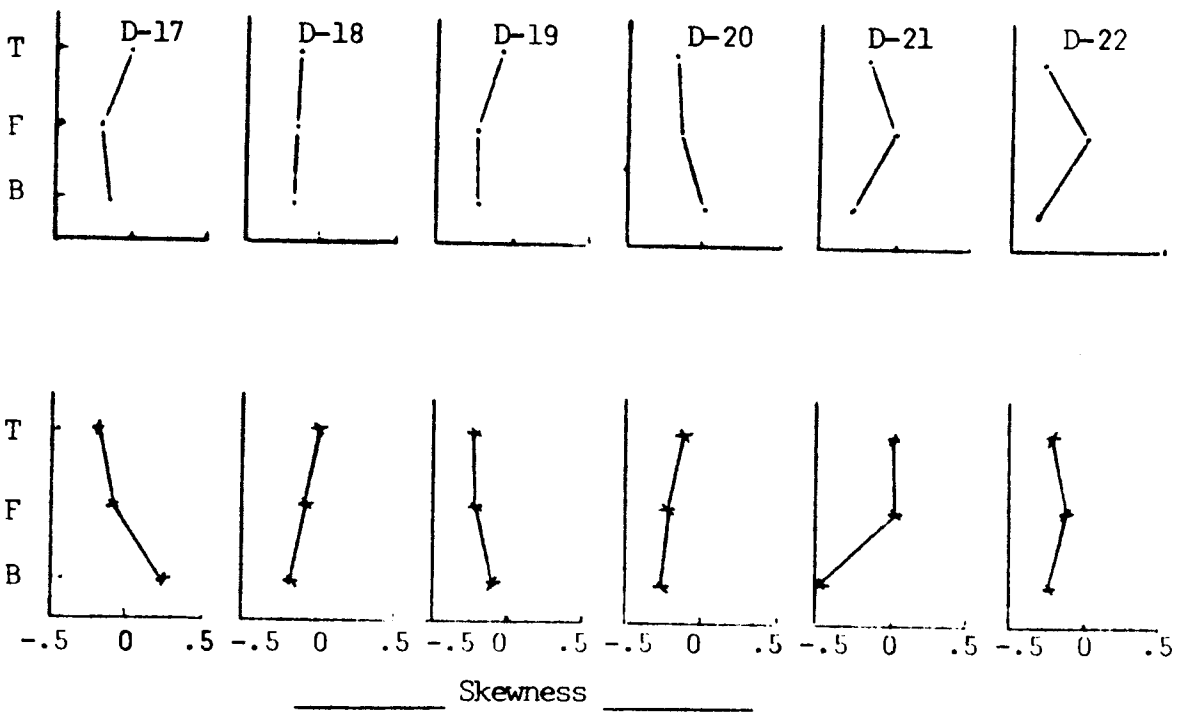

Figure 24a. Skewness of Top-, Fore- and Bottom-set Deposit.

symmetrical to coarse-skewed. On the average, the skewness of foreset materials is "near symmetrical". Although bottom-set materials show some degree of "coarse-skewed", there is a clear tendency for these materials to skew symmetrically beyond the delta front (tables 8 and 9). One of the reasons for this tendency lies in the fact that the bottom deposit is often contaminated by the larger particles which slipped down from the slumping. The relation of top-, fore-, and bottom-set material's skewness to average velocity and sediment supply rate is shown in figure 25. There appears to be no consistent relationship among skewness, average velocity, and sediment supply rate.

Kurtosis is the quantitative measure used to describe the departure from normality. For normal curve kurtosis is equal to 1.00; Leptokurtic curves have kurtosis over 1.00 and platykurtic curves have kurtosis under 1.00 (Folk and Ward, 1957).

Data in tables 8 and 9 (Figure 26) show that kurtosis of foreset materials is mostly platykurtic and that of top and bottom-set sediment are leptokurtic. The platykurtic tendency of foreset materials correlates two modes of deposition. The relationships among the kurtosis of top-, fore- and bottom-set deposits, average velocity and sediment supply rate are shown in figure 27. The trend of the plot indicates that the relationship among kurtosis, average velocity and sediment transport rate are very insensitive.

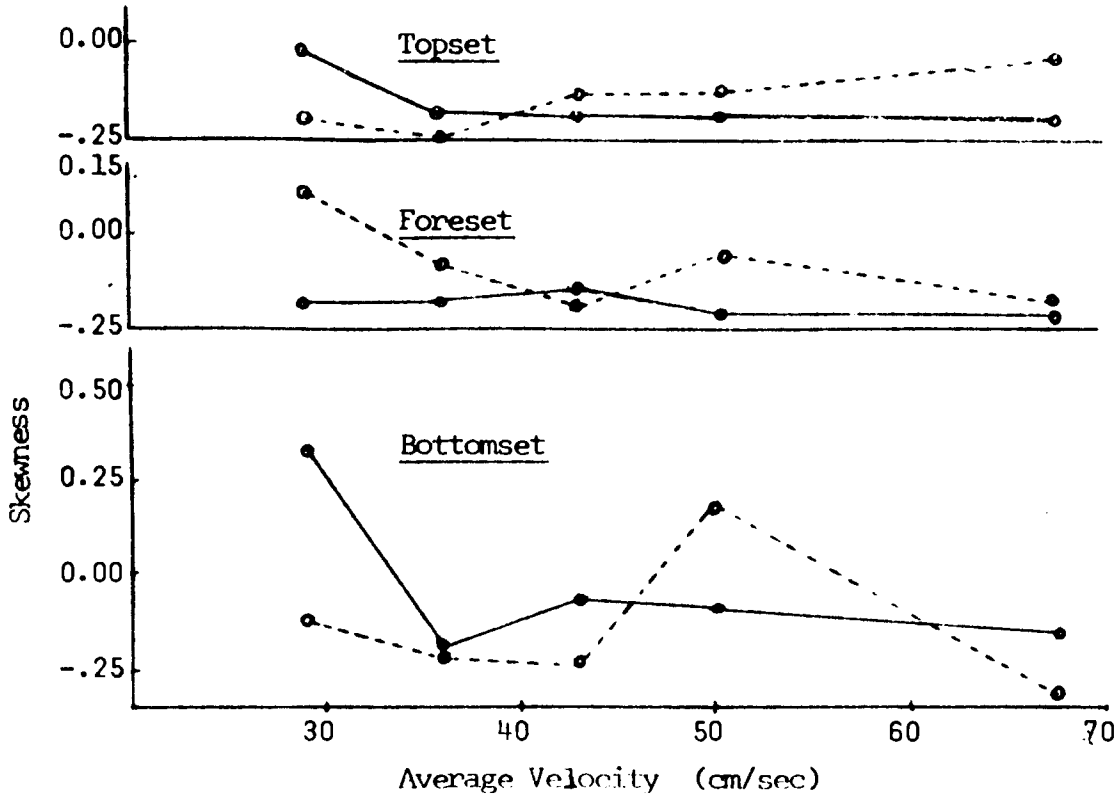

Figure 25a. Average Velocity versus Skewness.

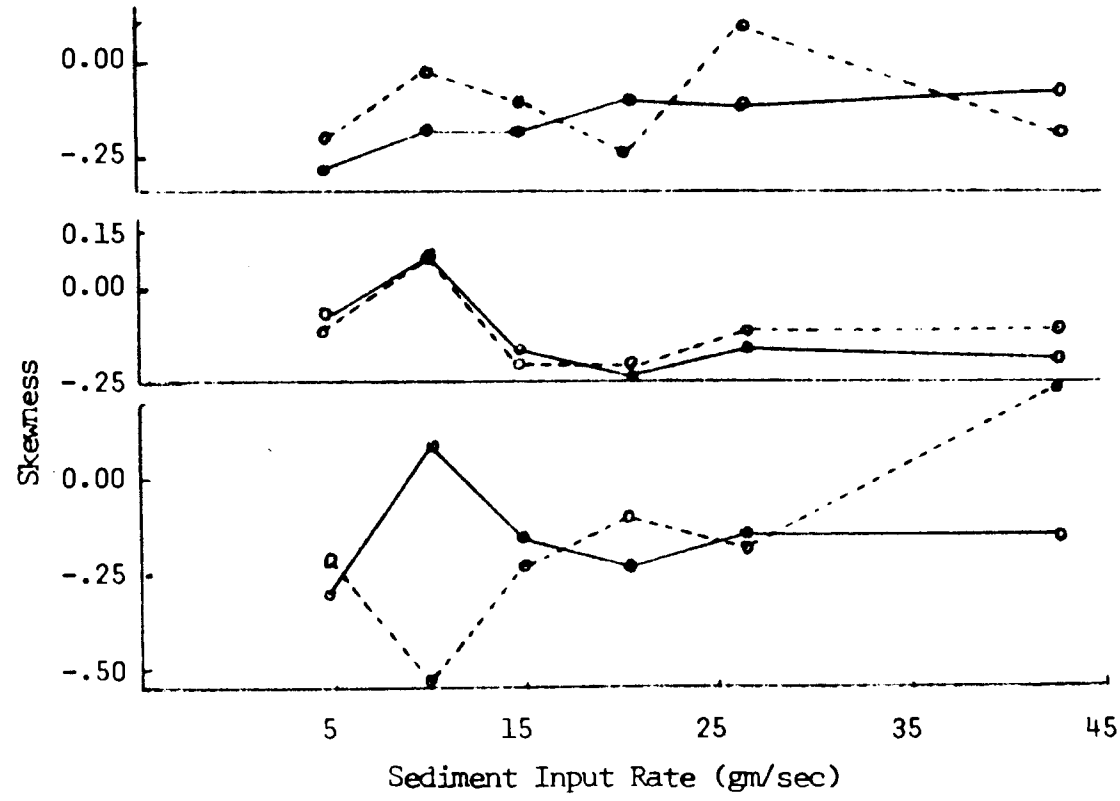

Figure 25b. Sediment Input Rate versus Skewness

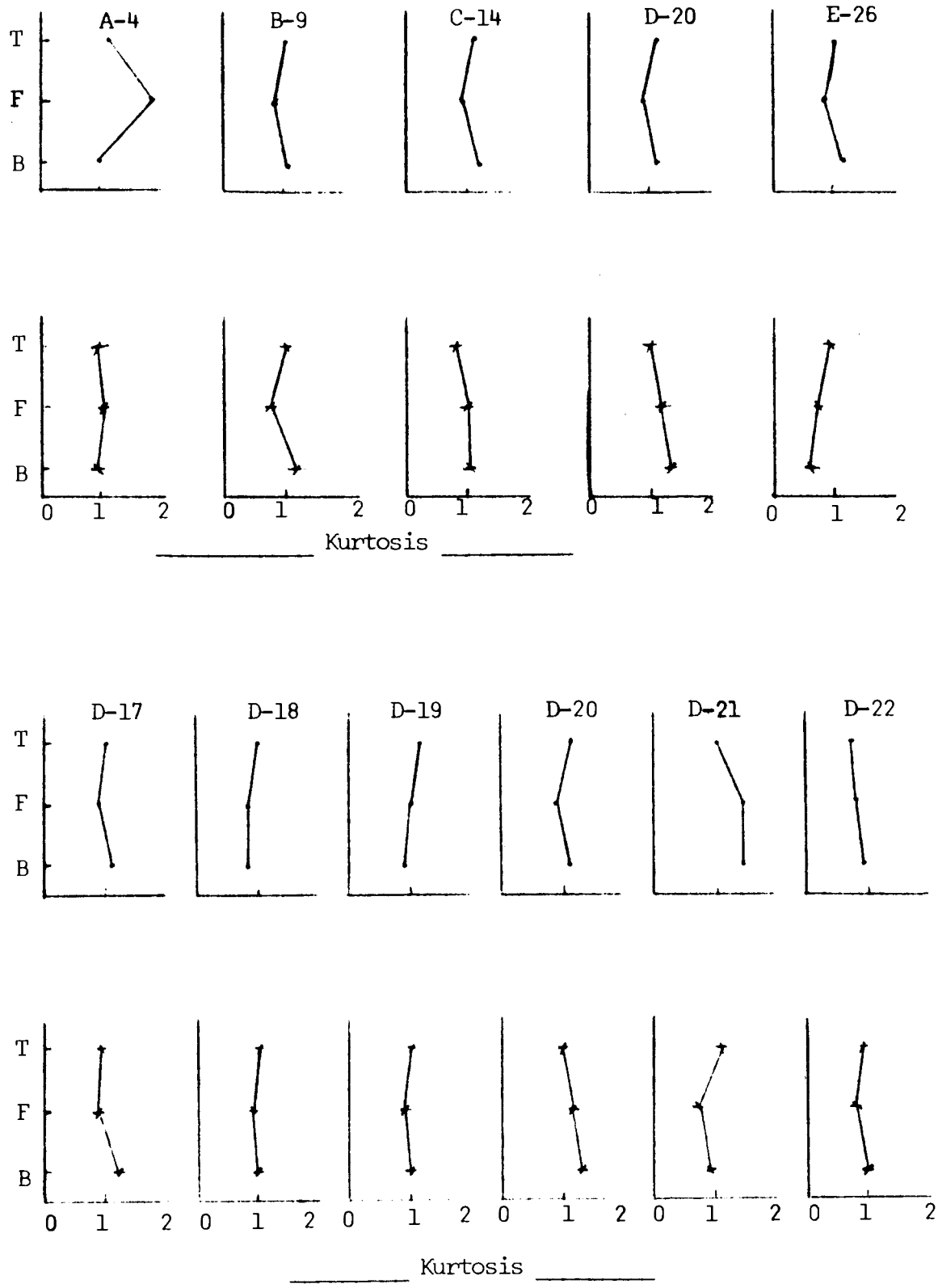

Figure 26. Variation in the Kurtosis Measure of Top-, Fore- and Bottom-set Deposit.

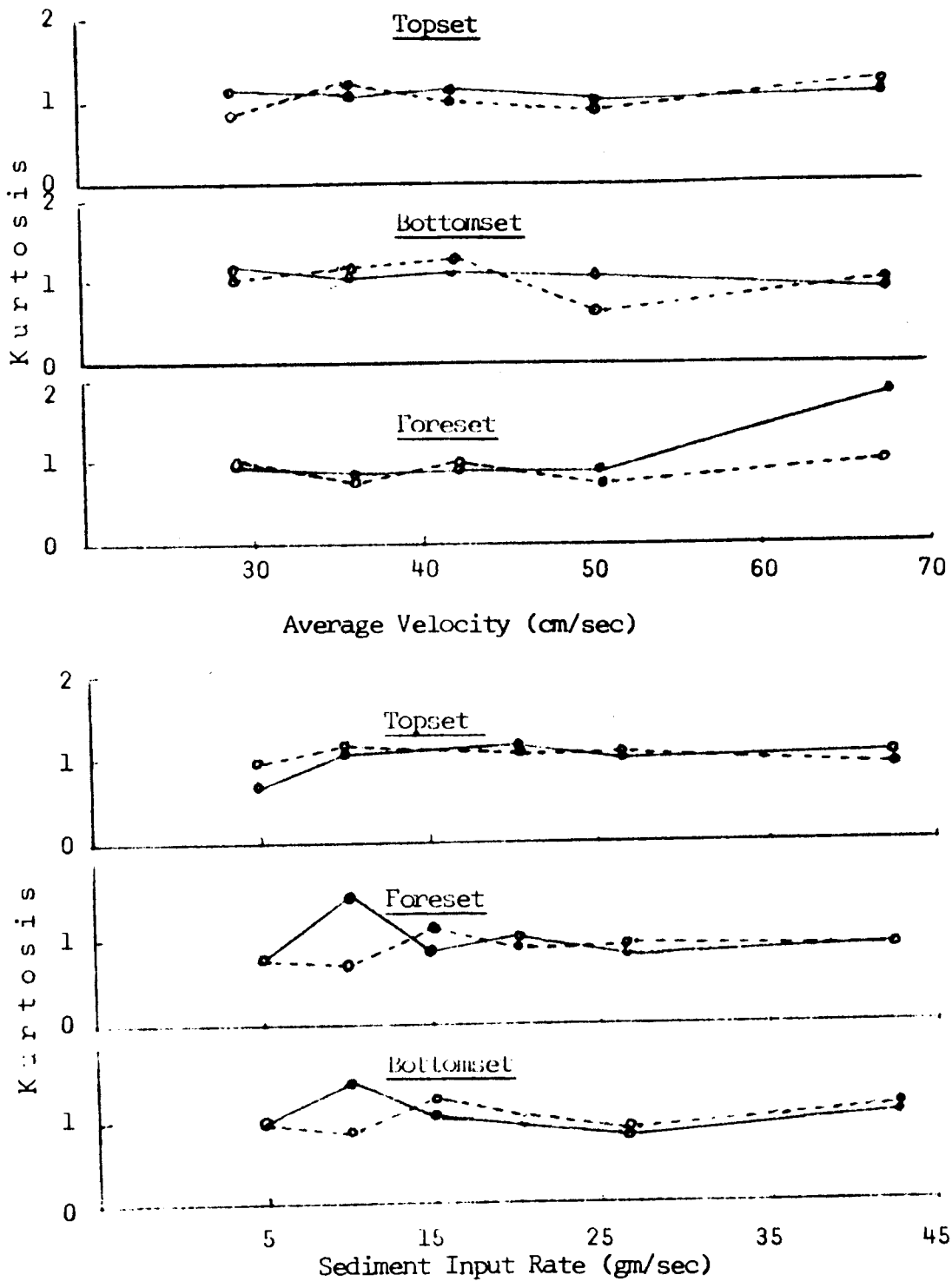

Figure 27. Relation between Kurtosis and Average Velocity and Sediment Input Rate.

VI. Discussion, Results and Research Problems

6.1 Discussion

The channel mouth is the dynamic dissemination point where sedimentation occurs to build a delta. The interaction between river effluent and the ambient water, resulting in the deconcentration of the outflow momentum and consequent loss of transporting power, is regarded as the primary cause of sedimentation. The majority of delta investigations have been of the stratigraphy and geology of an individual delta. Some of the works are morphological and purely descriptive. There have been relatively few attempts to analyse and detail the relation between the fluviatile processes and delta formation. Bates (1953) explored the submerged free-jet theory (Albertson et al, 1950) and proposed that a delta is built by jet flow. He recognized three types of inflow conditions on the basis of relative density differences between the river and basin water. One of these is the homopycnal situation, and it has been adopted in the present experiment.

The formulation of the present experimental delta model is relatively abstract and simple. It employs a rectangular flume system in which combinations of different discharge and sediment

input conditions have been incorporated to produce twenty-eight laboratory deltas. The model provides a simple method of exploring relationships between axial jet and deltaic deposition, and of describing interactions and interrelationships among flows, sediment transport conditions and the morphological delta pattern.

Measurements of the velocity-field along the longitudinal lateral and vertical directions of the expanding jet have been shown to be in substantial agreement with the analytical expression of the axial jet (Albertson et al, 1950; Bates, 1953). A dynamic similarity in the hydraulic expansion of the jets was also observed in the sediment-free flow conditions and under different discharge regimes.

The sediment transport through the flume channel involved two major mechanisms: relatively finer sediments were transported in suspension, while coarser materials moved along the channel bed. Proportionally high bed-load transport was characterized by low discharge and to some extent by high sediment-input conditions. Consideration of the bed-load transport is particularly important in the delta situation. This is because sediments moving along the bed are instantly affected by the variation in flow conditions, leading to deposition as soon as flow velocity falls below the critical limit for transportation. The lowering of the critical velocity limit is greatly influenced by the rapidly changing boundary conditions

at the channel mouth. On the other hand, the suspended materials are affected much more slowly and are carried away far beyond the delta-front.

Likewise, the initial deposition in the flume basin occurred in two different ways. The materials moving along the bed settled collectively at the efflux-section forming a pile, while the suspended-load settled discretely and in accordance with the hydraulic expansion of the jet flow. It may be pointed out that Jopling's (1964, 1965) model of lee-side deposition of a small laboratory delta has much in common with the present experiment. The model showed that the discrete settling of the individual particles and collective settling of a mixture of sediment grains are both important in the mechanics of delta growth. A sharp discontinuity in a channel floor causes flow separation and flow expansion. As a result, particles moving along the bed settle as a collective unit, and the finer materials carried in suspension tend to settle as discrete units in accordance with the particles' differential settling velocity.

One of the shortcomings in the interpretation of delta sedimentation has been the lack of a clear distinction between the occurrence of bed-load and suspended-load transport, and their different roles in the formation of deltas. It is more important when jet analogy is taken as a basis of deposition. This seems to be one of the basic deficiencies in Bates' (1950)

model for delta sedimentation. Van Straaten (1960) pointed out that the essential part of the river delta sediments, both subaqueous and subaerial, are formed by processes other than that of jet flow. Axelsson (1967) and Allen (1968) noted that the distribution of bed-load on the delta front is significant especially with respect to the sliding materials. Allen (1968) was critical about the "path-line method" used by Bonham-Carter and Sutherland (1967) in their computer simulation of delta sedimentation because their approach does not account for the bed-load transport.

There have been clear demonstrations in the experiment that dumping of bed-load at the channel efflux-section causes rapid vertical accretion. The upward growth of the deposition, in turn, tends to constrict the flow inducing bed shear stress. Such a change in the bottom boundary condition of the flow will imply intensification of turbulent activities, thereby affecting sediment transport and deposition. Following this occurrence, the top of the deposit becomes a flat-bed representing a rudimentary surface of equilibrium or local base-level. As a logical sequel of this development, the vertical flow expansion and diffusion is precluded, necessitating greater lateral spreading. As the delta builds, the front forms a sharp break of slope over which the slip-face (Jopling, 1960) mode of deposition continues. This has been the major observation concerning the mode of delta progradation in the present

experiment, and all other observed morphological features are of secondary importance.

In the case of low discharge and high sediment transport conditions the sediment-water interface (base-level) of the upward growth reaches a higher level. In other words, the thickness of the vertical accretion attains a relatively greater height. Concomitant with the development of the rudimentary base-level there has been a marked tendency for the flow to diverge. The formation of this divergent pattern of flow atop the depositional surface may be viewed in the following ways. As soon as the channel flow leaves the confinement of the channel banks it has a natural tendency to flare, resulting in the reduction of flow velocity and thus in the competence and capacity of the transporting power. The flaring is heightened by the gradual upward growth of the vertical accretion when flow fails to resist or truncate the surface. Since a greater quantity of sediment is transported along the mid-channel, the rate of deposition along the middle of the divergent flow is also higher. As a result, some kind of low-height sediment bulge evolves, which causes further flaring.

In response to the divergent flow pattern, materials are carried to the periphery of the depositional surface, building metastable sediment-wedges. The sediment-wedges periodically collapse due to shear failure and slip down the gravity-controlled foreset slopes, causing lateral expansion of

the delta. It seems highly significant that divergent flow and slumping process mainly contribute to the lateral expansion of the delta. As a result, the submerged natural levees are least developed because of their shifting position. It also seems reasonable to think that the increasing divergence of the flow over the depositional surface increases the bed shear stress, and in response to a critical value of the bed shear stress, certain bed forms are created (ripples, sandwaves). The formation of these bed forms causes localized damming effects to the flow and subsequently leads to formation of the distributary pattern over the delta surface.

On the other hand, the level of vertical accretion (base-level) at high discharge and low sediment transport operates at a relatively higher flow depth. That is, the thickness of the vertical accretion is relatively less. For inertial reasons the flow is relatively less divergent. However, the effects on the flow of the bottom boundary, which was formed through the upward growth of the vertical deposition, is significant because the interaction between them results in the intensification of turbulence, forming a strong eddy system, often violent in nature. It involves a turbulent exchange process where some of the sediment is propelled and moved to the sides of the flow, building submerged natural levees on either side. The formation of the levees gradually confines flow into a single channel. Following the formation of the levees, two

threads of maximum turbulence related to wall-drags are formed. As a result, a mid-channel longitudinal shoal slowly builds up and subsequently bifurcates the flow.

The present experimental observations demonstrate that the morphological delta pattern is directly dependent on the degree and nature of flow divergence that develops as a result of mutual interaction between the flows and depositional form. The flow causes certain forms to evolve but when this happens the character of the flow is itself altered in certain fundamental ways. It is this reaction which allows the development of different kinds of morphology in the deltaic environments. The efficacy of this interaction, involving various processes, depends in a complex manner upon the nature of the flow regime and the characteristics of the sediment transport.

Despite the above fact, the overall magnitude of the deltaic mass reflects the totality of the hydraulic regime and sediment transport conditions of the present experiment. From the standpoint of morphometry, areal mapping, surficial morphology, and the internal structure of the deltas produced in the present experiment, it may be inferred that the delta morphology is more than a passive product of the jet diffusion process. Most of these points have been discussed in chapter five and are summarized in the following section.

6.2 Synthesis of the findings

The major findings of the present laboratory flume study involving homopycnal inflow situation are summarized as follows.

1. The sedimentation process associated with the present experimental delta formation in a laboratory situation has been described, and the axial jet analogy proposed by Bates (1953) has been found to be inadequate in interpreting the overall delta morphology.
2. In the sediment-free flow system measurements of the velocity-field have been shown to be in substantial agreement with the general conception of the axial jet perceived by different authors including Alertson et al (1950) and Bates (1953).
3. A dynamic similarity in the hydraulic expansion of the jets forming at different flow regimes has been observed.
4. Initial deposition derived from the suspended load has been observed to correlate with the jet expansion pattern, but it was subsequently obscured by further deposition associated with reverse flow.
5. The coarse granular sediments moving along the bed have been observed to settle as collective units forming a pile at the channel efflux-section. The pile ultimately turned into the gravity-controlled foreset slopes along which slumpings occurred to prograde the delta.

6. As visually observed, slumping has been more frequent and almost continuous at high bed-load transport and low discharge conditions. Also, slumping related to the peripheral sediment wedge formation caused by divergent flow (forming over the delta surface) directly prevents stabilization and growth of submerged natural levees, but promotes lateral expansion of the delta.
7. It has been demonstrated that the morphological delta pattern developed differently in different discharge and sediment input conditions. However, linear measurements of the delta morphometry demonstrate that the magnitude of the deltaic mass is a log-linear function of the channel velocity and sediment-input rate.
8. It has also been shown that for a given sediment discharge, an increase in flow velocity causes a relative rate of increase in the longitudinal length of the delta, with concomitant decreases in both vertical and lateral growth. Conversely, at a given constant discharge of flow, an increase in sediment-input rate tends to retard the rate of longitudinal advances, a process effectively related to compensatory increases in both width and upward growth of the deltaic mass.
9. It has been demonstrated that morphological delta features are surficially formed and reasonably correlative with the nature and degree of flow divergence occurring over the

delta platform. Hydrodynamically more efficient or less divergent flow causes intense turbulent exchange, building submerged natural levees and a mid-channel longitudinal bar. A bar may lead to bifurcation of the flow, forming two distributary channels. Bed-forms such as sandwaves, sediment bulge, or broad-based shoal forming in response to fairly divergent flow pattern (hydraulically inefficient flow) and high bed-load transport, caused localized damming effects, and subsequently lead to the formation of distributary patterns and are usually shallow and short-lived.

10. The tripartite arrangement of topset, foreset, and bottomset beds has been examined and described qualitatively and quantitatively in section 5.3.4. The foreset deposit contributed the gross structural organization of the laboratory deltas. Cross-bedded structure of the foreset deposit is directly related to low discharge regime and the phenomenon of flow separation. The findings support Jopling's model of leeside deposition of a small laboratory delta (1964).

6.3 Problems and Future Research

The present flume experiment illustrates that by restricting the degree of freedom, the role of specific variables involved in the delta building mechanism can be

isolated for detailed observations. However, it is to be remembered that the condition generated in the flume is a gross simplification of the prototype in nature. Furthermore, the scale barrier is difficult to negotiate in extrapolating the results to large-scale natural occurrences. Despite these difficulties, the fundamental processes of deposition can be studied efficaciously in the laboratory flume.

Experimental procedures and equipment currently used are adequate. However, it is recommended that future studies of the kind incorporate the following suggestions:

a) Because of a probable variation in the pressurized water-flow system of the tap-points, it is necessary to provide an independent flow circuit system having an independent reservoir and a power driven mechanism for the flume.

b) The channel-component of the flume system should have sufficient longitudinal reach to provide adequate time and space for the flow to adjust with the boundary conditions.

c) Determination of velocity components in time and space is very important in such an investigation. Because of certain shortcomings, the Pitot static tube is not suitable for determining velocity heads at low discharge, or when the water is charged with sediments.

d) Because a part of the finer sediment is always lost during the runs, it is better not to recycle sediment when

the material is river sediment.

e) It would be better if a very large flume system is employed to overcome a certain scale barrier encountered in the present study.

f) It is felt that this study could be better performed by a team of workers rather than by an individual.

The present flume experiment has provided a valuable insight into the mechanism of delta formation in a variety of discharge and sediment transport conditions. But delta-building processes are very complicated, involving many variables rather than a few dominant ones. There is an obvious need for a comprehensive experimental study of the effective roles of the interdependent and interacting variables. A very promising laboratory flume research exists for consideration of the variation of channel width and slope, sediment grain-size, basin slope and morphology, and off-shore energy conditions. Further work could give better understanding of the natural processes, and also provide a renovated methodology for dealing with natural problems.

Another promising avenue of flume experimental research suggested by the present study is the consideration of morphological delta features and internal structures of laboratory deltas; that is, the formation of bars or shoals, and the building of natural levees, distributary system, and the deformation of the internal delta structure.

Appendix A

The flume system

The flume system used in the present experiment was designed and built by the writer, and was financed by the Department of Geography, Simon Fraser University. The flume system consists of three major components: the flume basin, the flume channel, and the hopper. The flume was placed on two tables with necessary supports as shown in figure A-1.

The flume basin, 300 cm long, 120 cm wide is made of 1.27 cm (0.5 inches) plywood (see figure A-2). The plywood was sized and nailed together to build the tray-shaped basin. The joints were sealed with fibre glass to prevent leakage. A few innovations were introduced into the basin. Six foam slabs covering a longitudinal distance of 240 cm to raise the basin-bottom by 10 cm. Twenty-five lateral-lines (A to Y) and 48 longitudinal-lines (0 to 48), 5 cm apart, were drawn on the foam surface to provide necessary grid-references. Eight outlet tubes (dia. 0.4 cm) were connected to the basin for draining out the water at the end of the run. To control the water-level of the flume basin, a 22 cm high weir was built at a longitudinal distance of 180 cm. Two outlet tubes (dia. 2.5 cm) were fixed at

a distance of 190 cm from the channel mouth to provide a necessary exit for the spilled-water over the weir during the run.

The flume channel, 100 cm long, 10.2 cm wide and 10 cm deep, is made of plywood (Figure A-1 and A-2). It is a rectangular open-channel whose bottom and sides were capped with very thin metallic sheets. The upper end of the channel was supported by a block of wood. Water was drawn into the flume system through two flexible hoses (dia. 2.54 cm).

The hopper is a rectangular cone-shaped box built with four pieces of plywood. The upper and lower ends represent squared-openings, measuring 30 cm x 30 cm and 8 cm x 8 cm, respectively, and the vertical height of the cone wall is 65 cm (Figure A-1 and A-2). The lower end of the hopper is fixed on a rectangular piece of plywood with a hole (diametre 3.5 cm) at the middle. A metal plate with six openings was used to regulate the sediment-feed rates into the flow system. The hopper was suported by three bricks on either side of the flume head (Figure A-1).

The flow circuit for the flume is shown in figure A-3. Water was drawn from two tap-points through flexible hoses into the flume channel, and thence to the flume basin. During the test run, the spilled-water over the weir was drained out through the two exit-pipes without recirculation.

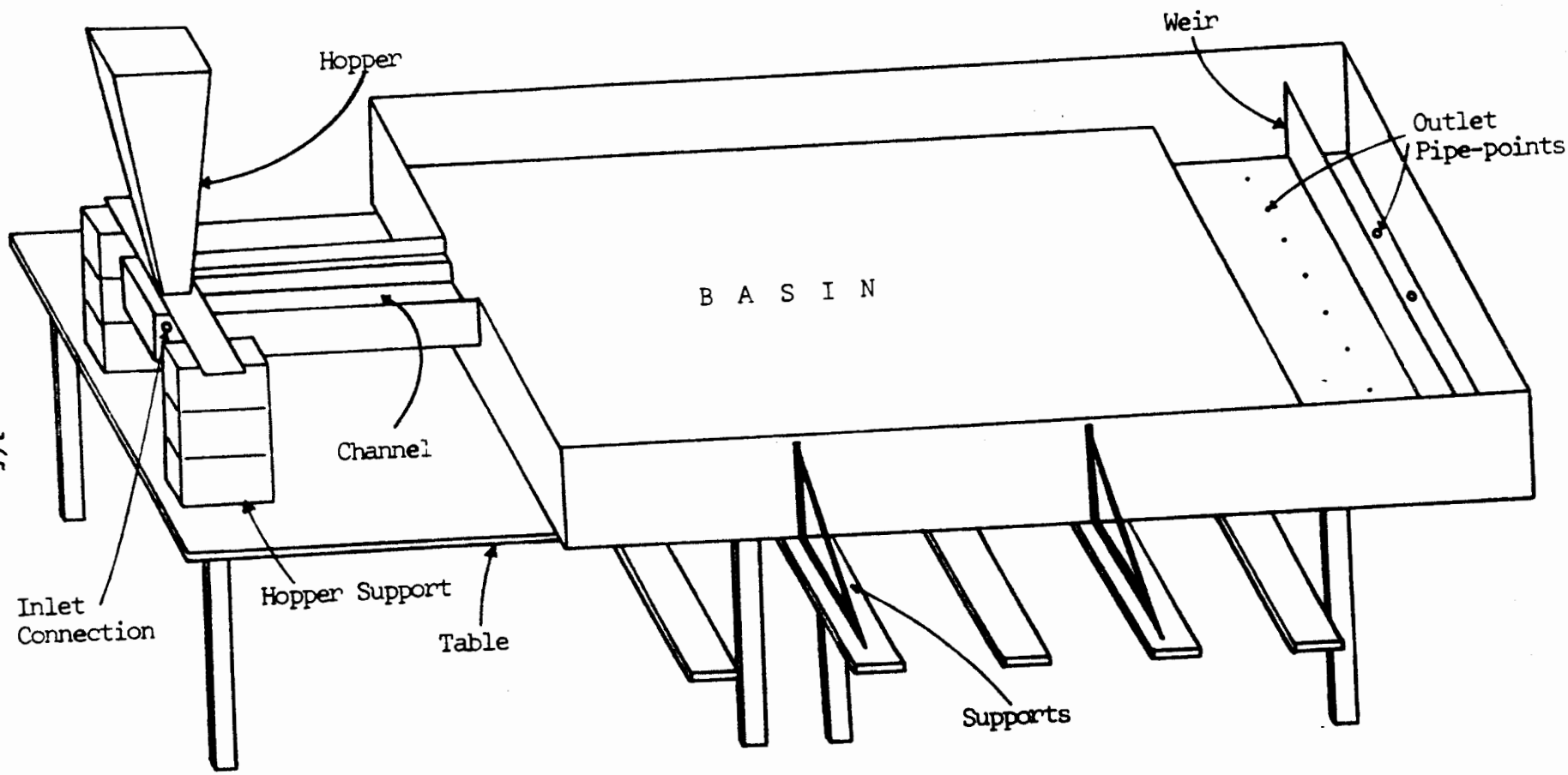

Figure A-1. Diagrammatic Representation of the Flume System.

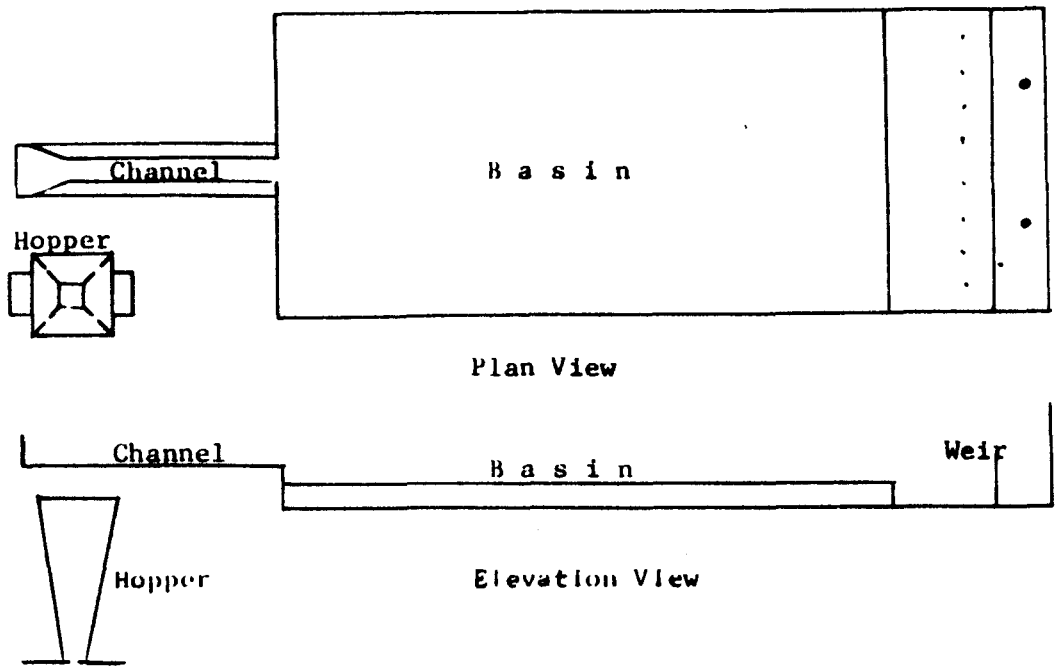

Figure A-2. Plan and Elevation of the Flume System.
Scale is 1 cm to 30 cm.

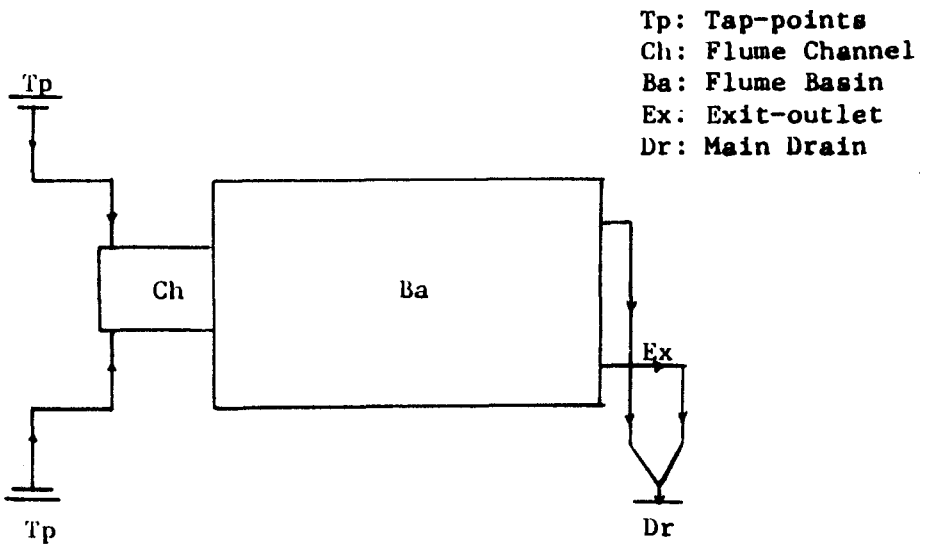

Figure A-3. Flow-Circuit of the Flume.

Appendix B

Computations of Velocity, Discharge and Froude Number

The flow-velocity of a location, V, was computed from the relation: $V = 2gh$ where g is the acceleration due to gravity (980 cm/sec) and h represents velocity-head measured at the location.

A pitot static tube was used to determine the velocity-head. The instrument consists of two separate parallel parts in a single tube with a right angle bend at one end. One of these parts indicates the sum of the pressure head and velocity head (i.e. total head), and the other part indicates the pressure head. The heads of the pitot tube are connected with the glass tube fixed vertically on a board. The pitot tube is immersed at a required flow-depth and water is sucked up through the glass-stems to remove all air. When the instrument is held tight facing the current, differential water rises are indicated by the vertical glass-stems. The vertical distance between these two rises is the velocity head. Tables B1, B2, and B3 represent the velocity-head, flow-velocity and discharge of the different locations of the runs.

Table B-1

Velocity-head and flow variables

Contained in this section of the table are data relating to velocity-heads (cm) and flow velocities (cm/sec) recorded at the mouth of the flume channel in the sediment-free flow system. The locational references on the measurements are shown in figure B-1.

Ref.	Variables	Series-A	Series-B	Series-C	Series-D	Series-E
P	h/V	1.90	0.30	0.15	0.80	1.00
1		61.02	24.25	17.15	39.29	44.27
P	h/V	4.40	0.85	0.60	2.15	2.95
2		92.86	40.81	34.29	64.91	76.04
P	h/V	5.20	1.25	0.85	2.65	3.55
3		100.95	49.49	40.81	72.07	83.41
P	h/V	4.40	0.85	0.60	2.15	2.95
4		92.86	40.81	34.29	64.91	76.04
P	h/V	1.90	0.30	0.15	0.80	1.00
5		61.02	24.25	17.15	39.29	44.27
P	h/V	0.85	Measurements of the		0,20	0.40
6		40.81	above data involved 6/10th of the		19.79	28.00
P	h/V	1.80	flow-depth from the		0.45	0.75
7		59.39	water-surface		29.69	38.34
P	h/V	2.20			0.70	1.10
8		65.66			37.04	46.43
P	h/V	1.80			0.45	0.75
9		59.39			29.69	38.34
P	h/V	0.85			0.20	0.40
10		40.81			19.79	28.00

Other variables computed from the above figures or otherwise measured are shown below.

V cm/sec	67.50	36.00	29.00	42.00	50.50
d cm	2.00	1.35	1.00	1.50	1.75
w cm	10.20	10.20	10.20	10.20	10.20
Q cm^3/sec	1377.00	495.72	295.80	642.60	901.07
Fr.	1.525	0.9897	0.9234	1.0954	1.2189

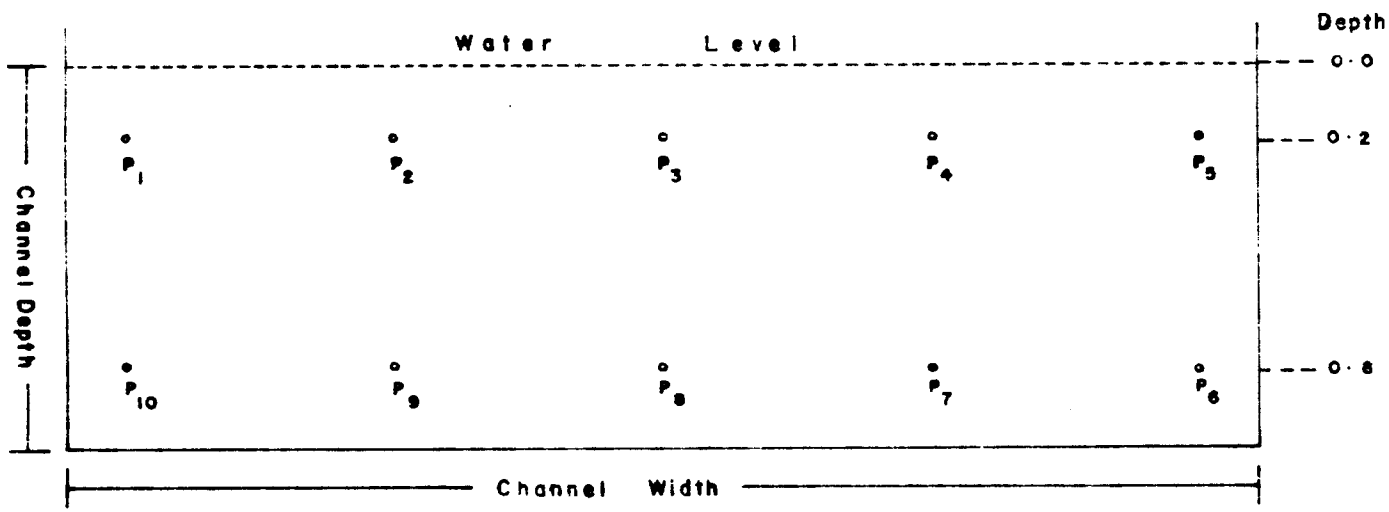

Figure B-1. Diagrammatic Representation of Locational References Across Channel-Mouth.

TABLE B-2

Velocity-head data of the jets

Contained in this section of the table are data relating to velocity-heads (cm) and flow velocities (cm/sec) recorded at the mouth of the flume channel in the sediment-free flow system. The locational references on the measurements are shown in figure 7

Grid Ref.	Series-A	Series-B	Series-C	Series-D	Series-E
M/0	5.20	1.40	0.85	2.65	3.55
M/4	5.20	1.40	0.85	2.65	3.55
L/4	2.55	0.65	0.40	1.30	1.70
K/4	0.00	0.00	0.00	0.00	0.00
M/7	5.20	1.35	0.80	2.65	3.55
L/7	1.85	0.50	0.30	0.95	1.25
K/7	0.05	***	***	***	***
J/7	0.00	0.00	0.00	0.00	0.00
M/11	3.50	0.90	0.60	1.75	2.35
L/11	1.60	0.45	0.30	0.80	1.10
K/11	0.75	0.20	0.10	0.30	0.50
J/11	***	***	***	***	***
I/11	0.00	0.00	0.00	0.00	0.00
M/15	3.00	0.80	0.50	1.50	2.00
L/15	1.55	0.40	0.20	0.75	1.05
K/15	0.65	0.15	0.10	0.30	0.45
J/15	0.20	0.05	***	0.10	0.15
I/15	***	****	***	****	****
H/15	0.00	0.00	0.00	0.00	0.00
M/20	1.75	0.45	0.30	0.85	1.20
L/20	1.30	0.35	0.15	0.65	0.90
K/20	0.80	0.20	0.10	0.35	0.50
J/20	0.45	0.10	0.05	0.20	0.25
I/20	0.20	0.05	***	0.10	0.15
H/20	0.05	***	***	***	***
G/20	0.00	0.00	0.00	0.00	0.00

(Table continued on next page)

Table B-2 (continued)

Velocity-head data of the jets

Grid	Series-A	Series-B	Series-C	Series-D	Series-E
M/25	1.30	0.30	0.20	0.65	0.85
K/25	0.80	0.15	0.15	0.40	0.55
I/25	0.25	0.05	***	0.10	0.15
G/25	0.15	***	***	0.05	0.10
E/25	0.00	0.00	0.00	0.00	0.00
M/30	1.10	0.25	0.20	0.55	0.75
K/30	0.80	0.15	0.10	0.35	0.55
I/30	0.55	0.10	0.05	0.25	0.35
G/30	0.20	0.05	***	0.10	0.15
E/30	0.10	***	***	0.05	0.05
C/30	0.10	***	***	***	***
A/30	***	***	***	***	***
M/35	0.95	0.25	0.15	0.50	0.65
M/40	0.85	0.20	0.15	0.45	0.55
M/45	0.80	0.20	0.15	0.45	0.50

*** represents h is less than 0.05 i.e., velocity < 9 cm/sec.

Computations of the flow velocity of the channel were done by measuring the velocity-head at ten locations across the channel width. They involve the determination of the velocity head at 0.2 and 0.8 of the total flow-depth of the channel. Another method involving six-tenths of the flow depth from the water surface was employed to determine the velocity-head where the channel flow depth was shallow. The average velocity was computed by taking the arithmetic mean of the ten or six locations. Table B1 lists the measurements and the velocities of

the channel flow.

The flow-discharge was computed from the equation Q = V.A, where V rerpresents the average velocity and A is the cross-sectional area (width x depth) of the channel flow. The flow depth and width were directly measured, and are shown in table B1.

The Froude Number was computed from the relation,

$$Fr. = \frac{V}{\sqrt{2gd}}$$

where Fr. = Froude Number
V = Average velocity of the channel flow
g = Acceleration due to gravity (980 cm/sec)
d = Channel flow-depth.

The velocity of the jet at different locations along longitudinal, lateral, and vertical directions was computed from direct measurements of the velocity-heads at those locations. The locations of the velocity-head measurements are shown in figure 7 (Section 5.1) and data related to these measurements are listed in tables B-2 and B-3.

Table B-3

Velocity-head data of the jets

Contained in this table are all the data relating to the velocity-heads of the jet flows measured along the vertical axis of the jets. The locations of the measurement are shown in figure 7. The data are in cm.

Ref.	Depth	Series-A	Series-B	Series-C	Series-D	Series-E
	0.4	5.20	1.40	0.95	2.65	3.55
M/4	2.0	3.30	0.90	0.60	1.70	2.25
	4.0	0.35	0.10	0.05	0.15	0.20
	6.0	0.00	0.00	0.00	0.00	0.00
	0.4	5.20	1.35	0.95	2.65	3.55
	2.0	2.90	0.76	0.55	1.50	2.00
M/7	4.0	1.05	0.25	0.20	0.55	0.70
	6.0	0.10	0.05	***	0.05	0.05
	8.0	0.00	0.00	0.00	0.00	0.00
	0.4	3.50	0.90	0.60	1.75	2.35
	2.0	2.40	0.65	0.45	1.20	1.65
	4.0	1.30	0.35	0.25	0.65	0.85
M/11	6.0	0.30	0.15	0.10	0.30	0.40
	8.0	0.10	****	****	****	0.05
	10.0	0.00	0.00	0.00	0.00	0.00
	0.4	3.00	0.80	0.50	1.50	2.00
	2.0	1.30	0.35	0.25	0.65	0.85
M/15	4.0	0.65	0.20	0.15	0.35	0.45
	6.0	0.30	0.10	0.05	0.15	0.20
	8.0	0.10	***	***	0.05	0.05
	10.00	***	***	***	***	***
	0.4	1.75	0.45	0.30	0.85	1.20
	2.0	1.10	0.30	0.20	0.55	0.75
M/20	4.0	0.65	0.15	0.10	0.30	0.45
	6.0	0.35	0.10	0.05	0.20	0.25
	8.0	0.20	0.05	***	0.10	0.15
	10.0	0.05	***	***	***	***

(Continued on next page)

Table B-3 (continued)

Velocity-head data of the jets

Ref.	Depth	Series-A	Series-B	Series-C	Series-D	Series-E
	0.4	1.30	0.30	0.20	0.65	0.85
	2.0	0.85	0.25	0.15	0.45	0.60
M/25	4.0	0.50	0.15	0.10	0.25	0.30
	6.0	0.25	0.05	0.05	0.15	0.15
	8.0	0.10	***	***	0.05	0.05
	10.0	***	***	***	***	***
	0.4	1.10	0.25	0.20	0.55	0.75
M/30	2.0	0.55	0.15	0.10	0.30	0.40
	6.0	0.15	0.05	***	0.05	0.10
	10.0	***	***	***	***	***
	0.4	0.95	0.25	0.15	0.50	0.65
M/35	2.0	0.40	0.10	0.05	0.20	0.25
	6.0	0.05	***	***	***	0.05
	10.0	***	***	***	***	***

All values are within the range of +/-1 0.02cm.
**** indicates that velocity-head is less than 0.05

Appendix C

Sampling and size of sediment analysis

Samples of sediment were taken from eight locations covering topsoil, foreset, and bottomset materials. Sediment samples were dried at room temperature and analysed by a visual accumulation tube.

The equipment consists of a sedimentation tube and a special recorder. The tube has a length of 120 cm and an inside diameter of 2.54 cm., except for the lower end, which has a constricted sediment-accumulation section with a diameter of 5.00 mm. The size analysis is based on a stratified sedimentation system in which a sample (weighing within 5 to 7 gm) is introduced at the top of a settling tube containing water. A manually operated pen is used to trace the height of sediment accumulation on a chart which moves at an uniform speed. Analyses are in terms of fall velocity of individual particles of which the sample is composed. The cumulative size frequency distribution is determined graphically by the intercepts on the ordinate axis.

The sediment sizes corresponding to percentiles of 5, 16, 25, 50, 75, 84 and 95 were read from the chart and are listed in

tables C - 1 and C - 2. All percentiles are expressed in phi units.

The sediment parameters used in this study are those suggested by Folk and Ward (1957). The parameters are expressed as follows:

$$\text{Mean Size} = \frac{016 + 050 + 080}{3}$$

$$\text{Sorting (standard deviation)} = \frac{084 - 016}{4} + \frac{095 - 05}{6.6}$$

$$\text{Skewness} = \frac{016 + 084 - 2050}{2(084 - 016)} + \frac{05 + 095 - 2050}{2(095 - 05)}$$

$$\text{Kurtosis} = \frac{095 - 05}{2.44(075-025)}$$

The measure of central tendency is the median diameters, 50% value on the cumulative frequency graph. The median separates the sample into two equal halves by weight. The other way of expressing the central tendency is to use the mean value. If the sample has a symmetrical distribution the mean and median are the same; if the mean differs from the median the

Table C-1

Contained in this table are the data relating to the sediment sizes corresponding to various percentiles expressed in Phi units. The data are read from graphs traced by the visual Accumulation tube. The sediment samples represent topset (T), foreset (F) and bottomset (B) deposits collected from the longitudinal distances of 25, 65, 105 and 145 cm from the channel mouth. They are listed below in the increasing order of distances.

References		05	016	025	050	075	054	095
	T	1.0	1.395	1.615	2.015	2.24	2.40	2.73
Run -4	F	0.705	1.09	1.29	1.69	2.0	2.07	2.195
	B	.64	1.00	1.185	1.59	1.91	2.045	2.23
	T	1.56	2.015	2.16	2.56	2.78	3.00	3.18
Run -9	F	0.705	1.045	1.235	1.695	2.045	2.15	2.40
	B	1.09	1.67	1.845	2.16	2.495	2.58	2.76
	T	1.515	1.845	2.045	2.325	2.62	2.75	3.08
Run -14	F	0.775	1.185	1.395	1.845	2.16	2.29	2.58
	B	0.40	0.595	0.705	0.845	1.135	1.29	1.64
	T	1.185	1.67	1.94	2.29	2.60	2.73	3.02
Run - 20	F	0.705	1.09	1.29	1.775	2.12	2.23	2.51
	B	0.92	1.34	1.515	1.785	2.09	2.195	2.48
	T	1.09	1.535	1.695	2.10	2.36	2.52	2.75
Run - 26	F	0.845	1.135	1.34	1.73	2.015	2.09	2.29
	B	1.0	1.29	1.515	1.785	2.07	2.195	2.44
	T	1.09	1.29	1.515	1.785	2.10	2.195	2.40
Run -4	F	0.40	1.00	1.185	1.56	1.91	2.06	2.195
	B	1.045	1.395	1.56	2.015	2.195	2.29	2.585
	T	1.395	1.845	2.07	2.415	2.65	2.75	3.03
Run -9	F	0.575	0.705	1.00	1.515	1.94	2.13	2.40
	B	1.135	1.755	1.94	2.29	2.58	2.66	2.91

(Continued on next page)

Table C-1 (continued)

References		05	016	025	050	075	054	095
	T	.575	.845	.09	1.56	1.91	2.045	2.195
Run -14	F	.575	.845	1.045	1.29	1.67	1.895	2.10
	B	1.785	2.16	2.325	2.63	2.91	3.03	3.23
	T	1.29	1.64	1.845	2.22	2.55	2.65	3.035
Run -20	F	.705	1.135	1.535	1.845	2.195	2.325	2.62
	B	.845	1.535	1.755	2.15	2.48	2.585	2.84
	T	1.535	1.845	2.015	2.275	2.55	2.60	2.80
Run - 26	F	0.575	0.775	1.00	1.515	2.015	2.13	2.53
	B	1.67	2.015	2.13	2.48	2.65	2.75	3.02
Bottomset deposit only								
Run - 4		0.705	1.45	1.67	2.12	2.44	2.57	2.80
Run - 9		2.045	2.415	2.585	2.86	3.10	3.20	3.55
Run - 14		2.36	2.67	2.83	3.15	3.47	3.56	3.80
Run - 20		1.45	1.67	1.97	2.26	2.58	2.67	3.05
Run - 26	F	1.97	2.16	2.325	2.62	2.84	3.00	3.18
Run 4		1.845	2.10	2.26	2.585	2.80	3.00	2.27
Run - 9		2.36	2.65	2.84	3.10	3.31	3.45	3.69
Run - 14		2.69	3.03	3.17	3.44	3.61	3.705	3.88
Run - 26		2.015	2.26	2.44	2.73	3.035	3.16	3.54
Run - 26		2.12	2.48	2.62	2.91	3.14	2.28	3.63

Table C-2

Sediment grain size analysis

Contained in this table are the data relating to the sediment sizes corresponding to various percentiles expressed in Phi units. The data are read from graphs traced by the visual Accumulation tube. The sediment samples represent topset (T), foreset (F) and bottomset (B) deposits collected from the longitudinal distances of 25, 65, 105 and 145 cm from the channel mouth. They are listed below in the increasing order of distances.

References		05	016	025	050	075	054	095
	T	1.09	1.59	1.815	2.13	2.53	2.62	2.95
Run - 17	F	0.705	1.09	1.29	1.755	2.06	2.195	2.48
	B	1.00	1.395	1.56	1.94	2.18	2.31	2.67
	T	0.92	1.535	1.695	2.16	2.55	2.66	3.01
Run - 18	F	0.705	1.045	1.235	1.695	2.07	2.15	2.455
	B	0.705	1.00	1.185	1.615	1.97	2.06	2.29
	T	1.56	1.97	2.10	2.385	2.62	2.72	3.05
Run - 19	F	0.92	1.235	1.515	1.91	2.16	2.275	2.60
	B	1.185	1.515	1.64	2.015	2.23	2.325	2.58
	T	1.185	1.67	1.94	2.29	2.60	2.73	3.02
Run - 20	F	0.705	1.09	1.29	1.755	2.12	2.23	2.51
	B	0.92	1.34	1.515	1.785	2.09	2.195	2.48
	T	0.845	1.395	1.615	2.015	2.325	2.51	2.71
Run - 21	F	0.40	0.64	0.845	1.235	1.73	1.91	2.23
	B	0.845	1.235	1.715	1.91	2.195	2.36	2.58
	T	0.775	1.185	1.515	1.94	2.23	2.36	2.63
Run - 22	F	0.285	0.64	0.845	1.395	1.91	2.07	2.325
	B	1.235	1.56	1.695	2.045	2.23	2.29	2.495

(Continued on next page)

Table C-2 (continued)

References		05	016	025	050	075	054	095
	T	.845	1.185	1.395	1.875	2.16	2.31	2.62
Run - 17	F	0.705	1.09	1.29	1.73	2.10	2.23	2.58
	B	1.045	1.615	1.845	2.16	2.51	2.82	3.01
	T	.705	1.235	14.5	1.73	2.29	2.48	2.69
Run - 18	F	0.705	1.09	1.29	1.73	2.10	2.24	2.55
	B	1.135	1.64	1.845	2.195	2.52	2.61	2.86
	T	1.395	1.185	2.045	2.36	2.62	2.69	2.91
Run - 19	F	0.775	1.185	1.395	1.875	2.44	2.195	2.58
	B	1.045	1.59	1.755	2.10	2.44	2.57	2.84
	T	1.29	1.64	1.845	2.22	2.55	2.65	3.035
Run - 20	F	0.705	1.135	1.535	1.845	2.195	2.325	2.62
	B	.845	1.535	1.755	2.15	2.48	2.585	2.84
	T	1.29	1.73	1.97	2.260	2.57	2.67	3.00
Run - 21	F	.575	.705	.92	1.34	1.785	2.015	2.0195
	B							
	T	1.00	1.515	1.67	2.12	2.455	2.585	2.76
Run - 22	F	.575	.845	1.045	1.515	1.97	2.09	2.36
	B	1.185	1.56	1.73	2.10	2.325	2.48	2.62

Bottomset deposit only

17		1.56	1.815	2.015	2.29	2.60	2.69	3.05
18		1.64	1.94	2.07	2.35	2.60	2.67	2.93
19		1.615	1.91	2.06	2.325	2.58	2.67	2.96
20		1.535	1.755	1.97	2.23	2.495	2.58	2.72
21		1.45	1.67	1.97	2.26	2.58	2.67	3.05
22		1.615	1.94	2.07	2.36	2.61	2.80	3.01
Run - 17		2.045	2.36	2.55	2.82	3.12	3.34	3.41
Run - 18		1.97	2.23	2.36	2.68	2.98	3.07	3.41
Run - 19		2.015	2.26	2.44	2.71	3.00	3.12	3.38

(Continued on next page)

Table C-2 (continued)

Run - 20		2.015	2.26	2.44	2.73	3.035	3.16	3.54
Run - 21		2.015	2.26	2.36	2.63	2.90	3.03	3.26
Run - 22		1.67	2.015	2.13	2.44	2.68	2.78	3.12

distribution is asymmetrical or bimodal in character.

Folk and Ward (1957) suggested a verbal scale to describe sorting as follows:

St < 0.35	very well sorted
0.35 < st < 0.50	well sorted
0.50 < st < 1.00	moderately sorted
1.00 < st < st 4.00	poorly sorted extremely poorly sorted.

It is suggested that when sediment is bimodal, the sorting will most likely be poorer than when it is unimodal. The degree of sorting depends to a considerable extent on the method of sediment transport. The skewness of a sediment indicates the departure of the mean from the median. In symmetrical distribution the mean and median values are the same. If skewness is negative the mean is less than the median; the distribution is skewed towards smaller 0 value or coarser particles. On the other hand, if skewness is positive the distribution is skewed towards the higher 0 values or finer particles.

Kurtosis is a measure of peaknedness. Very high or low values of Kurtosis suggest that one type of material was sorted

in a region of high energy, and then transported without change in character to another environment, where it becomes mixed with another sediment, possibly of low energy.

Selected Bibliography

Abrahams, A. D., 1968., "Distinguishing between the concepts of Staedy State and Dynamic Equilibrium in Geomorphology": Earth Sci. Jour., v.2, No. 2, pp. 160-166.

Albertson, M.L., Dai, Y.B., Jensen, R.A., and Rouse, Hunter, 1950; "Diffusion of Submerged Jets": Am. Soc. Civil Engineers Trans., v.115, pp. 629-697.

Allen, J.R.L., 1964; "Sedimentation in the Modern Delta of River Niger": West Africa: in Straaten, V. (ed.), Deltaic and Shallow Marine Deposits, Amsterdam (Elsevier), pp. 26-32.

Auerbach, M., 1939; "Die Obserflachen und Tiefenstrome im Bodensee": Deutcsche Wasserwirtschaft, v.34(8), pp. 358 -366.

Axelsson, V., 1967; "The Laiture Delta": Geografiska Annaler, 49A (1).

Bagnold, R.A., 1968; "Deposition in the Process of Hydraulic Transport": Sedimentology, v.12, pp. 45-56.

Barrell, J., 1912; "Criteria for the Recognition of Ancient Delt Deposits": Bull. Geol. Soc. Am., v.23, pp. 377-446.

Bates,C.C., 1953; "Rational Theory of Delta Formation": Bull. Am. Assoc. Petrol. Geologists, v.37, pp. 2119-2162.

Bates, C. C., and Freeman, J. C., 1953; "Interrelations between Jet Behaviour and Hydraulic Processes Observed at deltaic River Mouths and Tidal Inlets": Proceedings of the 3rd Conf. Coastal Eng., Council on Wave Research, Berkeley, California.

Blatt, H., Middleton, G., and Murray, R., 1972: Origin of Sedimentary Rocks: Prentice-Hall, New Jersey.

Bonham-Carter, G.F., and Sutherland, A.J., 1967; "Diffusion and Settling of Sediments at River Mouth - a Computer Simulation Model": Gulf Coast Assoc. Geol. Soc. Trans., v.17, pp. 326-338.

Borichansky, L.S., and Mikhailov, V.N., 1966; "Interaction of River and Sea Water in Absence of Tides": in Scientific Problems of the Humid Tropical-Zone Deltas and Their

Implications, Proceedings of Dacca Symposium (1964), UNESCO., pp. 175-180.

Brush, L.M. Jr., 1965; "Sediment Sorting in Alluvial Channels": Soc. Eco. Paleontologists and Mineralogists, Spe. Pub. No. 12, pp. 25-33.

Chorley, R. J.; 1962; "Geomorphology and general systems theory": U. S. Geological Survey, Professional Papers, 500 - B.

Chow, V.T., 1959; Open-Channel Hydraulics: McGraw-Hill, New York.

Church, M., and Gilbert, R., 1975; "Proglacial Fluvial and Lacustrine Environments": Soc. Eco. Paleontologists and Mineralogists, Spe. Publ. No. 23.

Cobb, W. C., 1952; "The Passes of the Mississippi River": Am. Soc. Civil Eng., pp. 13-23.

Coleman, J.M., and Wright, J.D., 1971; "Analysis of Major River Systems and Their Deltas - Procedures and Rationale with Two Examples": Louisiana State Uni., Coastal Studies Series No. 28.

Crickmay, C.H., and Bates, C.C., 1955; "In Discussion of Delta Formation": Am. Assoc. Petrol. Geologists Bull., v.39, pp. 107-114.

Crowell, J. C., 1952; "Submarine Canyons Bordering Central and Southern California": Jour. Geol., v.60 (1), pp. 58-83.

Dent, E. J.; 1924; "The Mouths of the Mississippi River": Trans. Am. Soc. Civil Eng., v.85(1545), pp. 997-1006.

Dozier, J., 1973; "An Evaluation of the Variance minimization principle in river Channel adjustment": Ann Arbor Michigan Uni., Unpubl. Ph.D. Thesis.

Elrod, H.G., 1954; "Computation Charts and Theory for Rectangular and Circular Jets": Heating, Piping and Air Conditionings, v.26, no.3, pp. 149-155.

Fisk, H. N., 1944; "Geological Investigation of the Alluvial Valley of the Lower Mississippi River": Mississippi River Comm., Vicksburg, Miss. 78p.

Folk, R. L. and Ward, W. C., 1957; "Brazos River Bar: a Study in

the Significance of Grain Size Parameters": Journ. Sed. Petrology, V. 27, No. 1, pp. 3-26.

Forel, F. A., 1904, Le Leman, v.II, Lausanne, Switzerland.

Gilbert, G. K.; "Report on the Geology of the Henry Mountains": U.S. Geogr. and Geol. Surveys of the Rocky Mountain Region, 170 p.

Gilbert, G.K., 1885; "The Topographic Features of Lake Shores": U.S. Geol. Survey Annual Report, v.5, pp. 104-108.

Gilbert, R., 1973; Observations of Lacustrine Sedimentation at Lillooet Lake, British Columbia: Unpubl. Ph.D. Thesis, University of British Columbia.

Harbaugh, J.W., and Bonham-Carter, G.F., 1970; Computer Simulation in Geology: John Wiley & Sons, New York.

Harleman, D.R.F., 1966; "Diffusion Processes in Stratified flow": in Ippen, A.T. (ed.), Estuary and Coastline Hydrodynamics, McGraw-Hill, New York.

Heezen, B. C., and Ewing, M., 1952; "Turbidity Currents and Submarine Slumps, and the 1929 Grand Banks Earthquake": Am. Jour. Sci., v.250(12), pp. 849-873.

Hickin, E.J., 1970; Sedimentation in Sand-Bed Channels: Unpubl. Ph.D. Thesis, University of Sydney.

Holle, C. G., 1952; "Sedimentation at the Mouth of the Mississippi River": Proc. Second Conf. Coastal Eng. Council on Wave Research, Berkeley, California, pp. 111-129.

Howard, C. S., 1953; "Density Currents in Lake Mead." Internat. Assoc. hydraulic Research, 5th. Cong. Proc., Minneapolis, pp. 355-368.

Inman, D.L., 1973; "Sorting of Sediments in the Light of Fluid Mechanics": Jour. Sed. Petrology, v.19, no.2, pp. 51-70.

Ippen, A.T., 1971; "A New Look at Sedimentation in Turbulent Streams": Jour. Boston Soc. Civil Engineers, v.58, pp. 131-161.

Jopling, A. V., 1960; "An Experimental Study on the Mechanics of Bedding": Ph.D. Thesis, Harvard Unoversity, 358 p.

----------, 1962; "Mechanics of Small Scale Delta Formation -

Laboratory Study": Natl. Shallow Water Research Conf. Proc., Natl, Sci. Foundation, Washington, D.C., pp. 291-195.

----------, 1963; "Hydraulic studies on the Origin of Bedding": Sedimentology, v.2, pp. 115-121.

----------, 1964; "Laboratory Study of Sorting Process Related to Flow Separation": Jour. Geophys. Research, v.69, pp. 3404-3418.

----------, 1965; "Hydraulic Factors Controlling the Shape of Laminae in Laboratory Deltas": Jour. Sed. Petrology, v.35, pp. 777-791.

King, C.A.M., 1966; Techniques in Geomorphology: St. Martin's Press, New York.

Kolb, C.R., and Lopik, J.R.V., 1966; "Depositional Environments of the Mississippi River Deltaic Plain - Southeastern Louisiana": in Shirley, M.L., and Ragsdale, J.A. (ed.), Deltas, Houston Geological Society, pp. 17-62.

Kuiper, E., 1960; "Sediment Transport and Delta Formation": Proc. Am. Soc. Civil Eng., Jour.Hydr. Div., v.86.

Lipsey, T. E. L., 1919; "Currents at or near the Mouth, Southern Pass, Mississippi River": U. S. Eng. School, Prof. Mem., v.11 (55), pp. 65-122.

Middleton, G. V., (ed.), 1965; "Primary Sedimentary Structures and their hydrodynamic interpretation": Soc. Econ. Paleontologists and Mineralogists, Spec. Pub. 12, 265 p.

Middleton, G. V., 1966; "Experiments on Density and Turbidity Currents - II Uniform Flow of Density Currents": Canadian Jour. Earth Sci., v.3, pp. 627-637.

Mikhailov, V.N., 1966; "Hydrology and Formation of River Mouth Bars": in Scientific Problems of the Humic Tropical-Zone Deltas and Their Implications, Proceedings of Dacca Symposium (1964), UNESCO., pp. 59-64.

Nixon, M., 1959; "A study of the bankfull Discharge of Rivers in England and Wales": Proc. Inst. Civil Eng., 12.

Novak, I.D., 1973; "Predicting Coarse Sediments Transport - the Hjulstorm Curve Revisited": in Morisawa, M. (ed.), Fluvial Geomorphology, Pub. in Geomorphology, State Uni. of New York, Binghamton, N.Y..

Prandtl, L. 1925; "Bericht Uber Untersuchungen Zur Ausgebildeten Turbulenz": Z. ang. Math. Mech., 5.

Rouse, H., 1945; Elementary Mechanics of Fluids, John Wiley & Son, Inc., New York.

Russell, R. J., 1936; "Physiography of the Lower Mississippi River Delta": Louisiana Dept. Cons. Geol. Bull. 8, pp. 3-199.

Russell, R.J., 1967; "River and Delta Morphology": Louisiana Uni. Coastal Studies Series No.20.

Samojlov, I.V., 1956; Die Flussmundungen: (Translation from original Russian).

Schwarzacher, W., 1975; Sedimentation models and Quantitative Stratigraphy: Developments in Sedimentology-19, Elsevier Sci. Publishing Co., New York.

Scruton, P.C., 1956; "Oceanography of Mississippi Delta Sedimentary Environments": Am. Assoc. Petrol. Geologists Bull., v.40, pp. 2864-2952.

----------, 1960; "Delta Building and Delta Sequence": in Recent Sediments, Northwestern Gulf of Mexico, Am. Assoc. Petrol. Geologists.

Shepard, F. P., 1951; "Transportation of sand into Deep Water": Soc. Econ. Paleon. and Mineral., spec. Pub. 2, pp. 53-65.

Shepard, F.P., 1955; "Delta Front Valleys Bordering the Mississippi Distributaries": Bull. Geol. Soc. Am., v.66, pp. 1489-1498.

----------, 1960; "Mississippi Delta: Marginal Environments, Sediments and Growth: in Recent Sediments, Northwestern Gulf of Mexico": Am. Assoc. Petrol. Geologists.

Simmons, H. B., 1950; "Applications of Hydraulic Model Studies to Tidal Problems": Comm. Tidal Hydraulics Rept 1, U. S. Corps of Eng., pp. 127-45.

Singamsetti, S.R., 1966; "Diffusion of Sediment in Submerged Jets": Am. Soc. Civil Engineers, Hydraulics Div.Jour., v.92, no.HY-2, pp. 153-168.

Sutherland, A.J., 1967; "Proposed Mechanism for Sediment in Entrainment by Turbulent Flows": Jour. Geophys. Research,

v.72, pp. 6183-6194.

Takano, K., 1954a; "On the Velocity Distribution Off the Mouth of a River": Jour. Oceanographic Soc. Japan, v.10(3), pp. 60-64.

----------, 1954b; "On the Salinity and Velocity Distributions Off the Mouth of a River": Jour. Oceanographic Soc. Japan, v.10(3), pp. 92-98.

Tollmien, w., 1926; "Berechnung Turbulenten Ausbreitungsvongaange": Zeitschrift fur Angewandte Mathematik und Mechanik, v.6, p. 468.

Wolman, M. G., and Leopold, L. B., 1957; "River Flood Plains: Some Observations on their Formation." U.S. Geol. Survey, Prof. Paper No. 282-C.

Wright, L. D., 1970; "Circulation, effluent diffusion and sediment Transport, Mouth of South Pass, Mississippi River." Louisiana State Uni., Coastal Studies Institute Tech. Report. No. 84